Zeolite Synthesis under Nonconventional Conditions: Reagents, Reactors, and Modi Operandi — Source link ↗

Aron Deneyer, Quanli Ke, Julien Devos, Michiel Dusselier

Institutions: Katholieke Universiteit Leuven

Related papers:

- Small-Pore Zeolites: Synthesis and Catalysis

- The hydrothermal synthesis of zeolites: precursors, intermediates and reaction mechanism

- The distribution of aluminum in the tetrahedra of silicates and aluminates

Zeolite Synthesis in Non-Conventional Conditions: Reagents, Reactors and *Modi Operandi*

Aron Deneyer, Quanli Ke, Julien Devos, and Michiel Dusselier*

Center for Sustainable Catalysis and Engineering (CSCE), KU Leuven, Celestijnenlaan 200F, 3001 Heverlee, Belgium.

ABSTRACT: A myriad of tetrahedral molecular sieve frameworks, often siliceous, can be calculated *in silico*. Only a tiny fraction (<0.1%) of these can be synthesized on purpose. Only a small fraction of these available frameworks, mostly those composed of only Si and Al as T-atoms, *i.e.* true zeolites, are used commercially. A gap thus exists between what should be possible (thermodynamically) and what can be produced (kinetically) and used in real life. Even if a synthesis is successful (in industry or academia), flexibility with regard to synthesis parameters - in terms of time, amount of unit operations, OSDA-efficiency, *etc.* - as well as the obtained material properties - in terms of Si/Al ratio, Al-distribution, T-atom variety, crystal size, *etc.* - remains limited. These limitations are not surprising since conventional zeolite syntheses, *i.e.* hydrothermal synthesis in batch from amorphous or soluble Si- and Al-sources, have limited degrees of freedom (DOF). Typically, the type of ingredients, their ratios, a constant temperature, synthesis time and the absence or presence of agitation are varied. In order to take new steps towards more cost-competitive syntheses, and more importantly, zeolites with a greater flexibility in terms of structural properties, this review highlights all DOFs that can be introduced in addition to or on top of the conventional way of synthesis. By doing this, a distinction is made between non-conventional DOFs that influence the chemistry of the system (*e.g.* interzeolite conversion, charge density mismatch approach, ionothermal or free-radical assisted synthesis) and non-conventional DOFs that influence the physical environment (*e.g.* ultrasounds, alternative energy *via* microwaves or continuous set-ups). The review concludes with learnings, practical insights and future opportunities. In other words: which zeolite synthesis strategies really make a difference and which ones are just tweaking around the edges?

INTRODUCTION

Zeolites are crystalline microporous materials composed of tetrahedral silicon (Si) and aluminum (Al) oxides.[1] The chemical composition of zeolites has also been extended to include other tetrahedral atoms, such as the non-metallic B or P, metallic Sn, Ga and Ge, and transition metal Zn and Ti.[2] These so-called T-atoms are tetrahedrally connected *via* shared oxygens (TO$_2$), resulting in an ordered framework with characteristic microporosity in form of cages and channels (*e.g.* FAU topology in Figure 1). Multiple types of (catalytic) sites can be found in zeolites: framework Lewis acids, extra-framework Brønsted acidic protons and cations (compensating framework charge derived from isomorphic Al^{III}O$_2^-$ substitution) or active nanosized clusters (metal, oxide, *etc.*).[1,3,4]

Zeolites, both in academia and in industry, are typically synthesized hydrothermally in a batch set-up from amorphous or soluble Si- and Al-sources. In academia, this batch is typically a metal-encased Teflon cup.[1,3,5] To a certain level, this way of working limits the rate of formation (*cfr.* activity in chemical reactions) as well as the type of material that is formed (*cfr.* selectivity in chemical reactions). Most of the time, synthetic innovation (*i.e.* new frameworks, properties or rates) is encountered by using different types and ratios of classic zeolite ingredients, effectively altering the starting composition. The most common variation is using different organic cations that direct to a specific structure (selectivity). Apart from ingredients, the batch temperature is chosen and sometimes a mode of agitation. The purpose of this work is to review research in the field of zeolite synthesis with special attention to non-conventional conditions. Non-conventional here means either modified conventional batch hydrothermal synthesis by added features (*e.g.* non-aqueous solvents, zeolites as Si- and Al-source, different types of heating or agitation); or entirely different *modi operandi* (*e.g.* continuous flow synthesis). Note that non-conventional does not mean that these techniques are currently not well-examined (*cfr.* the broad range of examples in this review) or not used at a commercial scale. Non-conventional routes are likely indispensable for the production of some commercial zeolites.

In what follows, the conventional way of working is introduced and the current zeolite market is briefly overviewed. Then, certain limiting factors deriving from synthesis are discussed, as these provide rationales to aim for non-conventional strategies. In what follows, the most important "non-conventional" strategies are discussed with a focus on better or different output in terms of activity (rate) and/or selectivity (topology as well as material properties). Non-conventional conditions, highlighted in this

review, will either aim to influence the chemistry of the system directly or change the physical environment during synthesis. Finally, hybrid strategies combining multiple chemical and/or physical techniques, as well as some interesting post-synthetic strategies are briefly discussed. This review ends with some conclusions, practical insights and a future outlook.

CONVENTIONAL HYDROTHERMAL SYNTHESIS

Typically, hydrothermal zeolite synthesis starts by mixing a Si-source (*e.g.* colloidal silica, alkali silicates, silicon alkoxides such as tetraethyl orthosilicate, *etc.*), an Al-source (*e.g.* aluminum (hydr)oxides, nitrates, alkoxides, *etc.* or minerals such as gibbsite), water, a mineralizing agent and (organic) structure directing agents ((O)SDA) in one pot, *i.e.* a batch.[1–3,5] The Si- and Al-source are the amorphous or soluble raw material from which the crystalline aluminosilicate will be formed. If zeotype molecular sieves are synthesized, an additional or different heteroatom source needs to be added such as phosphoric acid when synthesizing SAPOs.[6] The mineralizing or mobilizing agent, which is typically OH^-, ensures the balance between the hydrolysis of amorphous Si- and Al-species, and the formation of new T-O-T bonds in crystalline aluminosilicate species and an intermediate sol-gel if applicable.[3–5] In addition to OH^-, fluoride media (F^-) is also regularly used as mineralizing agent, shifting from an alkaline to a (neutral or) low pH environment. By doing this, the solubility of certain species as well as the formation and stabilization of different oligomers and secondary building units and thus the hydrothermal synthesis itself, is heavily affected in comparison to OH^- media. As SDA, both inorganic (*e.g.* Na^+, K^+ or Cs^+) and organic cations (*e.g.* quaternary ammonium cations such as tetraethylammonium (TEA^+)) are common and often both are used at the same time. Frequently, inorganic SDAs come with the sources and/or with the mineralizing agent, *e.g.* sodium silicate and NaOH respectively. SDAs exert influence on different stages of zeolite synthesis leading to the creation and stabilization of a specific zeolite geometry.[3–5,7] Most of the times, especially with OSDAs present, a particular zeolite with characteristic topology and composition can only be obtained from specific ingredients. While an OSDA can be seen as a template, using this term is avoided because the fit between guest and host is often not perfect, and often there is the possibility to get multiple frameworks from one OSDA.

In addition, reaction conditions play a crucial role in steering the final product properties.[3–5] Especially the temperature profile is a dominant parameter in synthesizing the "right" zeolite topology. Often the batch autoclave containing the ingredient mixture is aged at moderate temperature (room temperature - 363 K). Aging can be used to promote the contact between Si and Al species, to direct their framework distribution, to dissolve or depolymerize crystalline or solid T-atom precursors (*e.g.* Al_2O_3 often requires prior contact with the mineralizing agent) and sometimes to generate a specific aluminosilicate gel. Aging often accelerates nucleation and crystallization later.[3,5]

Thereafter, the temperature will be raised to somewhere between 363 K and 473 K for 'real' hydrothermal synthesis. Normally, a classic zeolite synthesis process is thought to consist of three consecutive phases, being *(i)* the induction period, *(ii)* nucleation and *(iii)* crystal growth.[3] The induction period typically starts when the final temperature of the hydrothermal synthesis is reached. This higher temperature is accompanied by an increased concentration of soluble Si- and Al-species, going from a stable, over a meta-stable, towards a labile phase.[5] In this latter phase, it is possible to form new crystals. This phenomenon is called supersaturation and is often, together with reaching the final synthesis temperature in the liquor, seen as the start of the induction period (τ).[4] In turn, the induction period is often subdivided into three different stages[3]: *(i)* time to obtain a quasi-steady-state distribution, *(ii)* time to transform from a quasi-steady-state towards a nucleus, *(iii)* time to be able to detect the growing nucleus.

In reality, the different stages are hard to identify and often overlap. Moreover, two or more phases are regularly competing, and their crystallizations are often at different stages. The starting precursor mix (gel or colloidal suspension) or also any kind of primary amorphous phase, represents a non-equilibrium (heterogeneous) situation. Thereafter, an increase in temperature (as well as longer synthesis time) will lead to an equilibrium state between the liquid phase on the one hand and the solid aluminosilicate phase on the other hand (secondary amorphous phase). This is still not crystalline, but it can already closely relate to the target zeolite in terms of structure and composition. At this moment, so called "islands of order" or "proto-nuclei" will spark nucleation. A regular ordered network will be obtained from these basic, but still amorphous, structures. Primary nucleation is thus taking place in a homogeneous or heterogeneous way with the SDAs as orienting factor towards the preferred zeolite geometry. In order to increase the rate of crystallization, zeolite seeds can be added during the hydrothermal synthesis (secondary nucleation). This increasing speed can be ascribed to the presence of new crystals and/or a higher external surface. In the end, zeolites crystals will further grow at the crystal-liquor interface *via* successive monomer addition at the expense of the amorphous Si- and Al-source (or solution) or by aggregation of available nanoparticles in non-classical ways.[3–5,8–14]

In summary, molecular sieves synthesis in general consists of a complex sequence of steps. For a more detailed understanding, the reader is referred to the reviews of Corma and Davis (2004)[2], and Cundy and Cox (2003 and 2005)[1,3] and the book "zeolites and catalysis" of Cejka, Corma and Zones (2010)[4]. Since discussions are ongoing, Mintova and co-workers recently published an update on zeolite growth mechanisms and remaining questions.[9]

BRIEF OVERVIEW OF THE ZEOLITE MARKET

Porosity, active site diversity and stability explain the value of these unique high surface area materials. Important industrial applications for synthetic zeolites are *(i)*

separation, *(ii)* ion exchange and *(iii)* catalysis (Table 1 and Figure 1).[1,15] For example, multiple molecules can be separated as a result of differences in molecular dimension, diffusion rate and adsorption capacity with the porous host, which corresponds to the processes of size-sieving, kinetic separation and equilibrium separation respectively.[16] With regard to ion exchange, zeolites are frequently used as fabric softener while doing the laundry in order to remove water hardening Ca^{2+} and Mg^{2+}. These materials are also valuable catalysts, improving (petro)chemical as well as environmental-oriented reactions. Examples include fluid catalytic cracking of hydrocarbons into shorter ones with zeolite Y[17] or the reduction of NO_X in automotive exhausts with Cu-zeolites[18]. The list of industrial zeolite applications is always expanding. In research as well, zeolites are often at the basis of new processes, *e.g.* in the activation of small molecules (CH_4[19,20], syngas[21,22] and CO_2[23-26]) or biomass[27-29]. Given the soaring interest in converting small molecules, an increasing focus is now found on materials with pores containing at most 8 T-atom members in the ring (8MR) opposed to larger 12 or 10MR pore systems.[15,30,31] Such small-pore zeolites are used in automotive catalysis, and they also excel in the production of olefins from methanol (MTO)[18,32]. In contrast, large-pore or mesoporous materials (*e.g.* 12MR beta or hierarchical MFI) can aid in the upgrading of larger biomass-derived molecules.[28,33-37]

Although zeolites are highly-praised at an industrial level, only a few topologies are available at this scale (right box in Figure 1). According to Vermeiren and Gilson a decade ago, only 18 topologies are produced and used commercially.[38] The laundry detergent market is the largest in terms of volume (LTA, GIS), but with regard to value, the differences with catalyst and adsorbent applications are smaller. Further growth is expected especially for those zeolites that are used as catalysts and certainly as adsorbents (Table 1). Recently, the silicoaluminophosphate (SAPO)-34 (CHA) was commercialized for use as MTO catalyst in China. Part of the 25-year period between discovery and commercialization demonstrates the difficulty of going from a promising material and its activity to an industrial zeolite process.[32,38]

WHY AIMING FOR NON-CONVENTIONAL STRATEGIES?

Novel catalytic applications or better-than-benchmark results are often reported for new or modified zeolite materials or synthesis routes, but their large scale implementation lacks. In addition to synthesizing a material without impurities at the gram scale (a first hurdle) with a significantly better performance for a certain application (second hurdle), upscaling can present important roadblocks (third hurdle). Ideally, a synthesis is safe, environmentally friendly, fast, and with a limited number of unit operations

(*e.g.* filtration or washing steps) and an efficient use of raw materials (*e.g.* optimizing the use of a, preferably cheap, structure directing agent). Even when fulfilling most of the above, new materials can still lose out against established ones due to less efficient post-synthesis procedures (*e.g.* ion-exchange or dealumination *en route* to the final required properties), less suitable catalyst shapes for industrial reactors (*e.g.* minimizing pressure drop and having enough mechanical strength) or just because of economies of scale.[38,39] Molecular sieve synthesis research with a focus on protocols and scalability is thus required, in order to render their manufacture more sustainable and cost-competitive, with efficient use of feedstocks and energy.

According to Zones, safety, waste management, synthesis time, consumption of raw materials and the use of (often energy-intensive) unit operations are the biggest obstacles in commercial zeolite synthesis.[39] Slow kinetics, and especially those of the nucleation step, are likely one of the more pronounced stumbling blocks at this moment. Ideally, a synthesis procedure will be shortened, from the scale of days-weeks to a few hours-days (*cfr.* activity in chemical reactions).[40] At the same time, one has to be aware of the metastability of zeolites, meaning that these materials are not favorable end-points from a thermodynamic point of view (*cfr.* stability/phase selectivity).[3,41] Eventually, the thermodynamic drive leads to more dense phases such as quartz (SiO_2). It is thus extremely important to play with the kinetics in a way to speed up synthesis and at the same time end up with the desired zeolite, while avoiding different metastable zeolites on the way to the dense 'bottom'.[15,42,43] If new procedures are fast and selective, material and energy balances need to be relatively good and operations safe, for workers and environment.[39,44]

Besides speed, a second major drawback of the current molecular sieve inventory is that not every structure is accessible in every composition in terms of T-atoms. Although more than 260.000 frameworks are theoretically calculated, only 248 can be synthesized, of which approximately only one third are zeolites (only Si and Al as T-atoms).[42,45,46] Moreover, these synthetic zeolites are only available in a limited range of Si/Al ratios from synthesis. Even for the commercial zeolite catalysts, there is often a lack of control over both the amount of Al-incorporation[47] and the Al-distribution.[48] Examples of the latter are paired vs isolated Al, specific crystallographic T-site locations[49] or Al zoning[50], which impact catalytic selectivity and activity.[51] In addition, the accessibility of the active sites in the zeolite interior strongly influences their performance. Therefore, it is also key to control the crystal size and the morphology of the zeolite in order to prevent coke formation and enhance their long-term stability as catalyst (*cfr.* selectivity).[52]

Table 1. [a] **Worldwide zeolite consumption.**[38,53]

Application	Share (V%) 2004 [b]	Share (V%) 2016 [b]	Market evolution	Used topologies at commercial level [c]
Synthetic zeolites (± 40% of all consumed zeolites; average annual growth rate = *1.5%*) [d]				
Ion exchanger	78.2	66.6	↙ (efficient use + other detergents)	LTA (most frequently used)
Catalyst	14.2	18.0	↗ (rising demand of fuels + lower oil quality)	AEL, BEA, ERI, EUO, FAU, FER, LTA, LTL, MFI, MOR, MTW, MWW, RHO [e]
Adsorbent	7.4	14.0	↗↗ (many environmental projects)	CHA, EDI, GIS, HEU, MER [e]
Natural zeolites (± 60% of all consumed zeolites; average annual growth rate = *status quo*) [d]				
e.g. Clinoptilotite, Chabazite, Mordenite are used				

[a] In 2004, the consumption of natural zeolites was > 2 500 kilotons . year^{-1} and the consumption of synthetic zeolites was 1 692 kilotons . year^{-1}. [b] Percentages are Volume% (V%). [c] Based on the review of Vermeiren and Gilson (2009).[38] [d] Data for 2016. [e] Topologies (used commercially as catalyst) can also be used industrially as adsorbent for separations (*e.g.* LTA, FAU).
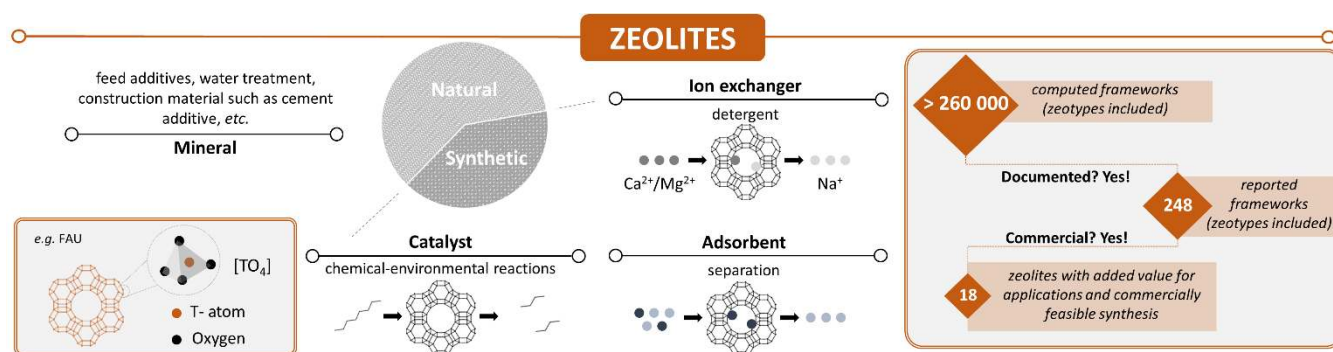

Figure 1. Schematic pie chart of the worldwide natural (60%) and synthetic (40%) zeolite consumption (2016).[53] In addition, their major applications are highlighted. The typical zeolite structure with its tetrahedra is visualized in the left box (here: FAU, viewed along [111]). Some numbers of commercial versus computed frameworks (including zeotypes), are represented in the right box.

In order to improve the efficiency of zeolite syntheses - in terms of synthesis time, unit operations, crystallinity, yield, OSDA-efficiency, *etc.* - and to broaden the current zeolite diversity - in terms of topology, composition, T-atom diversity, morphology, *etc.* - researchers are constantly looking for new techniques.[54] In what follows, the most striking non-conventional strategies, either changing the chemical or the physical environment, will be discussed and compared with the conventional way of working. The latter, in batch, is represented in Figure 2. Classic ingredient variations such as novel OSDAs, HF or conventional T-atom sources, are not the scope here. Zeolite membrane synthesis and its strategies[55,56] will not be discussed in this review, only bulk synthesis. Zeolites (Si, Al composition) are the main focus.

CHANGING THE CHEMICAL ENVIRONMENT

In hydrothermal systems, the chemical synthetic parameters, such as silicon source, alkaline cations and pH, play a vital role in the product selectivity, crystallization rate, crystal size and morphologies. Even a minor variation in these can eventually lead to significant differences in the products. For example, playing with the alkaline or silicon sources could enhance the nucleation rate and lead to smaller crystals.[57,58] In this section, non-conventional techniques will be discussed that change the chemical environment during synthesis, *i.e.* different ingredients (or types) compared to ones used in conventional hydrothermal synthesis. Within this group, six subtopics are highlighted: *(i)* reducing or avoiding some of the conventional ingredients, *(ii, iii)* solvo- and ionothermal syntheses *(iv)* interzeolite conversion (IZC), *(v)* charge-density mismatch (CDM), and *(vi)* free radicals-assisted synthesis (overview in Figure 3). In the context of waste management, the first strategy aims to consume less (conventional) raw materials, while the second and third aim at replacing solvent and/or OSDA. The fourth strategy uses a microporous crystalline Si- and Al-source instead of typical amorphous or soluble precursors. Fifthly, in CDM, the types as well as the amount of SDAs are varied, initially starting with a mismatch in charge between SDA and aluminosilicate. The last strategy complements the usual OH$^-$ mineralizing agent with ·OH radicals.
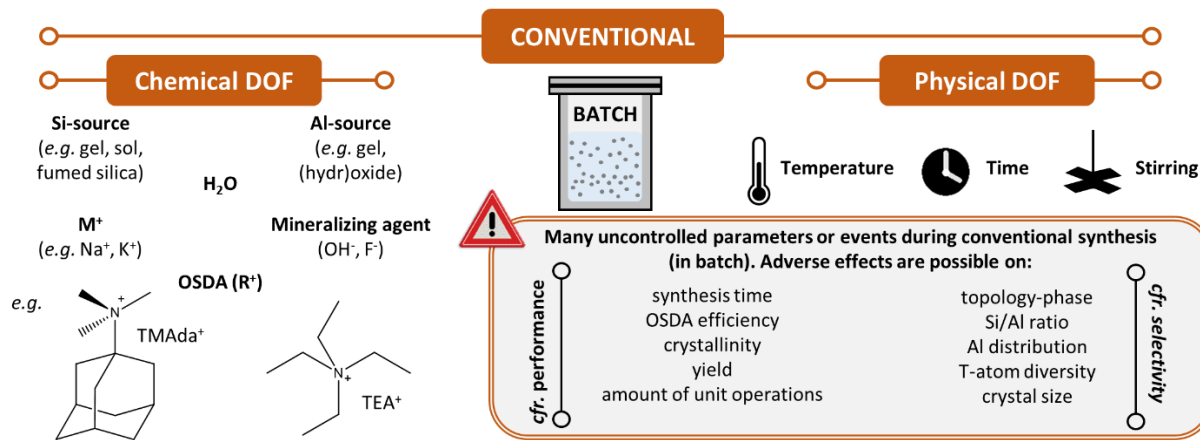
Figure 2. Standard hydrothermal synthesis of zeolites in a batch autoclave (*e.g.* with Teflon cup). All conventional degrees of freedom (DOF) as well as important bottlenecks are listed. TMAda+ = N,N,N-trimethyl-1-adamantylamine+; TEA+ = tetraethylammonium+.
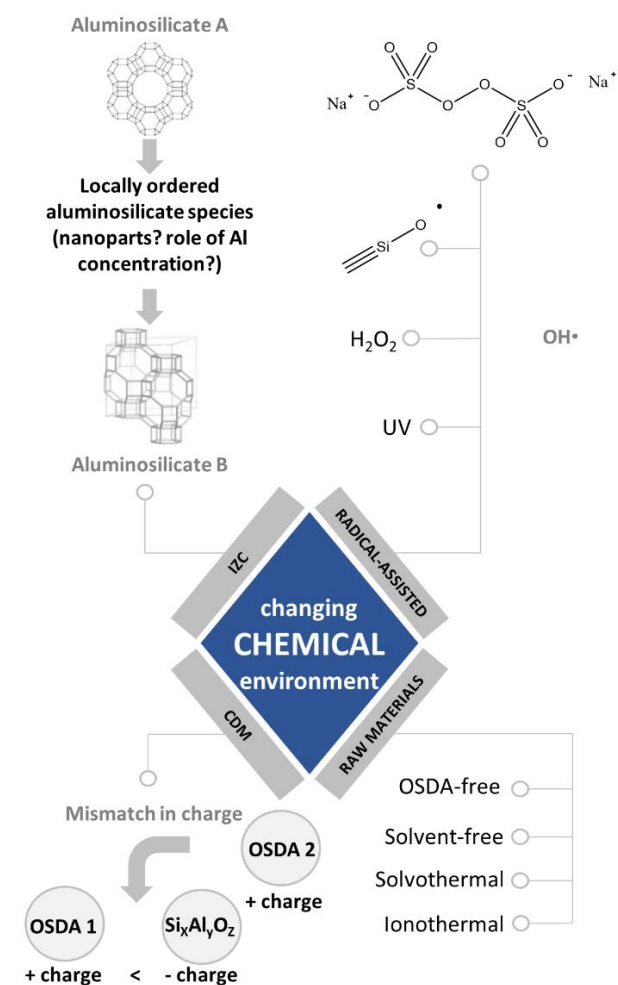

Figure 3. Schematic representation of non-conventional strategies that change the chemical environment during zeolite synthesis, not based on simple compositional variation: avoiding, reducing or replacing certain **raw materials** (e.g. OSDA-free or ionothermal); **interzeolite conversion**; **charge-density mismatch** and free **radical-assisted** synthesis (·OH radicals can be introduced in different ways)

Reducing or avoiding some of the conventional zeolite ingredients. Efficient use of raw materials in zeolite synthesis is getting more attention lately, to reduce waste or the use of toxic chemicals. Moreover, this way of working can have beneficial effects on the overall production cost (*e.g.* less unit operations required, higher productivity per synthesis batch volume and cheaper raw materials). Since OSDAs and solvents are no part of the final zeolite, the necessity of using these two conventional ingredients was mainly investigated, resulting in successful solvent-free and OSDA-free approaches. Solvent-free approaches, typically after a mechanochemical grinding step, are highlighted as a hybrid strategy later in this review. In the case of OSDA-free synthesis, several topologies, originally discovered with organics (*e.g.* BEA, EMT, MFI, RTH, MTW, MOR) can now also be synthesized, either by adapting the ratio of the starting ingredients[41,59] but mostly by using seeds[60–69]. Liu *et al.* (2014), for example, found a more uniform Al-distribution in RTH-frameworks from an OSDA-free method because there was no interaction between Al-species and organics.[69] For a detailed overview of 'ingredient-free' approaches, the reader is referred to the review of Feng-Shou Xiao et al., which also highlights OSDAs recycling.[70]

Solvothermal Synthesis. Conventionally, water is the solvent for most zeolite syntheses (*hydro*-thermal). Compared to solid state crystal syntheses for oxides for example, hydrothermal methods operate at lower temperature as transport of species is much easier. While high temperatures in solid state methods seem to produce more thermodynamically favored outcomes, kinetic control over the produced phase is more prevalent in hydrothermal routes. This results in kinetic restrictions for certain phases, or kinetics paths to others, and thus in general, the easier production of metastable phases.[71] Solvothermal synthesis, in the context of this review, refers to zeolite synthesis methods using organic solvents instead of water, *e.g.* pyridine, alcohols, hydrocarbons.[72] Compared to water, the autogenous pressure generated at elevated temperature can be

higher for certain solvents and also the polarity (hydrophobic/hydrophilic properties) varies widely.[71] Notably, most of the solvothermal syntheses are not exactly anhydrous, and the presence of minor amounts of water can be essential (or beneficial) for the zeolite crystallization.[73,74]

A patent from 1982 disclosed the use of dimethoxyethane (ether) as a solvent for zeolite synthesis.[75] In 1985, Bibby and Dale thoroughly reported the nonaqueous synthesis of aluminosilicate and all-silica sodalite (SOD, Table 2, entry 1) using ethylene glycol and propanol as solvents. Ever since, solvothermal methods have been considered to have great potential and some examples are listed in Table 2.[76] In 1993, Kuperman and co-workers reported a nonaqueous solvothermal method in conjunction with HF.[77] This solvothermal method is based on pyridine, propylamine, triethylamine or their combination and crucially employs F- as mineralizer, minor amounts of water, and occasionally TPA(Br) as OSDA.[77] The HF-pyridine and HF-alkylamine solvents allowed to prepare (very) large-crystal ferrierite (FER), silicate-1 (MFI) and dodecasil-3C (MTN) zeolites with uniform sizes and well-defined morphologies (Table 2, entries 2-4). Since water is less viscous than many organic solvents, the chance of secondary nucleation seems reduced in solvothermal environment and thus the formation of small crystals suppressed.[72] Similar strategy was later utilized by Weitkamp and co-workers to tailor the morphology of large-crystal FER zeolites by using various n-alkylamines as templates and pyridine as solvent.[78] Nitrate-containing SOD zeolites have also been synthesized using methanol and pentanol noting the need for increased reaction temperatures and times when using the more hydrophobic alcohol, with the result of larger crystal habits.[79]

Solvothermal synthesis has also been shown for the incorporation of heteroatoms into zeolite frameworks. Whether some of these compositions are unique to solvothermal routes though is hard to know, as control syntheses in water are often not reported or feasible. During the solvothermal synthesis of SOD zeolites, Yang and co-workers observed that germanium could be readily incorporated into the silica framework and accelerate the crystallization of SOD structure.[80] Likewise, iron, cobalt and boron could successfully substitute the aluminum within MRE-type, LIT-type and FER-type aluminosilicate frameworks respectively, with the assistance of alkylamine or methanol solvents (entries 5, 6, 2).[81-83] In addition to silica-based materials, solvothermal synthesis is often used with success in the syntheses of aluminophosphate (AlPO) frameworks (Table 2, entries 7-11).[84-86] One remarkable example is the novel AlPO structure of JDF-20 possessing 20-ring extra-large pores (Table 2, entry 10).[84] Typical analogues of AlPO structures, silicoaluminophosphate (SAPO), could be prepared by solvothermal routes as well, using alcohol media and/or alkylamine directing agents, such as SAPO-11 (AEL), SAPO-31 (ATO) and SAPO-35 (LEV) (Table 2, entries 8, 12 and 13).[87-90] In these cases, (small) effects on Si incorporation, catalytic performance and acidity have been noted when comparing non-aqueous to aqueous synthesis (e.g. ref [87]).

While water as a solvent is replaced, its presence in small amounts remains crucial, mainly because of its catalytic effect on the dissolution (of e.g. silicate species) or hydrolysis of oligomeric (e.g. chain[73]) species or the solvation of species[74] as well as its assistance in mass transport. However, the role of water seems synthesis-dependent. For instance, Yang et al. (2007) noted that the crystallization of siliceous sodalite is not sensitive to the presence of small quantities of water in ethylene glycol solvent because the latter can act as a transport agent, aiding in solvation and crystallization.[80] However, adding a lot more water to such systems (e.g. $H_2O/Si = 2$) drives the systems to neglect the solvent, diminishing the role of ethylene glycol to heat transfer agent only. In general, one can tentatively conclude that the interaction between solvent, OSDA and framework species is actually of greater importance in determining the final zeolite product topology, than the presence of water.
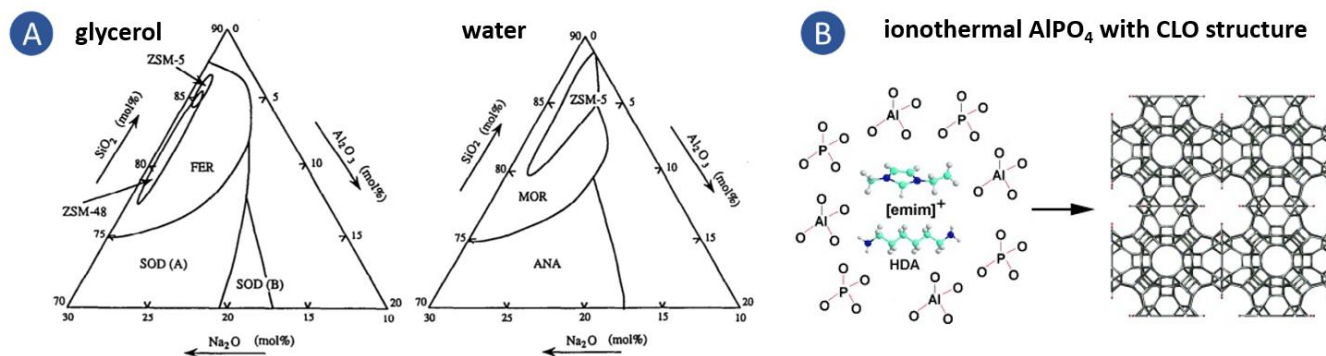
Figure 4. (A) Solvothermal exploration of Na_2O (10-30 mol%)-Al_2O_3 (0-20 mol%)-SiO_2 (70-90 mol%) in glycerol and water. For glycerol, 210 °C was used and the molar (SiO_2 + Al + NaOH)/glycerol ratio was 0.35 while for water, 190 °C and 0.035 were used. Reprinted from Zeolites, 14 (8), Kanno, N.; Miyake, M.; Sato, M., Syntheses of Ferrierite, ZSM48, and ZSM-5 in Glycerol Solvent, 625-628, Copyright (1994), with permission from Elsevier.[91] (B) Ionothermal synthesis leading to a CLO structure from 1 Al_2O_3 :1 P_2O_5: 2 HF: 1 hexanediamine : 80 EMIBr and traces of water at 210 °C for 2 h. Reprinted with permission from Wei et al.[92] Copyright 2010, Wiley-VCH.

In conclusion, solvothermal approaches have been widely applied for different topologies and compositions, and it seems lower supersaturation levels and nucleation rates in these systems relative to the hydrothermal ones are the main differences. This could be attributed to the organic solvent's distinct physical properties (polarity, viscosity, etc.) which give rise to different behaviors in dissolution and mass transfer.[72] Based upon these differences, solvothermal method could not only change the chemical rates of zeolite synthesis and give various sizes and morphologies, but also influence the selectivity.[77,82,91] A lot of studies however do not include an aqueous control, sometimes because it is simply not a possible to synthesize the zeolite from the same composition with only the solvent changed. An interesting study with comparisons (Fig. 4A) was given by Kanno et al, for an OSDA-free aluminosilicate system in glycerol and water. They discovered a new crystallization field for ZSM-48 (*MRE) likely caused by the low solubility of silica in glycerol, with the latter also acting as SDA (or pore filler). Intriguing to note in Figure 4A is that the crystallization fields of sodalites and ferrierite in glycerol, are nearly in accord with those of analcime and mordenite in water, respectively.[91]

It seems that for aluminosilicates, no new structures have been discovered using solvothermal routes, whereas this has been the case for phosphates. This phenomenon could be attributed to the different framework charge density of aluminosilicates and phosphates, which leads to changes in the interaction with solvents and OSDAs. For more information, the readers are pointed to an informative review from Morris and Weigel (1997).[72]

Ionothermal Synthesis. The competition between a solvent and an OSDA to interact with the zeolite framework being constructed can hardly be avoided when both are present. From this perspective, as well as others, researchers have been looking for a liquid to serve as template and solvent simultaneously. Ionic liquid solvents (ILs) are salt fluids containing predominantly ionic species under near-ambient temperature (<100°C).[93] From a large variety of ILs, those with strong polarity, good thermal stability and high solubility for inorganic reagents could be selected.[94,95] Morris and co-workers pioneered the preparation of a series of aluminophosphate (AlPO) zeotypes as well as interrupted structures (i.e. where not all oxygen atoms are part of Al–O–P linkages) by using the versatile ionic liquid, 1-ethyl-3-methylimidazolium bromide (EMIBr) as both solvent and template (Table 2, entries 14-17).[96,97] Thereafter, novel materials containing different heteroatoms, such as the cobalt aluminophosphate SIV with new topology, as well as siliceous frameworks have been prepared (Entries 18-20).[98,99] For the silicates (MFI, TON), the partial exchange of the 1-butyl-3-methyl imidazolium bromide for the hydroxide is needed, leading to an ionic liquid that is more compatible with dissolving silica.

During ionothermal synthesis, Morris et al. also observed widespread decomposition of alkyl chains (3-5 carbons) within 1-alkyl-3-methyl imidazolium bromide (AMIBr) ionic liquids, which suggests that the product selectivity is quite sensitive to the reaction conditions. The decomposition was aided by fluoride as mineralizer, and the resulting dimethyl imidazolium cation could generate the default CHA structure due to its pore-filling effect.[100] On the other hand, it is also noteworthy that the F$^-$ within ionothermal systems may not only serve as mineralizer, but also play a co-templating role together with the IL.[101,102] Ma et al. (2009) have systematically investigated the influences of alkyl chains, in presence of F$^-$ as mineralizer, on the synthesis of gallophosphate LTA (entry 21).[101] They note that when the alkyl chain length increases in AMIBr, the sizes of the as-synthesized crystals decrease sharply, while their morphologies transform from octahedron to truncated octahedron and finally to cube.[101] Even though decomposition could not be entirely excluded here, its influence seems less pronounced than in the conditions of Morris. Here, the alkyl chain mainly affects the crystal size and morphology of zeolite rather than topology.

Not all ILs are suitable because of their decomposition during zeolite synthesis.[100] Therefore, the introduction of additional amine as co-template with ILs was investigated to open up possibilities for new microporous materials. Wang et al. (2006) have investigated the evolution of AlPO frameworks emerging in ionothermal systems with amine species added, which indicated that the additional amine could increase the crystallization rate and improve the product selectivity (Table 2, entries 22-23).[103] It is interesting to note that the ATV AlPO was made at 280 °C, while temperatures this high are usually avoided in water due to the high pressure resulting from it. Furthermore, by co-templating, an open AlPO$_4$ framework with unique Al/P ratio (entry 24) and an AlPO with 20-ring openings (CLO, entry 25) could be indeed prepared using EMIBr as the ionic liquid but with 1-methylimidazole or 1,6-hexanediamine as the amine, correspondingly.[92,104] The CLO structure is seen in Fig. 4B. Combining solid-state NMR spectra and density functional theory (DFT) calculations, Xu et al. (2009) further concluded that co-template amine could interact with ionic liquids by hydrogen bonds and the consequent ionic liquid-amine hybrid could affect the nucleation of AlPO frameworks.[105]

Similar to solvothermal synthesis, a minor water content can always exist in the reagents. Table 2 lists some water/IL ratios. In this consideration, Ma et al. (2008) have carefully designed an anhydrous ionothermal system to explore the effects of varying amounts of water on the synthesis of AlPOs.[102] The results show that the addition of minute amounts of water (2 H$_2$O: 40 IL) could promote nucleation and crystal growth. It may be that the added water produces and transports H$^+$ and OH$^+$ hydrates in the ionothermal system and thus boosting the hydrolysis and condensation of reagents.[106] An autocatalytic effect could be present, as condensation water is progressively formed.

In conclusion, solvothermal and ionothermal methods are similar in nature, in that they replace water as the solvent. Additionally, ionothermal approaches also replace the OSDA with the cationic part of the ionic liquid. By this means, the competition between OSDA and solvent can be altered or influenced. It seems ionothermal systems are

quite sensitive to subtle changes in the synthesis environment, such as the structure of ionic cation and its decomposition, the concentration of water and fluoride, and the addition of organic templates.[96,100,103] Both solvo- and ionothermal systems have not really led to widespread discovery of new frameworks, although one can achieve more than tailoring crystal size and morphology, especially for ionothermal systems with co-SDAs. Ionic liquids often feature a low interface tension which likely influences the nucleation and crystal growth at the liquid surface interface. For zeotypes in particular these methods have shown a lot of promise, likely due to solubility differences in T-atom and their precursors. In certain of these syntheses, the selectivity is clearly affected. A downside of this synthesis route is the large volumes of costly ionic liquid (or solvent) needed. For more detailed discussions, the readers is referred to good reviews on this matter.[71,107,108]

Table 2. Summarization of zeolites prepared in solvothermal and ionothermal environment.

				Solvothermal Syntheses	
Entry[d]	Material	Top.	T-atoms[d]	Solvent(s) + OSDA (if used)[d,e]	T (°C)
1[76,79,80]	Sodalite	SOD	Si*, (Al)#, (Ge)/	EG*, /, propanol, methanol#, pentanol#	150*, #, 180*, /, 200#
2[77,78,82]	Ferrierite	FER	Si*, (Al)#, (B)ˡ	pyridine + n-propylamine*, Et_3N + TPABr#, pyridine + n-alkylamines *, #, ˡ	160*, 180*, #, ˡ
3[77]	Silicalite-1	MFI	Si	Et_3N +n-propylamine+TPABr	180
4[77]	Dodecasil-3C	MTN	Si	pyridine	200
5[81]	Fe-ZSM-48	MRE	Si, Al, Fe	Et_3N + diethylamine	200
6[83]	Lithosite	LIT	Co, Si, Al	methanol	200-250
7[85]	$AlPO_4$-5	AFI	Al, P	EG + Et_3N, 1,3-propanediol + Et_3N, hexanol+triethanolamine	180
8[85,87,88]	SAPO-11ᵀ, $AlPO_4$-11⊥	AEL	(Si)ᵀ, Al, P	EG + dipropylamine ᵀ, ⊥, ethanol+dipropylamineᵀ, EG + dibutylamine ⊥	180⊥, 200ᵀ
9[85]	$AlPO_4$-21	AWO	Al, P	EG or 2-butanol + dimethylamine or ethylamine	180
10[84 a]	JDF-20	-	Al, P	di, tri-or tetraethylene glycol + Et_3N, 1,4-butanediol + Et_3N	180
11[86]	$AlPO_4$-17	ERI	Al, P	methanol + EG + methylamine	180
12[87]	SAPO-31	ATO	Si, Al, P	EG + dipropylamine	200
13[89,90]	SAPO-35	LEV	Si, Al, P	hexamethyleneimine + EG	200
				Ionothermal Syntheses	
Entry	Material	Top.	Comp.	Ionic liquid + OSDA [e]	H₂O/ ionic liquid (mol/mol)	T (°C)
14[96 b]	SIZ-1	-	Al, P	EMIBr	0.07	150
15[96]	SIZ-3	AEL	Al, P	EMIBr	0.09	150
16[96]	SIZ-4	CHA	Al, P	EMIBr	0	150
17[97 b]	SIZ-6	-	Al, P	EMIBr	0	200
18[99]	SIZ-7 to 9 mixture	SIV+ AEI+ SOD	Co, Al, P	EMIBr	0.09	150
19[98]	[BMI]-Silicalite-1	MFI	Si	$[BMI]OH_{0.65}Br_{0.35}$	0.2	170
20[98]	[BMI]-Theta-1	TON	Si	$[BMI]OH_{0.65}Br_{0.35}$	0.2	170
21[101]	$GaPO_4$-LTA	LTA	Ga, P	EMIBr	0.225	180
22[103]	$AlPO_4$-25	ATV	Al, P	BMIBr + n-DPA	0.07 [f]	280
23[103]	$AlPO_4$-5	AFI	Al, P	BMIBr + n-DPA	0.07[f]	190
24[104]	JIS-1[c]	-	Al, P	EMIBr + MIA	0.53[f]	180
25[92]	DNL-1	CLO	Al, P	EMIBr + HDA	0.07[f]	210

[a] Novel structures without topology codes; [b] Interrupted structure; [c] Open AlPO framework; [d] In the case of multiple compositions across multiple records, composing T-atoms are linked with solvents and temperature. T-atoms between brackets are used in some reports only. [e] EG = ethylene glycol, Et_3N = triethylamine, EMI = 1-ethyl-3-methylimidazolium, BMI = 1-butyl-3-methylimidazolium, n-DPA = n-dipropylamine, MIA = 1-methylimidazole, HDA = 1,6-hexanediamine. [f] water calculated from HF and phosphoric acid sources, but it is possible that some of this water is removed in an open preheating stage (e.g. entry 25).

Interzeolite conversion (IZC). During IZC, earlier assembled zeolite parents are (partially) disassembled and reassembled into other zeolite topologies using hydrothermal synthesis, often in quite conventional conditions with classic *modi operandi*. Using zeolitic sources allows more rapid and selective syntheses for certain topologies, sometimes over a broader range of compositions as compared to classic syntheses starting from an amorphous or soluble T-atoms precursors or an amorphous aluminosilicate gel.[18,109] It also provides the opportunity to crystallize new frameworks (*e.g.* YFI[110]) or steer the selectivity to desired existing topologies. An example of the latter is IZC allowing to acquire CHA[111] from TEA[+]OH, in contrast to BEA often obtained with this OSDA.

The largest advantage of IZC is related to fast nucleation expressed by shorter synthesis times[112] and the broader compositional variety (Si/Al_F) of recipes than from conventional synthesis (*e.g.* for SSZ-13[18]). Other factors, often linked to the success of IZC, are framework density (FD) and structural similarity. As listed in Table 3, most of the zeolites are inclined to be transformed into structures with a denser framework. Faujasite (FAU) possesses one of the lowest framework densities (FD= 13.3 10^{-3} T/Å³) among the available zeolite topologies and plenty of zeolites (*e.g.* CHA, RHO, AEI and RTH) can be synthesized from a FAU precursor.[110–129] Thermodynamic studies have demonstrated that idealized frameworks with higher framework density are slightly more stable than structures with low framework density (with respect to α-Quartz).[130] Nevertheless, the use of an OSDA changes the stabilization of the materials resulting from synthesis significantly. Therefore, it is believed that energetic limitations are not a dominant factor in phase selectivity of particular reaction mixtures, but rather kinetic factors.[2,131] Recent literature demonstrates the possibility to perform IZC from sources with higher framework density to lower framework densities (Table 3, entries 11-13) or to similar framework densities (Table 3, entries 7, 9, 14-15). Although the thermodynamic drive to more dense materials in IZC is real,[130] this is likely stronger when only inorganics are used (no OSDA)[132]. This demonstrates the high importance of synthesis kinetics and allows a broader choice of zeolitic source materials to start from. For commercialization, the (additional) cost of the zeolitic source material should be balanced by satisfying synthesis parameters such as synthesis time, low SDA cost and improved physico-chemical properties.[39] In reverse, the same considerations also hold true for amorphous source recipes (conventional). SSZ-39 (AEI), a material first made by IZC, has only very recently been produced using cheaper amorphous sources. A very specific set of conditions are required to synthesize pure SSZ-39 in this way, and the synthesis lacks good atom efficiency (yield < 22%).[133] While synthesis from amorphous materials is still desirable, one cannot debate the value of IZC for this particular synthesis (AEI).

Table 3 A list of typical IZC (aluminosilicate) protocols reported to date.[a]

Entry	Parent zeolite	FD [b]	OSDA [c]	Descendants	FD [b]
1 [123–127]			TMAda[+], BTMA[+], TEA[+], *etc.*	CHA	15.1
2 [128,129]			TEA[+], BTMA[+], *etc.*	BEA	15.3
3 [113]	FAU	13.3	AMCE complex	RHO	14.5
4 [115–117,120,121]			DMDMP[+], TEP, DEDMP[+], *etc.*	AEI	15.1
5 [118,119]			MMPI[+], 123TMI[+], 1235TMI[+], 12345PMI[+], *etc.*	RTH	16.1
6 [120,122]			DBCOB[2+], etc.	AFX	15.1
7 [134,135]			TMAda[+]	CHA	15.1
8 [115]	BEA	15.3	TPA[+], *etc.*	MFI	18.4
9 [136]			DMP[+]	AEI	15.1
10 [113]	RHO	14.5	TMAda[+]	CHA	15.1
11 [136]	MFI	18.4	DMP[+]	AEI	15.1
12 [14]			TMAda[+]	CHA	15.1
13 [135]	LTL	16.7	TMAda[+]	CHA	15.1
14 [120]	CHA	15.1	DMDMP[+]	AEI	15.1
15 [120]			DBCOB[2+]	AFX	15.1

[a] OSDA-free, seeded and fluoride based IZCs are omitted; [b] The units of the framework density is 10^{-3} T-atom/Å³; [c] TMAda[+] = N,N,N-trimethyl-1-adamantanamine, BTMA[+] = Benzyltrimethylammonium, TEA[+] = Tetraethylammonium, AMCE complex = Alkali metal-crown ether complex, TPA[+] = Tetrapropylammonium, DMDMP[+] = N,N-dimethyl-3,5-dimethylpiperidinium, TEP = Tetraethylphosphonium, MMPI[+] = 2,6-methyl-N-methylpyridinium, 123TMI[+] = 1,2,3-trimethylimidazolium, 1235TMI[+] = 1,2,3,5-tetramethylimidazolium, 12345PMI[+] = 1,2,3,4,5-pentamethylimidazolium, DMP[+] = N,N-diethyl-2,6-dimethylpiperidine, DBCOB[2+] = 1,4-bis(1,4-diazabicyclo[2.2.2]octane)butyl dihydroxide

The success of commercially accessible FAU as source material for IZC can also be related to its intrinsic properties rather than its low framework density. Often, steamed and acid treated zeolites (US-Y) are used. These imperfect structures with larger external surfaces may be more inclined to dissolve,[137] since source dissolution is often an important prerequisite for further successful synthesis. Boruntea *et al.* (2019) postulated that a specific Si/Al (Si/Al=5.5-8.5) related to matching lattice parameters of dissolving FAU is required for SSZ-39 nucleation. Likely, specific intermediates with the correct 'lattice parameters' are crucial species to stir (heterogeneous) nucleation of SSZ-39 in the latter case.[120]

Like FD, 'structural similarity' is often invoked as key to a successful crystallization by IZC. Phase selectivity is sometimes thought to be guided by common building units (CBUs, *e.g.* double-6-rings). There may be a synergy between the disruption of the starting precursor into locally-ordered fragments and the simultaneous reassembly of these fragments into new topologies.[115,123,138] The potential role of units with 'structural similarity' has been extensively discussed by many research groups.[60,109,139] To this day, it is hard to proof the existence of these species of subunit cell size, especially under real synthesis conditions with observation *in situ*.[109] Table 3 lists many IZC syntheses (Table 3, entries 2-3, 5, 7, 9-12) that have little structural similarity. For example, suitable (kinetically fast) synthesis conditions allow MFI-to-CHA IZC (Table 3, entry 12), two structures with no CBUs. In OSDA-based IZC, strong ODSA-framework interactions are most likely the dominant factor in phase selectivity.[136] Additionally, Devos *et al.* (2020) also discovered the effects of Al- concentrations and growth modes on the Al-distribution and the whole IZC process, during the FAU-to-CHA IZC crystallization.[14] Perhaps the speciation of Al through the intermediate stages (concentrated in remaining amorphous solids, or in ring like structures?[140]) plays a crucial role in phase selectivity and crystallization.

Very recently, FAU-to-MOR IZC (with MFI as intermediate metastable phase) has been reported (without the use of OSDA).[141] None of these structures have common building blocks and the MFI-to-MOR transformation is one from a denser to more open structure. This nicely points out that simple or numerical parameters (framework density or structure similarity) are not adequate to explain the complex processes related to successful IZC crystallization: the kinetics and solubilities along the way matter more.

In short, IZC is a useful method for fast and selective synthesis of certain valuable topologies (*e.g.* CHA, AEI). Despite more expensive - but often very pure - source materials, the starting parents as well as the synthesis conditions can be tuned to obtain zeolite products with unprecedented physico-chemical properties and certain advantages. In general, IZC seems to benefit from fast nucleation, although understanding the underlying mechanisms is not an easy task. Novel or more profound insights here could accelerate zeolite catalyst designs for specific reactions.[14]

Charge Density Mismatch (CDM). Next to non-conventional Si and Al precursors, some protocols that employ charge-based effects of the organic templates in a distinct way are highlighted. Since the first use of alkylammonium species by Barrer and Denny in the 1960s, OSDAs have been widely adopted.[142] Generally, the purpose of introducing OSDAs into the synthesis gel is to prepare zeolites with higher Si/Al ratios and to enhance the structural stability.[143] Generally, less charge is added per volume for an OSDA (*e.g.* reflected in the C/N ratio for a quaternary ammonium) than for an alkali SDA (*e.g.* a hydrated cation).[142,143] However, the design and preparation of specific organics - a conventional ingredient-based strategy for zeolite discovery - especially those with complicated motives can be time-consuming, costly and hard to scale-up.[39]

Table 4. Zeolites synthesized *via* CDM strategy and the Si/Al ratios in the target zeolites.

Entry	Target zeolites	Initial SDA	Crystal inducing SDA	Si/Al ratios
1 [144]	UZM-4 (BPH)	TEA+	TMA+ and Li+	1.8-2.7
2 [145]		Choline+	Li+ and Sr²+	
3 [144]	UZM-5 (UFI)	TEA+	TMA+	5.2-7.0
4 [146–148]		TEA+	TMA+ and Na+	
5 [146,148]	UZM-9 (LTA)	TEA+	TMA+ and Na+	2.6-3.0
6 [149]	UZM-12 (ERI)	TEA+	[R-Diquat+]ᵃ and K+	5.6-7.3
7 [150]		TEA+ and HM+ᵇ	K+ and Na+	
8 [145,150]	UZM-22 (MEI)	Choline+	Li+ and Sr²+	4.0-5.1
9 [150]		Choline+	Rb+ and Sr²+	
10 [150]		Choline+	Cs+ and Sr²+	
11 [148,150]	Offretite (OFF)	TEA+	TMA+ and K+	2.6-3.3
12 [148,150]		TEA+	TMA+, Na+ and K+	
13 [150]	EU-1 (EUO)	TEA+ and HM+ᵇ	Li+	15.5
14 [150]	Merlinoite (MER)	TEA+ and TMA+	Rb+ and K+	2.6
15 [151]	Beta (BEA)	TEA+	TMA+ and Na+	8.1
16 [152]	CHA	TMAda+	TMA+	8.3-10.9

ᵃ [R-Diquat+] refers to a series of diquaternary cations; ᵇ HM+ refers to hexamethonium cation. Other abbreviations, see Table 3.

UOP researchers have developed the CDM approach in order to promote the cooperation between different simple organic templates and hence circumvent or avoid the adoption of complicated ones for new topology discovery.[153] In a typical CDM protocol, the initial synthesis gel is created from a positively charged OSDA, denoted as the initial OSDA, and an aluminosilicate precursor. Because of the mismatch between the low charge density in the initial OSDA and the higher one in the aluminosilicate framework that is expected to be formed, the synthesis gel can neither be crystallized (needs Coulombic stabilization of the charged framework) nor condensed.[146,154] In this case, a small amount of second OSDA with high charge density, often designated as the crystallization-inducing OSDA, is then added in order to overcome the crystallization barrier in the synthesis gel and trigger the condensation. Neither the initial nor the subsequent OSDA can guide the formation of the target zeolite independently, and thus synergy or 'collaboration' is required (or found) between the different OSDAs. Taking UZM-5 (UFI) as an example (Table 4, entry 4), the initial Si/Al ratio in the reactant mixture is 8, which corresponds to the framework charge density (= $-Al/(Si/Al)$) of -0.11. Meanwhile, the TEA$^+$/Al ratio therein is only 8, which gives the cation charge density. By virtue of additional (TMA$^+$ and Na$^+$) and heating, the charge densities of the solid and solution products could be diverged to different degrees, which subsequently realizes better match between the framework charge density and cation charge density in solid phase, stimulating zeolite crystallization.[146] Following this strategy, other zeolites with interesting topologies and properties such as UZM-4 (BPH), UZM-9 (LTA), UZM-12 (ERI), UZM-22 (MEI), offretite (OFF) and EU-1 (EUO) could be synthesized (Table 4). It is noteworthy that the inducing SDAs can either be an organic cation, an alkaline metal cation or even a combination of them.

Free radicals-assisted synthesis. Conventional hydrothermal synthesis often takes multiple days (weeks). Therefore, raw resources (*e.g.* Si and Al species, solvent and mineralizing agent) are frequently screened in order to shorten synthesis times. Recently, the mineralizing effect of free radicals, especially the hydroxyl free radical (·OH), was discovered. These can accelerate nucleation during synthesis when they are present on top of the classic mineralizer. This free radical-assisted protocol can also be used to incorporate specific heteroatoms into certain zeolite frameworks, hardly realized otherwise.

J. Yu and co-workers pioneered and systematically investigated the involvement of hydroxyl free radicals (·OH) in the hydrothermal synthesis of zeolites, with radicals generated by ultraviolet irradiation of a Fenton reagent.[155] Associating the crystallization processes with the concentration of the ·OH, they found that nucleation of Na-A (LTA), Na-X (FAU), NaZ-21 (LTN) and silicate-1 (MFI) zeolites could be accelerated *via* the introduction of ·OH (Figure 5 A and B *vs.* C).

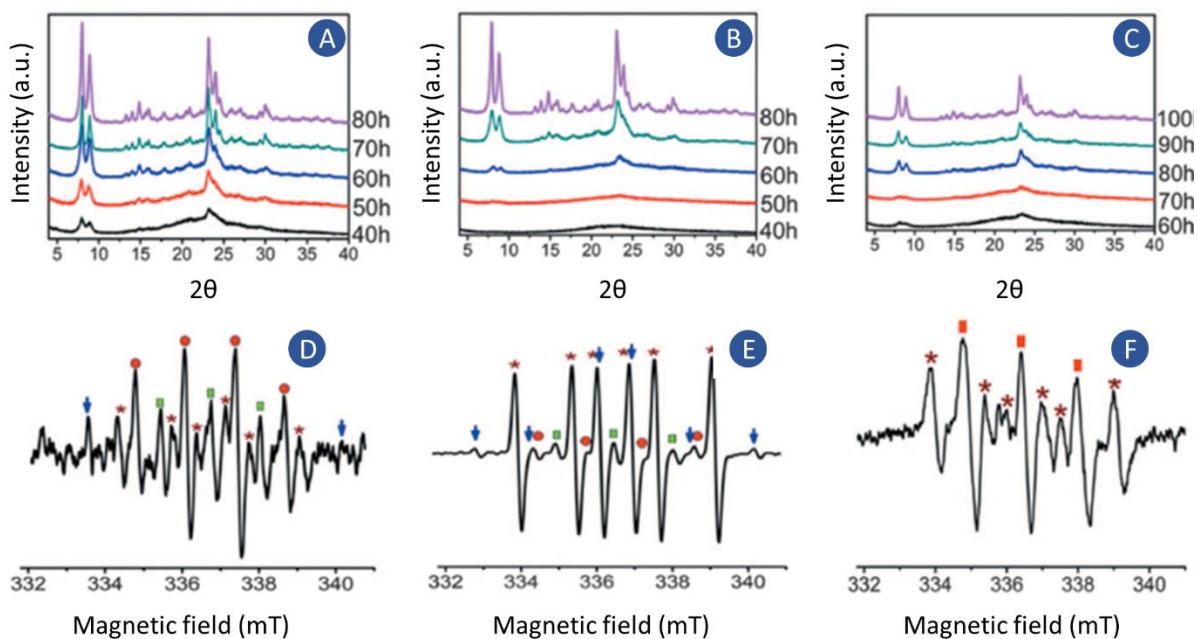**Figure 5**. Acceleration processes by ·OH radicals for the crystallization of silicalite-1 (MFI) at 343 K: (A.) Fenton conditions, (B.) UV conditions (4.0 mW . cm^{-2}), and (C.) dark conditions. EPR spectra of the TPA$^+$OH-TEOS-H$_2$O systems under (D.) Fenton conditions, (E.) UV conditions (4.0 mW . cm^{-2}), and (F.) dark conditions. The EPR signals are recorded *in situ* and marked as followed: ·OH = red circles, oxidized 5,5-dimethylpyrroline-N-oxide (spin trapping agent) radicals = green rectangles, silicon-based radicals = blue arrows, ethanol radicals = asterisks, oxidized 5-tert-butoxycarbonyl-5-methyl-1-pyrroline-N-oxide (spin trapping agent) radicals = red rectangles. From Feng, G.; Cheng, P.; Yan, W.; Boronat, M.; Li, X.; Su, J.; Wang, J.; Li, Y.; Corma, A.; Xu, R.; Yu, J. Accelerated Crystallization of Zeolites via Hydroxyl Free Radicals. *Science* 2016, 351 (6278), 1188–1192.[155] Reprinted with permission from AAAS.

Theoretical calculations further suggested that the ·OH radical is superior to the OH⁻ anion *via* a much lower activation energy barrier. This lower barrier would significantly affect the breaking of Si-O-Si bonds, the depolymerisation of the gel as well as the reassembly of new Si-O-Si bonds, especially in the most energy-demanding nucleation step.[155] Among different topologies, great attention has been paid to the radical promotor effect of sodium persulfate for silicate-1 (MFI) synthesis. Compared to the conventional hydrothermal method, both the synthesis period and the template consumption could be reduced with a small addition of sodium persulfate, while all the other reaction conditions were kept constant.[156] The UV-system can be considered a physical approach as well.

Free radicals could also be employed in the synthesis of mesoporous materials, as shown in a facile and acid-free protocol to directly prepare ordered mesoporous silica SBA-15 and [Fe]-SBA-15. The hydrothermal preparation of ordered SBA-15 frequently requires the addition of acid (*e.g.* HCl) to hydrolyze and condense silica species.[157] However, when the ·OH radicals are introduced both the hydrolysis and condensation processes could be facilitated, promoting the synthesis efficiency.[158] Moreover, up to 50% of the iron loading could be readily incorporated into the SBA-15 structure in this manner.[158] Without any acid addition to the system, safety issues and environmental concerns seem simultaneously tackled. In this respect, the impact of additional radical-generation reagents should off course be considered.

Apart from the more "traditional" radical promoters (UV irradiation and Fenton reactions), free radicals were also proven to originate from zeolite crystals that are milled and heated. In the work of Cheng *et al.* (2019), NaA (LTA) and silicate-1 (MFI) could both be made in a shorter period by the addition of those radicalized seeds. Comparing the XRD patterns of the milled and heated seeds to the normal ones, much weaker intensity was observed in the radicalized seeds, which was anticipated to be related to the disassembly of the ordered structure.[159] However, the disruption of the structure may also be responsible for the generation of surface silicon-based radicals (Si-O·) resulting from homolytic bond breaking[160–163], later confirmed by electron paramagnetic resonance. These radicals are said to further react with H_2O to form hydroxyl free radicals (·OH) and then boost zeolite crystallization.[159]

Finally, ·OH radicals have also been adopted in the stabilization of extra-large-pore zeolites, inspired by their positive role in the cleavage and restructuring of Si-O-Si. Germanium is frequently used to facilitate the construction of extra-large-pore structures. However, Ge-O bonds suffer severely from structural degradation *via* hydrolysis in the presence of moisture, which necessitates a mild post-treatment for Ge-removal. Shi *et al.* (2019) reported a facile post-treatment route in this context to prepare a highly siliceous and ultrastable 14 MR [Ti]-UTL zeolite by

the introduction of ·OH aiding in the hydrolysis and isomorphous substitution reactions.[164] The final catalysts showed excellent activity for oxidative desulfurization.

CHANGING THE PHYSICAL ENVIRONMENT

In the following sections, non-conventional techniques will be discussed that change the physical environment during synthesis, *i.e.* not the type of ingredients but the way in which these ingredients are treated. Within this group, five subtopics will be discussed: *(i)* temperature sequence/programs *(ii)* mode of agitation, *(iii)* semi-continuous or continuous set-up, *(iv)* microwaves and *(v)* ultrasound (overview in Figure 6). Temperature and agitation encompass minor adjustments to the conventional conditions: *e.g.* often, static or tumbling modes are considered a standard for small scale batches. These parameters will mainly influence the final zeolite properties (*e.g.* phase, crystal shape and size). In contrast, the usage of other reactor set-ups or the usage of microwaves or ultrasounds often aims to bring more (or in a different way) energy into the system, thus shortening the total synthesis time (*e.g.* to the order of minutes). Note: during the revision of this work, Wakihara *et al.* (2020) published an exploration of external extremely high pressures (up to 800 MPa) for zeolite synthesis.[165] Acceleration but also selectivity shifts were noted, indicating that both kinetic and thermodynamic aspects of zeolite crystallization were impacted by pressure. This mode can be seen as a new subfield in non-conventional synthesis via physical modifications (not in Fig. 6).[165]

Temperature sequence. Temperature is normally kept constant – excluding heating and cooling phases – during hydrothermal synthesis. In some cases, higher temperatures (> 473 K) are applied in order to shorten the synthesis drastically, but then (sometimes) special attention needs to be paid to OSDA-degradation (*e.g. via* Hofmann) and a higher operating pressure. Typically, solvent-free approaches are performed at higher temperatures[166] (see hybrid strategies section) while certain solvents also need or allow higher temperature (see Table 2). Nevertheless, only applying higher temperatures is fully in line with the conventional way of working and thus not discussed in this review. In contrast, temperature variations during synthesis can exert influence in different ways. In some approaches, a gradual temperature increase during synthesis (*e.g.* two-stage varying temperature crystallization) is programed, but also examples with intermediate cooling are reported. The rationale here is typically twofold: *(i)* control over the crystal size, as small crystals with a narrow distribution are often preferred, and *(ii)* to shorten long syntheses.

In the work of Li *et al.* (1999), silicalite-1 (pure silica MFI), was synthesized *via* a two-step temperature profile (starting at 333 K and ending at 373 K), leading to interesting insights into nucleation. It could be concluded that the first stage (lowest temperature) was responsible for a higher nuclei concentration, *i.e.* higher number and thus a lower average crystal size, while the second stage at higher temperature (after completing nucleation) resulted in a

faster growth of the crystals. By using this two-stage synthesis, small silicalite-1 crystals were obtained in high yield after a shorter synthesis.[167] Sun *et al.* (2000) came to similar conclusions synthesizing [Fe]-MFI *via* a two-stage strategy. The lower temperature (393 K) resulted in a much higher number of crystals and thus ultimately smaller sizes after completing growth at 443 K: ± 300 nm instead of ± 4000 nm in case of a single stage at 443 K.[168]

In line with these MFI findings in presence of OSDA, Sang *et al.* (2006) reported the synthesis of a NaY (FAU),

typically without OSDA, comparing a conventional hydrothermal synthesis and a non-isothermal route. A two-stage temperature program (24 h at 313 K followed by 48 h at 333 K) was applied to the precursor mixture. In this way smaller crystals (diameter of 0.4 μm instead of 0.8 μm) with a more narrow distribution are obtained in comparison with isothermal syntheses at 313 K or 333 K. The lower temperature stimulates nucleation, with growth takes place at the high temperature stage.[169] This does not mean that nucleation and crystal growth are always separate processes with a strict consecutive occurrence for all crystals.[170]
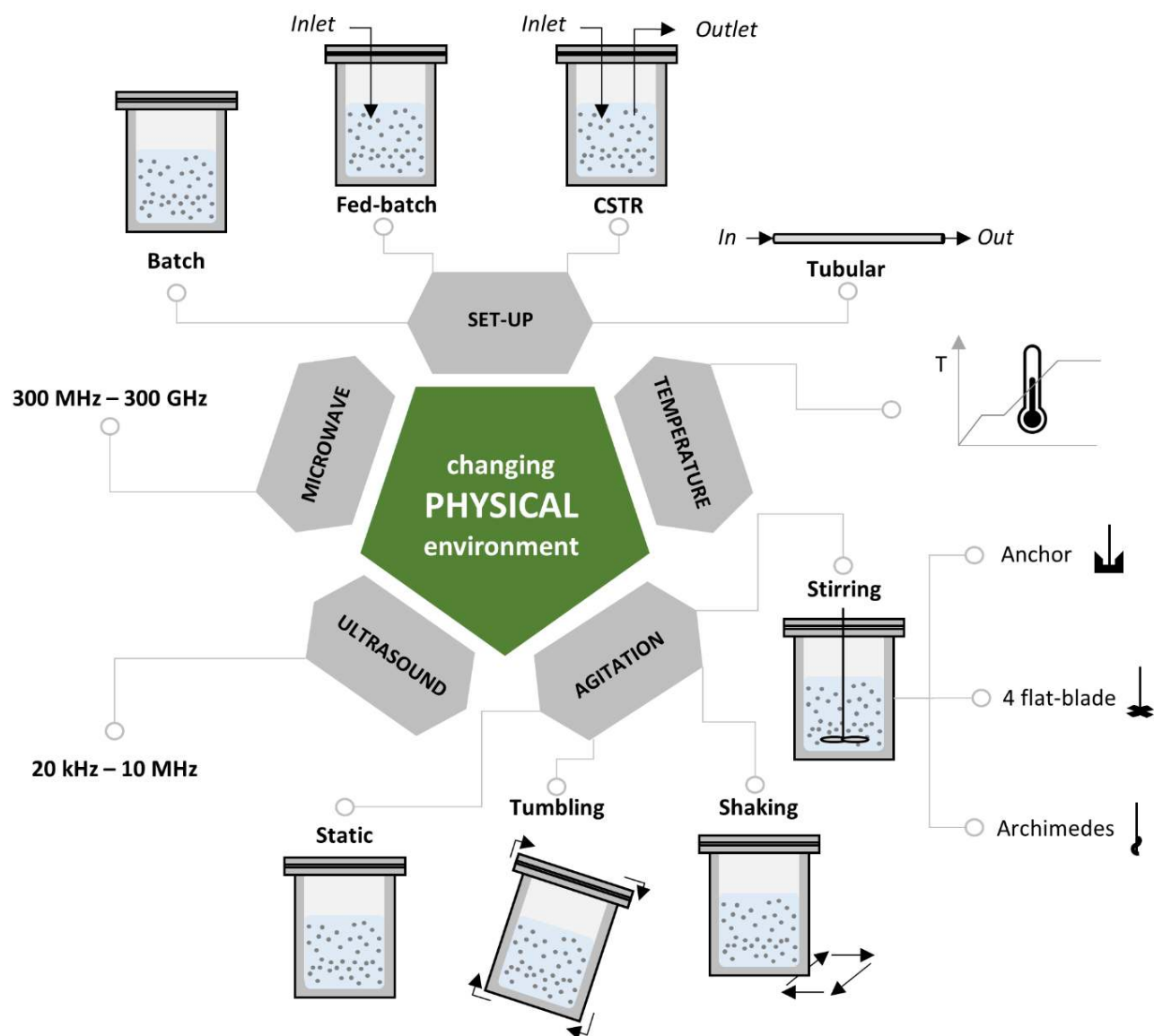

Figure 6. Schematic representation of the non-conventional strategies that change the physical environment during zeolite synthesis: *(i)* temperature sequence, *(ii)* agitation, *(iii)* semi-continuous or continuous set-up, *(iv)* microwaves and *(v)* ultrasound.

The influence of a multi-step temperature program on coal fly ash synthesis of zeolite 4A was also mapped. 4A is an LTA zeolite that is exchanged with Na^+, resulting in 8MR pore openings of ca. 4Å, while the ash is waste from power plants that can be used as Si- and Al-source. Hui *et al.* (2006) applied a temperature program of 1.5 h at 363 K followed by 1 h at 368 K instead of 5 h at 363 K again obtaining smaller particle size with a narrower distribution and a reduction of the synthesis time.[171] Yin *et al.* (2016) also claimed the twofold beneficial effect of the two temperature stage strategy for zeolite T (ERI-OFF) leading to smaller crystals with higher crystallinity in 4 days instead of 7.[172] In the case of MCM-22 (MWW), using rice husk as Si-resource, the synthesis period was said to be shortened with a three-stage strategy (aging at 323 K, synthesis at 373 K and 423 K) for a total of 3 days.[173] This was compared to the MCM-22 made by Güray *et al.* (1999), seen as some kind of reference, which was synthesized after 9 days at 423 K (pre-aged at 318 K) and with silicic acid (instead of rice husk).[174] Since one of the zeolite ingredients is different, conclusions about temperature effects are hard to draw.

Note that in these 'faster synthesis' approaches the conditions of control syntheses used to benchmark alleged improvements are crucial. Often, isothermal faster syntheses could also be possible (or exist in the art) using (slightly) higher temperature or different ingredients. In zeolite synthesis, where reproducibility is a challenge, a reference system, especially when assessing synthesis times based on (physical) reactor-approaches, should be performed in the same set-up, by the same authors and with exactly the same ingredients. Preferably, a benchmark is selected from the current state-of-the-art in terms of efficiency (i.e. short synthesis time, low energy, limited consumption of ingredients, high yield, *etc.*). Using multiple benchmarks would even be better.

Temperature profiles have also been applied for zeotypes with heteroatoms other than (or additional to) Si and Al. SAPO-34 (CHA) is the most encountered material in temperature variation research, because of its prominence as a catalyst for MTO. MTO has received increasing attention in the light of replacing current fossil-based routes for olefin production, such as light naphtha cracking.[32,175] Wang *et al.* (2013) reported the two-step crystallization of SAPO-34 with TEAOH as SDA, starting for 4 h at 403 K followed by 10 h at 453 K instead of 14 h at 453 K. Important to note is that the best material was obtained through removal of the remaining supernatant from the solid after the first stage, after which the solid was redispersed in deionized water for the second step at 453 K. While the shape of the crystals and the elemental composition is more or less equal when comparing to an isothermal sample, the two-step temperature strategy led to smaller crystal sizes (160 nm *vs.* 1100 nm), a slight increase in total surface area (30%), an enormous increase in external surface area (4.5 times more) and a doubling of the total pore volume. These effects were also present, but less pronounced in the two-step crystallization case without removal of the supernatant. Finally, the authors linked all these findings to an increase in the catalytic lifetime of the smaller crystals (596 min *vs.* 184 min), less coke formation and the lowest coke deposition rate. Using this material, olefin diffusion is likely more efficient leading to less heavy coke products.[176]

In the footsteps of this work, other research groups succeeded in reducing the crystal size of SAPO-34 by means of an advanced temperature program, for longer MTO catalyst lifetimes. The unique thing about the work of Guo *et al.* (2017) and Luo *et al.* (2018), both working with TEA as OSDA (but with slightly different procedures and Si-sources), is that cooling step(s) are introduced in the middle of the temperature sequence. According to the authors, this influences the nucleation in a positive way while inhibiting crystal growth. Although the general trend with regard to lower sizes and catalyst lifetimes is more or less equal, the influence on other properties seem to be minor or case-dependent. Besides, when considering any method, it is important to pay attention to the synthesis yields. For instance, yields in the work of Luo *et al.* were higher (>60%, and 45% for the isothermal synthesis) in comparison with those of Guo *et al.* (<30%).[177,178]

Recently, Bakhtiar *et al.* (2019) also reported the beneficial effect of a two-step hydrothermal synthesis of SAPO-34 (12 h at 473 K – cooling down to 293 K – 12 h at 473 K). Herein, the addition of extra morpholine (OSDA), prior to the second stage at 473 K, was said to further benefit the control over the crystal size *via* a degradation – recrystallization mechanism. Off course, decoupling the effects or interplay of adding an exotic organic and temperature variations should be carefully assessed. Summarized, the most complex synthesis procedure, in comparison with the convenient way of working (24 h at 473 K without addition of extra morpholine) led, in addition to smaller crystals (± 1 *vs.* ± 10 µm) and a longer catalyst lifetime, to higher surface area (545 *vs.* 293 $m^2 . g^{-1}$), micropore volume (0.25 *vs.* 0.13 $cm^3 . g^{-1}$) and acidity (234 *vs.* 139 $µmol . g^{-1}$).[179] Again, the convenient way of working here, used for comparison, seems suboptimal, as usually, micropore volumes in the region of 0.21 $cm^3 . g^{-1}$ are measured for a mature SAPO-34 (and not 0.13 $cm^3 . g^{-1}$).[180]

In a nutshell, a tailor-made temperature program is often chosen to limit the crystal size, shorten the synthesis time, and in the case of MTO chemistry, extend the catalytic lifetime[181] of the resulting materials. With regard to the other properties (acidity, porosity, crystallinity, *etc.*) different, sometimes contradictory, effects are observed and the 'usual or isothermal condition' control is often not the best found in literature. This implies that there is room to study the "temperature effect" in a more systematic way, given a critical benchmark and ample cross-control experiments. Since the rate of heating and cooling (and even the overshoot) in Teflon lined batch reactors in a convection or static air oven, can be quite hard to predict, *in situ* temperature measurements, or at least simulated profiles, are required in our opinion. Interesting examples are the usage of thermocouples in the work of Gharibeh *et al.* (2009) in combination with the use of microwaves[182] or the comparison between a tubular and a batch reactor (Figure 8)[183] in the work of Liu *et al.* (2014). The temperature control method holds promise to shorten synthesis times or affect

the purity/selectivity considerably. Careful controls and clever design of experiment are a must. With regard to the selectivity, Xu *et al.* (2012) highlighted the usage of a two-step temperature strategy, starting at 433 K and ending at 473 K, in order to suppress the formation of SAPO-5 and stimulate the synthesis of SAPO-47.[184]

Mode of agitation. The way in which the precursor solution is mixed during hydrothermal synthesis can play an important role for the final material characteristics and its kinetics of formation. In general, four different agitation strategies are described in literature: *(i)* static, *(ii)* tumbling, *(iii)* shaking or *(iv)* stirring (Figure 6). In the case of static synthesis, no additional mixing is performed on top of the natural diffusion of the various zeolite ingredients and with or without homogenization before the start. Diffusion and Brownian motion (random walk) depends on local gradients, interaction between ingredients and the installed temperature. In the case of tumbling, the entire autoclave undergoes a rotation (often circling around a central axis, i.e. not the middle of the autoclave), which is not the case for shaking. Stirring ensures mixing of the suspension, solution or gel (unless the viscosity is too high) without moving the autoclave. This fourth and last strategy can be performed by means of a stirrer that is magnetically driven or mechanically by an engine at the top of the autoclave. Within the group of (mainly mechanical) stirrers, different types such as anchors and 4-flat blades can be distinguished (Figure 6). Stirrers may serve as a site for heterogeneous nucleation, also in the case of PTFE (Teflon) degradation.[185] PTFE is the most common used material for internal stirrers and as soft material it is susceptible to mechanical deformations.[186] Finally, it is also important to mention that not only the type but also the stirring speed and the timing of stirring[187] can be an important parameter. In general, and similar to temperature variations, the type and the rate of agitation seem to mainly impact crystal sizes.[188]

In 2006, Ding *et al.* demonstrated the effect of agitation, either static in an oven or stirred (60 rpm) in an oil bath, on the synthesis of zeolite beta (BEA) from fumed silica, metallic Al-powder and TEA. During this study, special attention was paid to the relationship between the TEA/SiO₂ ratio and the agitation. If the TEA/SiO₂ molar ratio was high (here: 0.6 instead of <0.4), the influence of stirring was more pronounced, resulting in a smaller particle size (30 *vs.* 100 nm), a shorter induction period and a lower product SiO_2/Al_2O_3 ratio (31.6 *vs.* 38.8) in contrast to static conditions. To rationalize these observations, the authors used the solution phase nucleation mechanism: when the amount of TEA(OH) and thus basicity is high, the dissolution of the amorphous phase, required in order to form basic structures (nuclei) that are able to grow further, is efficient. This dissolution is restricted or less pronounced under static conditions, resulting in a longer induction and bigger particle size. At lower TEA/SiO₂, the dissolution rate from the amorphous gel as well as the amount of available SDA becomes lower resulting in a more restricted number of nuclei in any case (static or stirred).[189]

Another interesting investigation, by Bohström *et al.* (2014) compared static, tumbled and stirred syntheses of CHA zeolites. A small point of criticism in relation to this work is that the Al-source, in addition to the Si-source (TEOS) and TMAdaOH, is unclearly described as an "Aluminum hydrate", which can correspond to different forms of Aluminum. When focusing on minute variations in agitation or physical adaptation to conventional DOFs, ingredients must be rigorously defined in order to allow future comparison. Synthesis was performed at 433 K under tumbling or stirring (presumably magnetic), with rates of 35 or 750 rpm respectively. Two remarkable differences could be noticed when following crystallinity and particle size in function of time. First, nearly 100% crystallinity was already obtained after 24 h in a static or tumbled hydrothermal synthesis, while 72 h was required when stirring. Secondly, the particle size changed according to the type of agitation (Figure 7):

Static [2.2 μm] > Tumbling [1.8 μm] > Stirring [1.1 μm]

According to the authors, these three strategies lead to different shear and fluctuating forces, interrupting primary aggregates differently and resulting in the smallest sizes in the case of stirring. Line broadening, ascribed to a slightly less ordered structure, was observed in ^{27}Al and ^{29}Si MAS NMR of the calcined crystalline samples for the static and tumbling case in comparison to the stirred case (all three cases synthesized for 96 h at 433 K).[190] Zhan *et al.* (2002) also investigated the influence of these agitation modes,
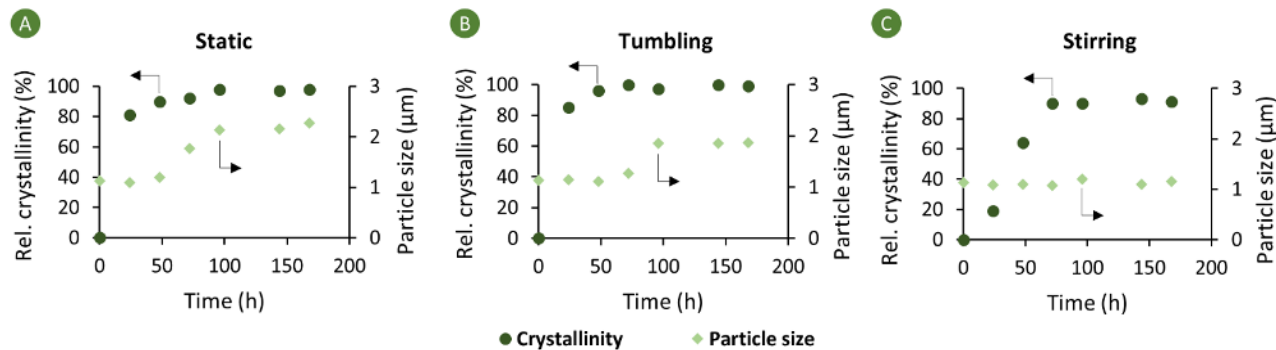
Figure 7. Comparison between three different modes of agitation for the hydrothermal synthesis of CHA zeolites: (A.) static, (B.) tumbling and (C.) stirring. For all modes, the crystallinity (primary y-axis) as well as the particle size (secondary y-axis) is presented in function of the synthesis time. The relative crystallinity is based on PXRD areas against those of the highest crystalline sample. The particle size is measured *via* dynamic light scattering. Prepared with data from the work of Bohström *et al.* (2014)[190].

on the synthesis of NaX (FAU). Although the temperature profile was not identical for all strategies, the biggest crystals (± 1 μm) seemed to form without stirring or shaking. The smallest zeolite crystals were obtained by stirring.[191]

Mainganye *et al.* (2013) investigated the effect of impeller design (4-flat blade, anchor or Archimedes) and stirring rate (150, 200 or 300 rpm) during the aging step of the hydrothermal Na-P1 (GIS) zeolite synthesis. The zeolite was synthesized from fly ash and NaOH with a stirred aging (48 h) at 320 K followed by a static step (48 h) at 413 K. By using the blade impeller (Figure 6), the highest phase purity was obtained. It seems that the solubility of fly ash during the aging is influenced by the type of stirrer and consequently it also influences the final material characteristics. It is important to realize that the type of impeller as well as the synthesis stage in which it is used can be crucial.[192] Remarkably, static syntheses could be accelerated (>50% faster) by quenching and opening the reactor during synthesis and (spatula) stir the substances for 1 min. The effect of this intermediate stirring step was monitored by a number of tests by Okubo and coworkers. Intermediate stirring, it seems, propels growth of existing nuclei, likely by providing macroscopic contact between the (pre-)nuclei and the liquid phase/by releasing nuclei from the solid amorphous phase.[187] Off course, effects of agitation are likely to be more pronounced when starting from more complex or inhomogeneous T-atom precursors. Güray *et al.* (1999) showed that the synthesis of MCM-22 (MWW) was possible under static as well as stirred conditions (during aging and crystallization) if silicic acid was used as Si-source. Remarkably, if silica gel or precipitated Si is used, characterized by a lower specific surface area (*vs.* dry silicic acid), stirring is required in order to obtain MCM-22, suggesting that silica dissolution is a rate-determining step in the crystallization. Again, stirring can be crucial in some cases to bring sufficient ingredients (here: Si) from the amorphous T-atom source in solution.[174]

An intriguing report shows that the selectivity of a synthesis can also be impacted by different types of mixing. Derewinski *et al.* (2004) found that in the case of tumbling (56 rpm) or stirring (400 rpm) the TON zeolite structure was synthesized while under static conditions the MEL structure formed. Important remarks in this respect are that no impurities of the other type (TON in MEL or *vice versa*) were observed and that both structures were synthesized starting from a gel with identical composition. Besides, the synthesis time in case of stirring was considerable shortened compared to tumbling. In an attempt to explain this MEL – TON selectivity, a hypothesis was formulated, taking into account two things. First, the unit cell of MEL is four times larger than the one of TON. Second, supersaturation will mainly take place in the pores of the gel under static conditions (*vs.* in the whole system under stirring) and thus limiting the number of crystals. The size of the crystals, after incorporation of all Si- and Al-species, is thought to be larger with a static system, stimulating MEL (unit cell: 96 T-atoms) instead of TON (unit cell: 24 T-atoms) formation.[193]

Semi-continuous or continuous set-up. An array of reactor types are available in the chemical industry. Figure 6 shows the four most basic types (conceptually). In its greatest simplicity, a reactor design can have no inlet as well as no outlet (batch set-up, filling and then closing a vessel), only an inlet (fed-batch or semi-continuous reactor) or an inlet as well as an outlet stream (continuous stirred tank reactor (CSTR) or plug flow reactor (PFR)). Nevertheless, zeolite synthesis, in contrast to many catalytic processes or large scale (petro)chemical organic reactions, is usually (almost exclusively) done in batch. Both the nature of the crystallization as well as the manageability of these solids and viscous liquids makes it difficult to use a (semi-)continuous set-up. Academically, an estimated >99% of zeolite synthesis reported are performed in closed systems. Industrially, batch reactors for zeolite synthesis also seem prevalent, but there, information on operational types is likely less visible (even in patent applications).[194–201] It is likely that industrial operational knowhow includes fed-batch feeding and temperature profiles. According to Roland (1989) industrial zeolite production is typically running in a semi-continuous way, *e.g.* continuous gel formation followed by crystallization in a batch set-up.[202] For sure, slow synthesis times (*e.g.* two weeks) from the lab cannot be assumed to be valid in large scale batch operations where tricks for faster operation are likely used.

Although (semi-)continuous examples are rather limited in the open art, Okubo, Wakihara and co-workers succeeded in using a tubular reactor with a continuously flowing liquid (in part suspension), effectively resembling a PFR.[40,203,204] The main advantage of this system is shortening the synthesis time, *i.e.* ultrafast zeolite formation in the order of minutes to hours, and its continuous nature, desirable from a large scale perspective. This strategy is often accompanied by higher efficiency in terms of yield, energy and/or material input. In what follows, the most striking examples of this PFR-resembling strategy are highlighted. For a detailed overview, the reader is referred to the comprehensive review of Liu *et al.* (2018) focusing on the tubular system.[205]

The significant differences in synthesis time between the conventional and the tubular method are illustrated in Table 5. An important remark is that in most cases (Table 5, entry 1-9) seeds are used, and thus the (slow) nucleation step is partially bypassed. Besides, an aging step can be required. Nevertheless, the hydrothermal synthesis time is still much shorter than would be expected in the case of standard synthesis and in some cases impossible to recreate in batch, no matter what the ingredient or compositional variation. The main reason is the slow heating step in a batch autoclave, whereas such thermal lag is more or less absent when a tubular reactor with a high surface to volume ratio is used. With regard to this tubular reactor, faster heating is observed if the reactor is placed in an oil bath (mostly conduction) instead of an oven (mostly convection).[205]

One of the first cases was reported for AlPO$_4$-5 (AFI, Table 5, entry 1). A tubular reactor was closed after loading the synthesis gel and thus not used continuously at first.

Based on the data of Liu *et al.* (2014), a temperature profile in function of time is depicted in Figure 8 for the different reactor designs (tubular *vs.* batch autoclave under agitation at 20 rpm).[183] The combination of seeds and the immersion of the tubular reactor in a preheated (463 K) oil bath is required in order to realize the ultrafast synthesis of 1 min for $AlPO_4$-5. In addition, there are also two important remarks, one relating to particle size and another to purity. First, the authors suggest that, in case of a shorter synthesis time, Ostwald ripening during crystal growth can be avoided and thus smaller particles are obtained. Second, VPI-5 (VFI) reflections, despite the usage of AFI seeds, are seen in XRD if the batch autoclave (with a slower heating profile) is used.[183] In general, not the reactor design, but presumably the different temperature profiles, seem to be responsible for the observed differences.
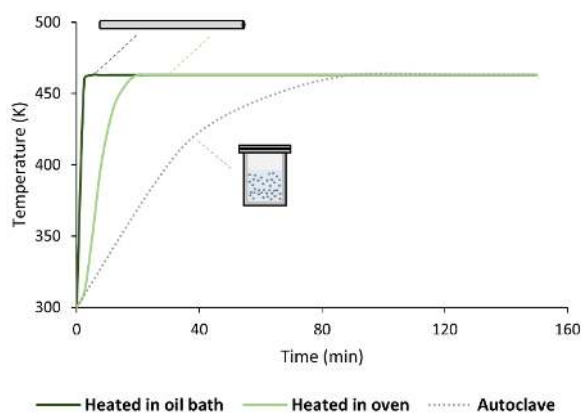
Figure 8. Temperature profiles in time, as measured for a tubular reactor (length: 13.5 cm, inner diameter: 4.4 mm) either heated in oil bath or oven and simulated for a batch autoclave (23 mL). Target temperature was 463 K. Prepared with data from the work of Liu *et al.* (2014)[183].

With regard to AFI, Peng *et al.* (2018), also reported the fast synthesis (1 h) of the pure silica version SSZ-24 (Table 5, entry 2). In contrast, the conventional hydrothermal synthesis in a batch autoclave took 48 h and SSZ-31 (STO) impurities could be observed. The tubular reactor thus offered all kinds of advantages (*e.g.* shorter synthesis time and higher purity). Note however that the fast synthesis was carried out at higher temperature (483 K instead of 423 K) and with a certain, long, aging period (72 h at 368 K). Taking this into account, it is complex to attribute the outcomes to a specific adaptation (aging, temperature, reactor type or a combination of these).[206]

In some examples (mentioned by an asterisk in Table 5), Okubo and co-workers were also able to construct a real continuous flow system, instead of only using a closed tubular reactor).[40,203,204] For instance, a two-stage set-up was designed in order to synthesize SSZ-13 (Table 5, entry 5) in a technical feasible continuous way. Blockage needs to be prevented by diluting the gel in the second stage (and thus decreasing the viscosity at a critical point) and by using an air-driven vibrator. This latter is responsible to ensure homogeneous mixing and to prevent precipitation of solids.

A scheme of this set-up is found in Figure 9, highlighting reactor dimensions and residence times.

For SAPOs, it is remarkable that the tubular reactor (with fast heating) can play an important role in the formation of either SAPO-5 (AFI) or SAPO-34 (CHA). According to the authors, short synthesis times (Table 5, entry 3 *vs.* 4) in combination with clear phase selection would not be possible in a classic batch.[203] In the case of SSZ-13 (Table 5, entry 5), a useful catalyst (in Cu-form) for the reduction of NO_X, the combination of seeds and efficient heat transfer also seems required in order to obtain the right topology (instead of, for instance, MTN) at 483 K in a very short synthesis time. In addition, ultrafast synthesis is often only possible if gibbsite (also used for batch references), in contrast to non-crystalline Al-sources, is used.[40] With regard to the ultrafast beta synthesis (Table 5, entry 8), it is interesting to note that the aging step, prior to the hydrothermal synthesis, can be omitted.[207] In general, final material properties, except for some examples, are often not that different when comparing zeolites from the conventional method with those from ultrafast synthesis.[205]
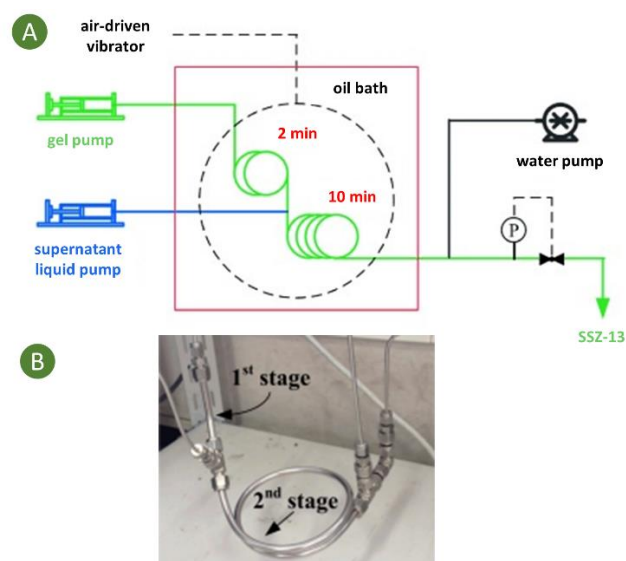
Figure 9. Representation of the continuous flow system, developed by Okubo and co-workers for SSZ-13: (A.) technical scheme for the continuous process, operating at 483 K with a residence time of 2 and 10 min for the first and second stage respectively; (B.) continuous-flow reactor with two stages of stainless steel and with an inner diameter of 4.4 mm. The aged gel is introduced (before the first stage) with a flow of 0.3 mL . min^{-1}. The supernatant liquid is introduced (before the 2nd stage) with a flow of 0.9 mL . min^{-1}. At the end, the obtained product is diluted with water (10 mL . min^{-1}). Adapted with permission from Liu *et al.*[40] Copyright 2015, Wiley-VCH.

The tubular reactor system has also been tried for erionite (ERI) synthesis with a high silica content (Table 5, entry 6). Typically, this material (Si/Al > 5.5) is synthesized *via* the CDM approach (see 'changing the chemical environment and Table 4, entry 7). By using a tubular reactor, Zhu *et al.* (2017) succeeded to shorten the synthesis time

from multiple days to 2 h (Si/Al = 5.5). In addition, the authors also found a better hydrothermal stability, based on degradation curves after hydrothermal aging at 973-1073 for 5 h, for the fast synthesized material *vs.* the CDM one. Besides the reactor system and its operation at a higher temperature (+60 K) in comparison with the CDM approach, changes in the composition of SDAs and the usage of seeds were present, certainly influencing the final outcome (e.g. no use of TPAOH but five times more KOH for the tubular one).[208]

The synthesis time, typically lasting for hours to days (weeks) for conventional batch syntheses, versus minutes to hours for the tubular systems, can be further reduced, to the order of seconds, by directly contacting the precursor mixture with a hot stream in a continuous flow reactor. By doing this, the thermal lag, which is already limited for a continuous tubular set-up, can be further eliminated. Liu *et al.* (2016) reported the ultrafast-synthesis of ZSM-5 zeolite in less than 10 seconds and without the presence of seeds (Table 4, entry 10). After mixing all ingredients and a crucial aging step at 363 K, the precursor stream is mixed with water under pressure at 643 K. Using water as heating medium, this strategy immediately results in a final temperature between 531 K – 573 K. Short residence times during synthesis are needed in order to prevent SDA decomposition as well as to guarantee zeolite stability in a hot water environment. It is important to notice that the aged mixture before flow synthesis was PXRD-amorphous and this aging step will require an additional tank (equipment) at temperature. Besides, it is also crucial that hydrodynamics, as with the above mentioned continuous flow reactor, are properly considered (*e.g.* avoiding blockage). Compared with the conventional set-up, similar material properties were obtained, with the exception of smaller particle sizes for the ultrafast flow synthesis.[204]

Table 5. Synthesis time of different zeolites and zeotypes, using a tubular (sometimes continuous flow*) reactor system. Besides, also the conventional synthesis time (reference time) is listed.

Entry	Material type	Topology	T (K)	P (MPa)	Seeds	Time	Reference time [a]
1 [183]	AlPO$_4$-5	AFI	463	1.4	N Y	>15 min 1 min	>1 h > 20 min
2 [206]	SSZ-24		483	2.1	Y	1 h	48 h (423 K)
3 [203]	SAPO-5*		483	2.1	Y	5 min	/
4 [203]	SAPO-34*	CHA	483	2.1	Y	10 min	/
5 [40]	SSZ-13*		483	2.1	Y	10 min	2 h 8 h (433 K) >3 days (433 K; without seeds)
6 [208]	Erionite	ERI	483	2.1	Y	2 h	5 days (CDM; 423 K; without seeds)
7 [68]	Mordenite	MOR	483	2.1	Y	10 min	8 h (443 K)
8 [207]	beta	BEA	483	2.1	Y	10 min	48 h (433 K)
9 [209]	Silicalite 1	MFI	483	2.1	Y	10 min	/
10 [204]	ZSM-5*		533	23	N	< 10 s	24 h (443 K)
11 [210]	NaA *	LTA	423	0.5	N	16 min	160 min (373 K)

[a] For the reference time, the synthesis time is taken at identical conditions (T, P, presence of seeds) in a batch autoclave. If different, these conditions are mentioned between brackets. * indicates continuous operation (PFR-like).

In addition to the work of Okubo and co-workers, other groups have also investigated the use of a continuous reactor system for the hydrothermal synthesis of zeolites. Ju *et al.* (2006) managed to shorten the crystallization time by a factor of ten approximately for zeolite NaA (LTA) in comparison with a conventional batch. In order to obtain this fast crystallization at 363 – 373 K, a continuous stainless steel capillary reactor (inner diameter of 0.75 mm and length of 1.5 m), placed in an oil batch, was used. During the synthesis, a flow of 0.2 – 0.85 mL . min⁻¹ was installed and related to this the residence time varied from 3.5 to 13.5 min. The authors also warned that aging was required in order to prevent blockage of the reactor.[211] Vandermeersch *et al.* (2016) synthesized zeolite NaA in a similar way by using a continuous flow reactor at 423 K without an aging step. The productivity of the continuous set-up was 160 g . h⁻¹ . (reactor volume)⁻¹, while it was only 33 in the case of batch. Also here the synthesis time could be reduced approximately ten times towards 16 min through an enormous reduction of the thermal lag (Table 5, entry 11). The authors examined that the heating step to 423 K required 68 s in continuous PFR mode while it took 1 – 2 h in an unstirred batch set-up. This seems to be slower in comparison with the batch data of Figure 8, but factors such as reactor volume (here: 80 mL instead of 23 mL), location of measurement (close to the edge or central in the gel/liquid), stirred or not, *etc.* can play an important role. In line with other PFR-type studies for zeolites synthesis, materials with more or less similar properties were obtained.[210]

In addition to systems resembling a PFR, there are a few examples that use a fed-batch system or a CSTR. First, Tassopoulos (1986) made a theoretical *in silico* comparison between a batch and a fed-batch set-up. Interesting differences can be observed if the traditional kinetic curve, representing the crystallinity in function of time, is plotted.

Typically, the induction period τ is longer for a fed-batch (semi-continuous) set-up through a frequent dilution with amorphous unreacted material (fed-batch addition). Also the speed of crystallization, *viz.* the slope towards 100% crystallinity, is lower *via* a lower particle concentration and thus lower available cumulative surface for crystal growth. Important to note is that the crystal size in fed-batch mode is typically larger since new reagents are added step by step (Figure 10).[212]

In line with these simulated results, Tassopoulos *et al.* (1987) investigated the lab synthesis of zeolite A in batch as well as in fed-batch mode. The latter was performed by adding the Si-source as well as the Al-source separately in the reactor vessel *via* a dual peristaltic pump, while synthesis was running at 373 K. As soon as the first reagents were added, the synthesis time started. The main (above mentioned) theoretical findings, such as longer induction period and slower crystallization rate, were confirmed. Besides, this also illustrated that the concentration and the mutual ratios of ingredients can vary significantly between a batch and fed-batch synthesis. Since zeolite synthesis always takes place within strictly controlled conditions, the slightest deviation can already result in a different material. For instance, in addition to zeolite A (LTA), also hydroxysodalite was formed during the fed-batch synthesis, although the input feed composition was identical to the initial batch composition. This seems to point to a role of the different concentration profiles of Si and Al species in the liquid (here higher for fed-batch).[213]
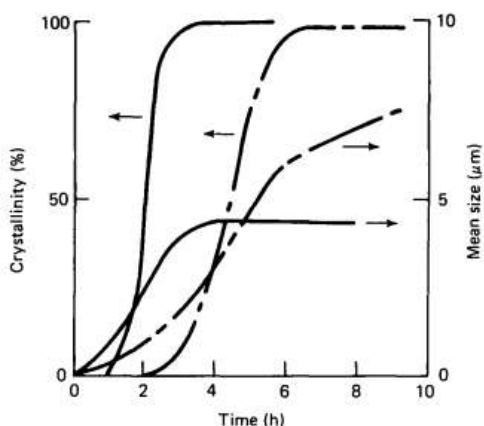

Figure 10. Population balance model simulations of crystallinity and size in time for a batch (full line) and a fed-batch synthesis (dotted). Reprinted from Zeolites, 7 (3), Tassopoulos, M.; Thompson, R. W. Transformation Behaviour of Zeolite A to Hydroxysodalite in Batch and Semi-Batch Crystallizers, 243-248, Copyright (1987), with permission from Elsevier.[213]

Cundy *et al.* (1995) also reported the continuous addition of reagents combined with regular sampling (slurry extraction), in fact resembling a kind of continuous set-up. In other words, products (in this study) were frequently removed in batches at regular intervals, but not in a continuous way (due to low flows). Additionally DOF, according to this research group, are an important advantage in comparison with the batch system: the concentration of reagents can be tuned in function of time and consequently supersaturation, nucleation as well as crystal growth can potentially be controlled more accurately. These (semi-)continuous systems render it possible to obtain information about the fundamental aspects of crystallization. Besides, this system can for instance also be used in order to vary the composition of the material in zones (*e.g.* radial variation of crystal composition in ZSM-5).[214,215]

The above summary suggest that in general, a tubular PFR reactor provides an additional advantage (next to continuous operation) in terms of synthesis time (*cfr.* activity in a chemical reaction), while a fed-batch or CSTR type of operation can influence the final material properties (*cfr.* selectivity in a chemical reaction). In the case of PFR, the thermal lag will be limited through a higher surface/volume ratio. In the case of fed-batch or CSTR, additional DOF are created since reagents can be added at specific times at a certain temperature and with certain dilutions. These findings are strongly in line with the basic principles of reactor engineering (Figure 11).[216] For instance, a PFR is theoretically identical to a batch reactor (in terms of selectivity and kinetics), but it is the length of (i.e. a plug moving along) the tube, instead of the time that determines the degree of conversion (or here the degree of crystallinity; Figure 11). Therefore, it is to be expected (somewhat) that material properties are more or less equal for the PFR vs batch studies, while the synthesis time can vary considerably: the residence time in PFR (V/F in Figure 11), typically operating at higher temperature and/or characterized by a faster heating profile is shorter than batch time). In comparison to a PFR, a CSTR set-up does not have a continuous decrease in concentration (consumption) of amorphous reagents (in the moving plug). Instead of an operating line with varying concentration and increasing conversion for a PFR, ideally a CSTR operates in a point with constant concentration and conversion during reaction/synthesis (Figure 11), in case of ideal mixing and a stable steady state. This difference in concentration (usually more dilute than in a plug) can have an important influence on what type of material (and how) is formed. Depending on the kinetics (and its corresponding order) as well as the type of material synthesis (reaction) steps (isolated (A to B), sequential or competitive formation of certain materials), the choice of the reactor could be decisive in order to obtain the right properties in terms of selectivity (*e.g.* Al content, crystal size) or phase (topology). For example, in a competitive synthesis, where parallel reactions can occur (*e.g.* A to B') or consecutive side-reactions (*e.g.* B to S), it could be recommended to select a CSTR if the order of the desired reaction is lower than that of the competitive one.[216] This hinges on devising (approximating) rate equations for a zeolite synthesis process and its multiple steps, which is not straightforward (not simply 1st order as in Figure 11). Given the limited number of reactor setup-based publications in zeolite synthesis, such hypotheses have not been tested. This theoretic potential of reactor design with respect to changing selectivity, and thus the materials formed, or their intrinsic bulk properties, is currently underexploited.
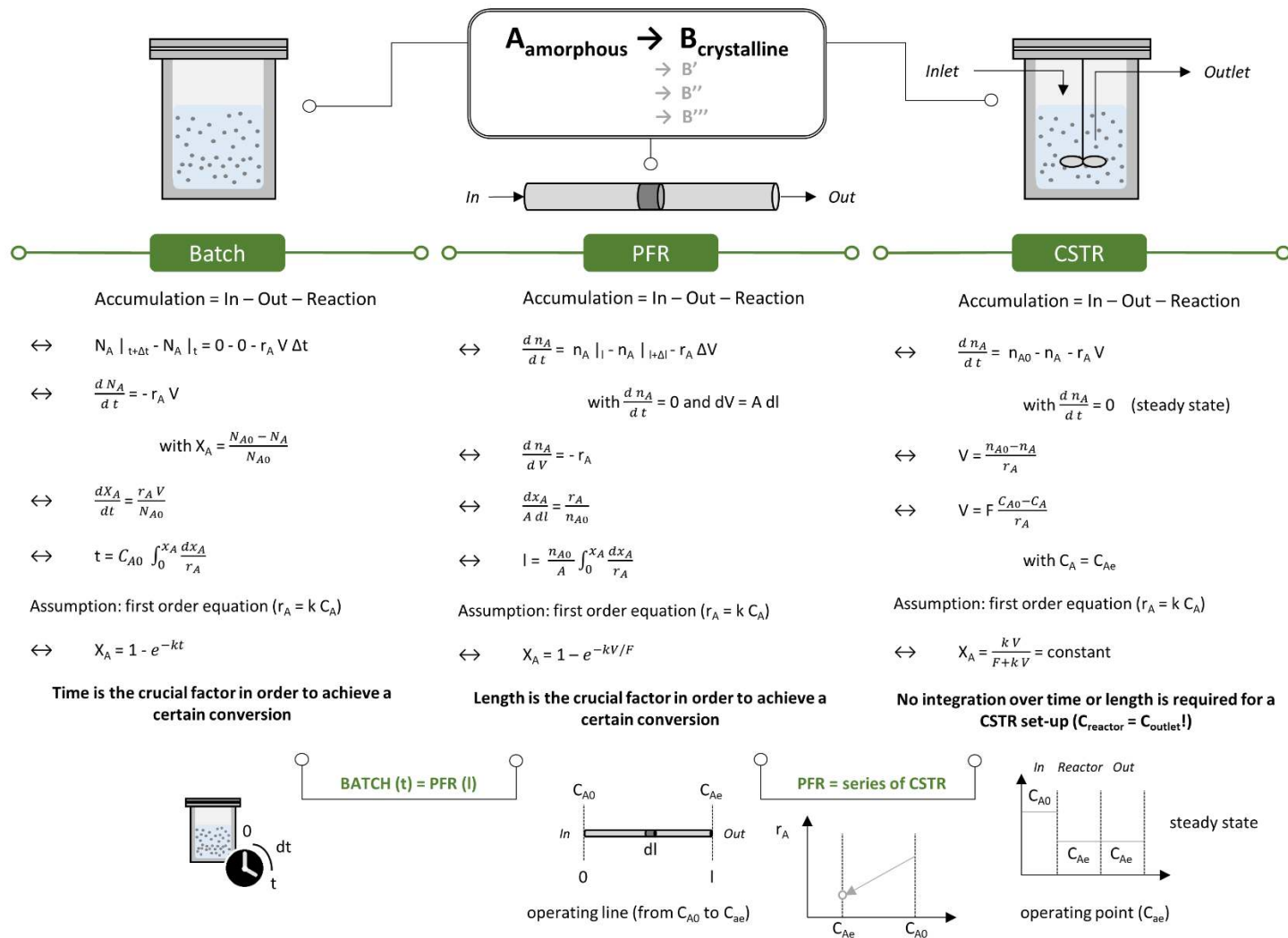
A_amorphous → B_crystalline
$$\rightarrow B'$$
$$\rightarrow B''$$
$$\rightarrow B'''$$

Inlet → ... → *Outlet*

In → ... → *Out*

Batch

Accumulation = In − Out − Reaction

$$\leftrightarrow \quad N_A\,|_{t+\Delta t} - N_A\,|_t = 0 - 0 - r_A V \Delta t$$

$$\leftrightarrow \quad \frac{d N_A}{d t} = - r_A V$$

$$\text{with } X_A = \frac{N_{A0} - N_A}{N_{A0}}$$

$$\leftrightarrow \quad \frac{d X_A}{dt} = \frac{r_A V}{N_{A0}}$$

$$\leftrightarrow \quad t = C_{A0} \int_0^{x_A} \frac{dx_A}{r_A}$$

Assumption: first order equation ($r_A = k\,C_A$)

$$\leftrightarrow \quad X_A = 1 - e^{-kt}$$

Time is the crucial factor in order to achieve a certain conversion

PFR

Accumulation = In − Out − Reaction

$$\leftrightarrow \quad \frac{d n_A}{d t} = n_A\,|_l - n_A\,|_{l+\Delta l} - r_A \Delta V$$

$$\text{with } \frac{d n_A}{d t} = 0 \text{ and } dV = A\,dl$$

$$\leftrightarrow \quad \frac{d n_A}{d V} = - r_A$$

$$\leftrightarrow \quad \frac{dx_A}{A\,dl} = \frac{r_A}{n_{A0}}$$

$$\leftrightarrow \quad l = \frac{n_{A0}}{A} \int_0^{x_A} \frac{dx_A}{r_A}$$

Assumption: first order equation ($r_A = k\,C_A$)

$$\leftrightarrow \quad X_A = 1 - e^{-kV/F}$$

Length is the crucial factor in order to achieve a certain conversion

CSTR

Accumulation = In − Out − Reaction

$$\leftrightarrow \quad \frac{d n_A}{d t} = n_{A0} - n_A - r_A V$$

$$\text{with } \frac{d n_A}{d t} = 0 \quad \text{(steady state)}$$

$$\leftrightarrow \quad V = \frac{n_{A0} - n_A}{r_A}$$

$$\leftrightarrow \quad V = F\,\frac{C_{A0} - C_A}{r_A}$$

$$\text{with } C_A = C_{Ae}$$

Assumption: first order equation ($r_A = k\,C_A$)

$$\leftrightarrow \quad X_A = \frac{k V}{F + k V} = \text{constant}$$

No integration over time or length is required for a CSTR set-up ($C_{reactor} = C_{outlet}$!)

BATCH (t) = PFR (l)

0 ... dt ... t

PFR = series of CSTR

C_{A0} ... C_{Ae}

In ... dl ... *Out*

0 ... l

operating line (from C_{A0} to C_{ae})

r_A ... C_{Ae} ... C_{A0}

In Reactor Out

C_{A0} ... C_{Ae} ... C_{Ae} ... steady state

operating point (C_{ae})

Figure 11. The basic principles of reactor engineering, for the 3 basic reactor designs (batch, PFR and CSTR). Symbols: $N_{A(o)}$ is number of moles of A in the system (o = at start) [mol]; n_A is molar flow rate of A [mol . s⁻¹]; t is time [s]; l is length [m]; A is cross-sectional area [m²]; V is volume of the reactor [m³]; r_A is reaction defined as moles of A disappearing per unit time per unit volume [mol . s⁻¹ . m⁻³]; C_A is the concentration of A [mol . m⁻³]; k is the rate constant [s⁻¹ for a first order]; F is the volumetric flow rate [m³ . s⁻¹]; X_A is the conversion of A [fraction].[216] The exact expressions these equations based on a first order rate are likely too simple for the transformation of liquids into solids (crystallization from gel or liquid)

Microwave-assisted. Microwave-assisted (300 MHz – 300 GHz) hydrothermal synthesis of zeolites is without any doubt the most reported unconventional strategy at this moment. Since employees of the Mobil oil corporation demonstrated the usefulness in 1988 for NaA (LTA) and ZSM-5 (MFI) synthesis[217], many studies for a myriad of zeolites have appeared.[70] In line with a continuous (PFR) reactor, the main driving force to use microwaves is to reduce synthesis time drastically.[205] Tompsett *et al.* (2006) listed several reasons why this technique can provide a more efficient synthesis. Up to this day, the deeper mechanisms (*e.g.* faster heating, creation of hot spots, better solubility of certain species) related to the benefits of microwaves in material synthesis, are sometimes still unclear. Nevertheless, differences in efficiency can, in general, be ascribed to thermal effects, originating from electromagnetic energy that is converted into chaotic motions and thus thermal energy. Furthermore, microwaves and their thermal effects can influence all different crystallization stages, being *(i)* gel formation, and thus the formation of the precursor species, *(ii)* nucleation and/or *(iii)* crystal growth.[218] In addition to shortening synthesis times, microwaves can also lead to a more uniform product (in terms of composition or dimensions) because of faster nucleation or a more uniform growth. Besides, it was also possible to expand the composition of certain materials.[70,218] Table 6 lists a selection of interesting examples.

Different groups have confirmed that the heating phase, *i.e.* the thermal lag, as well as the induction period can be shortened by using microwaves. For instance, Cundy *et al.* (1998) reported that the thermal lag for ZSM-5 (MFI) synthesis was less than 3 min, while it is typically 30 min in conventional synthesis. Katsuki *et al.* (2001) indicated that not only the heating step is faster, but also the kinetics seem to be influenced in a positive way. These faster kinetics could be observed by a (slightly) sharper (S-shape) crystallization curve. In general, a microwave treatment ensures that synthesis time can be shortened by a certain factor, which can go up to 1000 (*e.g.* Table 6, entries 1-4 for zeolite Y (FAU) and ZSM-5 (MFI)).[219-221]

Examples are also documented where it was possible to broaden the Si/Al ratio (*e.g.* up to 5 for zeolite Y (FAU); Table 6, entry 1, by Van Bekkum)[219], to realize successful tetrahedral incorporation of heteroatoms tetrahedrally (*e.g.* Ti in TS-2 (MEL); entry 6)[222] or even to change the phase selectivity (obtaining SAPO-5 (AFI) instead of SAPO-34 (CHA); entry 7)[223]. With regard to the latter, AFI and CHA are known to be competing topologies, and SAPO-5 is transformed into SAPO-34 if a longer crystallization time is used. Remarkably, under microwaves (and for short crystallization times) SAPO-5 synthesis is preferred at the expense of SAPO-34 (Figure 12). This means that synthesis kinetics of these competing/consecutive phases are influenced in another way. This effect was found for 2 different OSDAs. Such examples demonstrate the potential of alternative "non-conventional" conditions to influence, in addition to the *activity*, also the *selectivity* during zeolite synthesis.
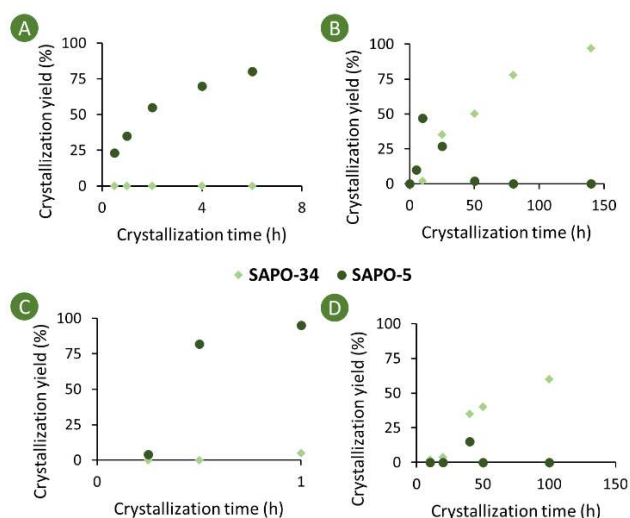
Figure 12. Competitive formation of SAPO-5 (AFI) *vs.* SAPO-34 (CHA) at 473 K using (A.) Microwave irradiation and (B.) Hydrothermal heating in oven, both with TEA OSDA. (C.) Microwave irradiation and (D.) Hydrothermal heating in oven, both with N,N,N,N-Tetraethylethylene diamine as OSDA. Prepared with data from the work of Jhung *et al.* (2003)[223].

In some cases, requirements are linked to the synthetic strategy in order to have success with microwaves. For instance, Slangen *et al.* (1997) discovered that an aging step is necessary for the fast synthesis of NaA (LTA) zeolites[224] and also Chandrasekhar *et al.* (2008), needed a long aging step (20 h) prior to the effective short microwave step of 2 min (Table 6, entry 8).[225] In contrast, Bonaccorsi *et al.* (2003) succeeded in circumventing a long aging, without the formation of impurities, by tailoring the used microwave energy.[226]

In addition to conventional Al- and Si-resources, microwave strategies can also be applied on zeolites synthesis starting from waste such as coal fly ash.[227] For instance, Querol *et al.* (1997) reported similar yields and zeolite types, but the activation time was shortened from 1 or 2 days towards 30 min.[228] Also Anuwattana *et al.* (2008) found an increase in efficiency using microwaves for ZSM-5 (MFI) synthesis from a Si-rich waste product that originates from the melting process of Iron. In addition to a six times faster synthesis, also a ten times reduction in particle size (± 0.3 instead of ± 3 μm) was observed.[229] An important remark is that microwaves do not always have a positive effect on the synthesis time of zeolites. For example, Inada *et al.* (2005) described a slower crystallization of Na-P-1 (GIS) zeolite from coal fly ash under continuous microwave irradiation in comparison with conventional synthesis. Remarkably, using microwaves partially (here, at the early stage: 0 – 15 or 15 -30 min), in the course of conventional heating (2 h in total), resulted in a higher XRD reflection intensity as well as cation exchange capacity (CEC) in comparison with only conventional heating for 2 h (Figure 13). According to the authors, this partial improvement was achieved due to better solubility of SiO_2 and Al_2O_3 from coal fly ash. In contrast, the use of microwave, especially between 45 – 60 min (middle stage) in the course of

conventional heating, caused a delay in zeolite formation since the usual dissolution-reprecipitation mechanism, going from an aluminosilicate gel into a zeolite, is thwarted (retardation of nucleation). The effect of using microwaves during the final step, *i.e.* crystal growth, was said to be negligible compared to only conventional heating.[230]
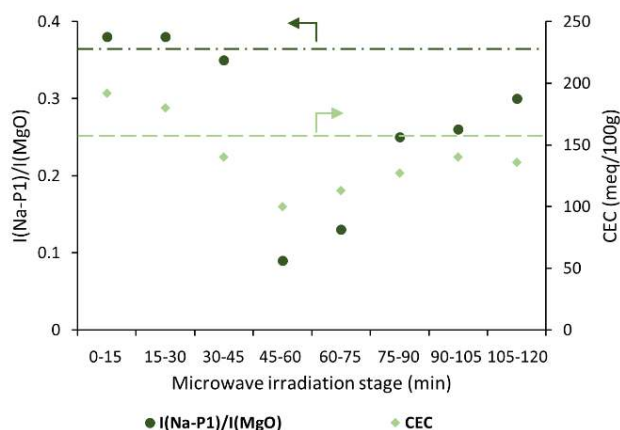

Figure 13. Representation of the XRD peak intensity and cation exchange capacity (CEC) of zeolite Na-P1 (GIS) by using microwave irradiation for 15 min in the course of the conventional heating (total synthesis time of 2 h). In other words, each data point corresponds with a total synthesis time of 2 h, but the timing of using microwaves (always 15 min) is different. The data for 2 h of conventional heating without microwave irradiation is indicated by dotted lines. Prepared with data from the work of Inada *et al.* (2005)[230].

It can be concluded that the synthesis time can be significantly shortened by microwave heating and that in some rare, but fundamentally interesting cases, material properties (*selectivity*) can be influenced. Understanding these effects is complicated. Conner and co-workers emphasized that the effects are extremely case/zeolite-dependent, and that even the choice of the amorphous resource (*e.g.* Si-source: Aerosil 200 *vs.* Ludox AS-40) can have a crucial effect on the observation of microwave benefit (or not). Not only the zeolite type and the ingredients, but also the dimensions of the used reactor can give rise to largely different outcomes. A comparison between a batch reactor with a diameter of 11 mm and a reactor with a diameter of 33 mm resulted in a completely different energy field (and thus heating profile). While a more or less homogeneous field was obtained with the 11 mm one, different minima and maxima, and thus also hot spots, were achieved with the 33 mm reactor. Botch reactors resulted in a faster synthesis in comparison with conventional heating, but the one with the hot spots led to larger uniform crystals (research on silicalite-1 (MFI)). In addition to time and exact location in the reactor (determining the exposure to microwaves), the supplied power can also play an important role. In the case of SAPO-11 (AEL), a non-stop irradiated experiment resulted in larger particles than with a pulse microwave experiment (Table 7, entries 1-3). Besides, the synthesis time as well as the crystal size of SAPO-11 decreased with increasing power (expressed in W, (Table 7, entries 4-6). Remarkably, no differences in synthesis time were observed for silicalite-1 if an average microwave power was changed. Finally, it is important to highlight that pulsed experiments can save energy, as the use of cooling gas in order to use a higher microwave power while keeping temperature constant, consumes energy.[182,231–233]

Ultrasound-assisted. Apart from microwaves, ultrasonic irradiation (20 kHz – 10 MHz) can also be employed during synthesis. According to Askari *et al.* (2013), no complicated facilities are required and this strategy can result in various benefits, *viz.* faster synthesis (*e.g.* shorter induction period and higher crystal growth rate) or better control over material properties (*e.g.* uniform particle size distribution and lower crystal size).[234] The reason for these changes is actually the constant formation, growth and collapse of bubbles (= acoustic cavitation) in the liquid during the exposure to ultrasonic energy. This is thought to finally result in better mixing, higher solubility of species, faster nucleation and/or faster crystal growth.[235–237]

Andac et al were among the first to study the effect of so called sonochemistry in zeolite synthesis.[238] LTA synthesis was studied from clear solutions, noting increased nucleation and crystallization rates and improved yields and particle size distribution. They also noted an effect on selectivity (LTA vs X vs …), relating this to changes to the relative rates of nucleation and crystal growth of the competing zeolites.[238]

In comparison with microwaves, ultrasounds are often used during the aging step prior to the effective hydrothermal crystallization. Wu *et al.* (2008) investigated the effect of different aging strategies: *i.e.* microwave-assisted, ultrasound-assisted, stirred aging and without aging. By doing this and simultaneously using different Si-sources (TEOS

Table 6. Synthesis time of different zeolite and zeotypes, using microwaves during hydrothermal synthesis.

Entry	Material	Top.	T (K)	Synthesis time	Benefits/Remarks
1 [219]	Y	FAU	393 + 373	30 s (reach 393 K) + 10 min (@ 373 K)	conventional synthesis takes > 10 h; widening the Si/Al ratio (up to 5); no other crystalline phases
2 [221]	Y		373	2 h	synthesis time is 3-4 times faster in comparison with conventional synthesis
3 [219]	ZSM-5	MFI	413	30 min	conventional synthesis (@ 453 K) takes several days; fast quaternary ammonium SDA degradation through microwaves; prismatic shape instead of conventional cubic shape
4 [220]	ZSM-5		448	3 h	conventional synthesis (@ 448 K) takes 5.5 h; the effects of seeds, SDA and microwaves are visualized *via* crystallization curves.
5 [239]	Beta	BEA	423	4 h	conventional synthesis takes several days; in addition to microwaves, also the presence of fluoride species (as well as seeds) seems to be required; the effect of seeds, fluoride species and microwaves are visualized *via* crystallization curves
6 [222]	TS-2	MEL	443	15 h	conventional synthesis takes 48 h; spherical particles (conventional) *vs.* irregular particles (microwave); Ti is tetrahedrally incorporated
7 [223]	SAPO-5	AFI	453 – 463	1 – 2 h	conventional hydrothermal synthesis by using the same ingredients as well as the identical temperature program will lead to the formation of SAPO-34 (CHA) after 24 – 48 h
8 [225]	A	LTA	358	2 h	conventional synthesis takes 6-8 h; synthesis from metakoalin; 2 min (@ 358 K) under microwaves and 20 h (@ RT) aging is required in order to have successful crystallization; no phase impurities
9 [240]	A		343 – 353	1 – 8 h	synthesis time is 2-3 times faster in comparison with conventional synthesis; good purity; influence of synthesis parameters
10 [241]	X	FAU	343	8 h	conventional synthesis takes 14 h (without stirring) or 8 h (250 rpm), 5 h (500 rpm) and 4.5 h (250 rpm); similar performance in toluene alkylation; spherical particles (microwave and conventional without stirring) *vs.* no definite shape (conventional with stirring)

Table 7. Effect of microwave parameters on the synthesis of SAPO-11 at 433 K. Prepared with data from the work of Gharibeh e*t al.* (2009)[233].

Entry	Average microwave power (W)	Nucleation time (min)	Crystallization rate (min⁻¹)	Yield (g)	Particle size (μm)
1	65 [c]	17	0.014	1.64 [a]	3.77 ± 0.55 [a]
2	62 [d]	17	0.014	1.44 [a]	2.70 ± 0.20 [a]
3	55 [e]	17	0.014	1.08 [a]	2.49 ± 0.24 [a]
4	65 [f]	17	0.014	1.64 [b]	3.77 ± 0.55 [b]
5	130 [f]	17	0.030	1.30 [b]	2.84 ± 0.41 [b]
6	210 [f]	13	0.066	1.11 [b]	2.04 ± 0.41 [b]

[a] at 95% relative crystallinity; [b] at 85% relative crystallinity; [c] continuous; [d] pulse (1 s on – 2 s off); [e] (pulse 1 s on – 3 s off); [f] cooling gas was used at various rates. Particle size from SEM.

or colloidal silica), large differences in final material morphology as well as in the crystallization curves of MCM-22 (MWW, Figure 14) could be observed. It is important to note that the synthesis protocol using TEOS (H_2O/SiO_2 = 20, Figure 14B) is more concentrated in comparison to the one with colloidal silica (H_2O/SiO_2 = 35, Figure 14A). Nevertheless, within the same protocol for MCM-22 synthesis, the induction period and synthesis time is the shortest in

the case of microwave-assisted aging while it is the longest in absence of an aging step. Ultrasound-assisted aging is situated between these two extreme cases.[242] Similar results for MCM-22 synthesis were obtained by Wang *et al.* (2008), also using ultrasound-assisted aging (in combination with seeds). In addition, they also investigated the effect of different ultrasound parameters (during aging). It was found that a longer aging time (30-90 min), a higher temperature of the ultrasonic bath (293 – 333 K) or a higher ultrasound power (25 -50 W) shortened the time of crystallization and/or improved the relative crystallinity. The authors suggested that ultrasounds were responsible for cracking of the seeds and higher solubility of the Si-species.[243] Further research is required in order to confirm such hypothesis. Besides, one ideally also reports product Si/Al ratios (and not only the starting ones) as well as the achieved yields.
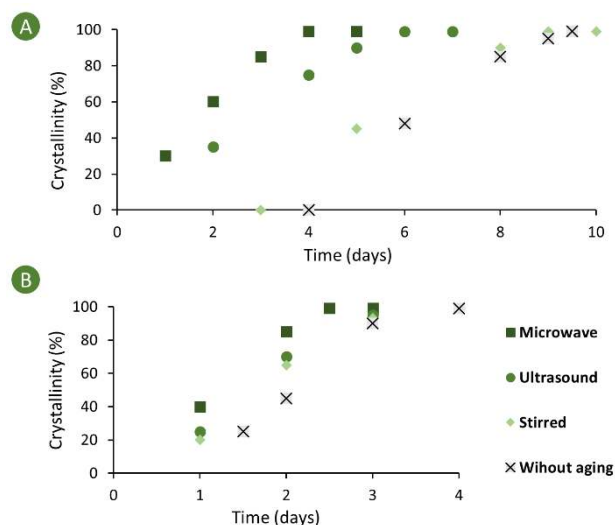
Figure 14. MCM-22 crystallization curves after different aging strategies and for different Si-sources: A. colloidal silica and B. TEOS. In the case of colloidal silica, the recipe was $1SiO_2$: $0.033Al_2O_3$: $0.075Na_2O$: $0.6HMI$: $35H_2O$. In the case of TEOS, the recipe was $1SiO_2$: $0.033Al_2O_3$: $0.075Na_2O$: $0.6HMI$: $20H_2O$. The aging time and temperature (for microwave, ultrasound and stirred aging) was 60 min and 333 K respectively. The microwave power was 120 W during the aging step, while the ultrasound power was not mentioned. Crystallization took place in a Teflon-lined steel autoclave at 431 K under static conditions. Prepared with data from the work of Wu *et al.* (2008)[242].

In addition to MCM-22, other examples are known in which ultrasounds are used prior to the hydrothermal crystallization. Mu *et al.* (2017) succeeded in shortening the total synthesis time of SSZ-13 (CHA) from 120 h to 72 h in comparison with conventional stirred aging.[236] Recently, Han *et al.* (2019) also showed this advantage (going from 30 h to 18 h), using ultrasounds during the preprocess of SSZ-13 (CHA) synthesis. In this latter work, a by-product of coal mining was used as one the zeolite ingredients.[244] Most of these studies show that, relatively speaking, (limited) time savings can be achieved, highlighting the (potential) profit of ultrasounds. The question is whether the effect on the synthesis time would be less, similar or more pronounced if another conventional synthesis protocol (with other ingredients, pretreatment, synthesis temperature, *etc.*) was used altogether. If researchers would like to make conclusions about the cost-competeness of alternative conditions, a conventional benchmark synthesis as reference is actually required.

Within the same CHA topology, Charghand *et al.* (2014) reported the synthesis of SAPO-34 and observed important differences in material properties. More specifically, ultrasonic-assisted aging under Argon atmosphere for 30 min at 90 W (instead of 3 h classic stirring without Argon atmosphere) of the formed gel resulted, after a final crystallization step at 473 K, in a material with higher surface area (384 *vs.* 607 m^2 . g^{-1}), better relative crystallinity (100 *vs.* 64.1%) and more uniform particle size. Among other things, it seems to be very interesting to examine the role of inert Argon during the ultrasonic aging step for SAPO-34. Using this material as MTO catalyst led to a slightly higher activity and selectivity towards olefins. This comparison is not entirely fair since the synthesis time of the samples were the same. Although this can be valuable to compare the two synthesis protocols, mature (fully crystalline) materials should be compared in catalysis. If a longer synthesis time was applied to the classically aged sample to reach a higher crystallinity, would it perform more similar to the Argon-assisted aged sample? A notable difference, however, is that the catalyst lifetime of this new material, based on a time-on-stream experiment, is improved by a factor of five in comparison with the conventional benchmark. According to the authors, the modified material properties were responsible for the better life time of the SAPO-34 catalyst.[245] Since cokes formation, and the related catalyst stability, is one of several key parameters for an efficient MTO reaction, at an industrial level and with fluidized bed reactors, this enhancement should be further looked into. Reproducibility as well as method genericity could be a focus for further studies as only SAPO-34 was tested.[245] For instance, recent work of Ahmadova *et al.* (2018) reported similar results, synthesizing SAPO-34 *via* ultrasonic-assisted aging and testing their MTO catalytic performance.[246]

Other sonochemistry studies have focused on EMT nanocrystals, [247] zeolite T (OFF/ERI)[248] and NaX (FAU)[249] with similar conclusions. In the case of NaX, irradiated volume, sonication time and power were thoroughly investigatd and sonication was also applied to reduce the agglomeration degree of the final powders.

Finally, the treatment with ultrasounds itself can be sufficient to alter the phase of certain zeolites. In this respect, Behin *et al.* (2016) found that clinoptilolite (HEU) can be converted in zeolite NaP (GIS) after only 3 h of sonication in alkaline media (15 mL of 1 M NaOH per g clinoptilolite). In order to realize this conversion, the sonochemical reactor operated at a constant temperature of 363 K with a wave frequency of 20 kHz and 15 W of power. Remarkably, it could be observed by means of SEM that the morphology of clinopitolite changed after 2.5 h. According to the authors, ultrasounds are responsible for cracks in the clinopitolite structure and consequently the concentration of

Si- and Al-species in solution will be higher. Achieving supersaturation results in the formation of zeolite NaP. After 5 h of sonication, almost 100% of NaP was yielded with a crystallinity of >70%. A conventional hydrothermal synthesis step after sonication did not affect the zeolite properties anymore, as only a minor increase in crystallinity was found. However, the authors did not measure the concentration of Si- and Al-species in solution and this could be revealing. One way to additionally verify sonication effects, would be to see whether there is a drop in crystallinity of other zeolites that do not easily undergo IZC after the same treatment. As well one should recognize that this phase transformation is in fact an interzeolite conversion (NaOH used and also heated) and that this IZC was also possible using only conventional hydrothermal synthesis at the same temperature without sonication step, but it takes much longer (72 h).[237] Besides, zeolite P can also be synthesized (*via* a conventional way) from other zeolite precursors such as zeolite A (LTA) or Y (FAU).[250,251]

HYBRID STRATEGIES

Obviously, the above mentioned strategies can be combined in all kinds of ways in order to improve synthesis or properties. Moreover, these techniques can be employed during different stages. Hence, an unlimited number of adaptations, compared to conventional synthesis, can be made. In what follows, four remarkable hybrid strategies are discussed: *(i)* aerosol, *(ii)* mechanochemical – solvent-free, *(iii)* continuous microwave experiment (CME), and *(iv)* microwaves in combination with ionothermal/solvothermal synthesis. Aerosol approaches use a continuous set-up where zeolite ingredients are sent through a heated tube in an aerosol by means of an atomizer. By doing this, a new type of amorphous precursor mix (often containing both Si- and Al-species) can be collected at the end of the tube which can then be used for classic synthesis. Consequently, this technique changes the chemical as well as the physical environment during synthesis. Second, a mechanochemical treatment of zeolite ingredients (*e.g.* ball-milling or grinding) is often performed in order to make the usage of solvents (water) less of a necessity. Third, CME combines two reactor based solutions, *i.e.* microwaves and a continuous reactor set-up. Both techniques are (individually) known to accelerate the synthesis of zeolites. Fourth, ionic liquids have proven to be excellent media for absorbing microwaves, which opens up the possibility to combine microwave heating and ionothermal synthesis.[252,253]

Aerosol. There has been renewed interest in aerosol processing for material synthesis. For a detailed overview of this technique with regard to the synthesis of heterogeneous catalysts, the reader is referred to the review of Debecker *et al.* (2018). Herein, the authors describe an aerosol as "a gas transport mist of liquid particles", being the transport of micron or submicron droplets through a tube. Within this group of aerosols, four different strategies are distinguished, *i.e.* drying, precipitation of certain species, a

reactive aerosol process and metal/alloy processing.[254] Although the reactive aerosol process, and mainly the aerosol-assisted sol-gel process, can be valuable for zeolite synthesis, examples are currently rather limited. This is mainly caused by the very short residence time of these droplets (in the order of seconds) in the aerosol tube, while the formation of a crystalline aluminosilicate, and especially their nucleation, takes a considerable time (minutes, up to several days). Nevertheless, certain groups have already succeeded in obtaining benefits from the usage of aerosols, which can be performed in two different ways.

First, the aerosol can be used prior to the crystallization step to convert precursors to an amorphous powder. In this case, the authors claimed that the synthesis procedure could be simplified with regard to certain steps in the protocol (*e.g.* using less SDA, less batch reactor volume and lower crystallization temperatures). Perhaps most interesting here is the possibility to prepare the precursors for better tetrahedral heteroatom incorporation in the framework. Nevertheless, the question remains whether the cost (and maybe also the increasing labor intensity) of additional equipment and its corresponding step will outweigh the achieved benefits if the aerosol only serves to better synthesize the amorphous precursor. Examples here are mainly reported by Xiong and co-workers studying the synthesis of several zeolites. According to the authors, the four major advantages, introducing aerosol in the synthesis procedures for TS-1 (MFI), are: *(i)* efficient incorporation of Ti (no precipitation of TiO_2), *(ii)* high OSDA-efficiency ($TPAOH/SiO_2 = 0.04$), *(iii)* low consumption of water and thus high batch loading (or less reactor volume), and *(iv)* lower crystallization temperature (403 instead of 443 K).[255] Besides, they also succeeded to synthesize silicalite-1 (MFI), ZSM-5 (MFI), [Zn]-ZSM-5 (MFI), [Fe]-ZSM-5 (MFI) and (hierarchical) beta (BEA) in this way.[255,256] Slightly different material properties (*e.g.* higher (external) surface area) were obtained in the aerosol-assisted synthesis of nano-sized ZSM-5 or beta aggregates, resulting in an improved activity and stability with regard to the catalytic cracking of 1,3,5-triisopropylbenzene.[257,258] Even the incorporation of Sn in zeolite beta, creating Lewis acidic sites (confirmed by Baeyer-villiger oxidation of cyclohexanone), as well as the synthesis of TS-1 zeolites with different Si/Ti ratios (only an absorption band for tetrahedral Ti-species at 207 nm in UV-VIS, when Si/Ti > 40) could be realized.[259,260] The most important conditions with regard to the synthesis of the latter material are added in Figure 15.

Second, aerosol itself can be used to synthesize the target material, but in contrast to the first aerosol strategy, amorphous materials (and thus no zeolites) have typically been synthesized. While strictly out of the scope of this review (zeolites), it is interesting to note that Pega *et al.* (2009) reported the synthesis of large pore amorphous aluminosilicates in basic media with TPAOH and a surfactant. In comparison with the conventional procedure, this aerosol or spray drying technique offers some advantages such as direct micellization, working sodium-free and in a continuous way. Moreover, it was possible to more or less control the texture of the material and less coke formation was

obtained if these materials were used as catalyst for the isomerization of *m*-xylene.[261] Fiorilli *et al.* (2016) investigated the effect of the Al-precursor, either aluminum isopropoxide or aluminum chloride, on the aerosol-assisted formation of mesostructured aluminosilicates. A higher amount of Al-incorporation could be obtained with aluminum isopropoxide.[262] Examples with Ti are also known.[263] The reason we mention this part is to show that an ordered aluminosilicate structure can be formed by using typical zeolite ingredients *via* aerosol. The critical step so far seems to be crystalline T atom ordering and/or nucleation in several seconds, but at this moment, there is also no certainty that ultrafast zeolite synthesis by an aerosol approach (and without additional crystallization step) is completely impossible. If successful, it would be interesting to investigate how aerosol parameters (*e.g.* starting droplet size after atomizer) would affect the synthesis protocol and final material properties of the zeolite.
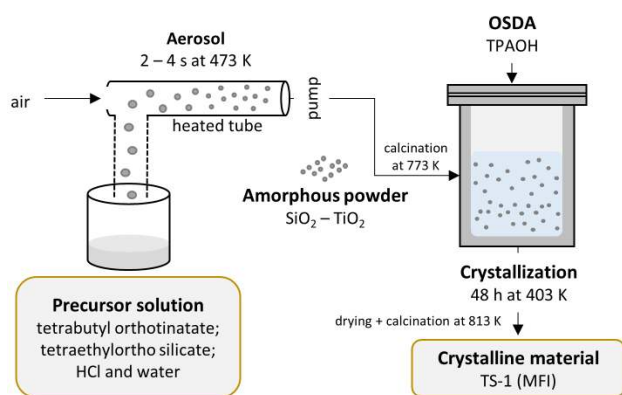

Figure 15. Schematic representation of the aerosol technique prior to the crystallization step. The conditions, which are used for synthesizing TS-1, are highlighted. Data obtained from the work of Guo *et al.* (2017)[260].

Mechanochemical and solvent-free. In contrast to what was originally thought, a mechanical treatment involves more than just a reduction in particle size and/or a densification of materials. For instance the introduction of mechanical energy makes it possible to break and form chemical bonds. Consequently, these kind of treatments can have an effect on different stages of zeolite synthesis. For a complete overview of zeolite mechanochemistry, the reader is referred to a review of Pérez-Ramírez and co-workers (2014).[264] In what follows, special attention is paid to mechanical techniques that influence the conventional hydrothermal synthesis outcome.

Ball-milling seeds is frequently used in order to create a positive effect during the crystallization step itself. As mentioned above (free-radical assisted synthesis), ball-milling in combination with heating can lead to the introduction of radicals and thus faster crystallization.[159] Okubo and co-workers also used milled seeds for their ultrafast synthesis of MOR in a PFR reactor.[68] This method has been known for quite some time. Among others, Valtchev *et al.*

already reported the simultaneous activation of gel and seeds for the synthesis of zeolite Y in 1995. More specifically, a treatment in a planetary ball-mill at 300 rpm for several minutes was performed prior to the conventional crystallization. It could be noted that for an activation time of 15 minutes, the induction period afterwards was much shorter and the crystallization speed higher. According to the researchers, this is induced by a higher number of nuclei and a larger specific surface area. A longer activation period (> 20 min) resulted in a lower crystallinity of zeolite Y (*e.g.* maximum ±15% for 30 min). Total nuclei deactivation was obtained after milling times longer than 30 min, leading to the formation of zeolite P and only trace amounts of zeolite Y (Figure 16).[265]
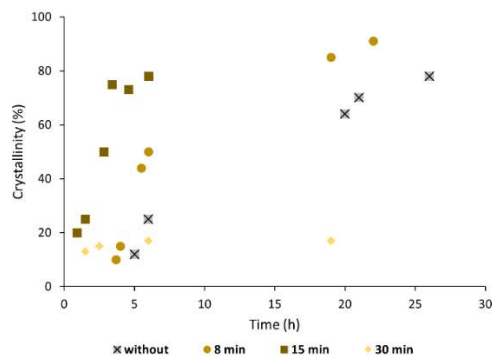

Figure 16. Crystallinity of zeolite Y in function of the synthesis time: the effect of simultaneous gel-seed activation *via* ball milling (for 0, 8, 15 or 30 min) prior to the crystallization step. 10 wt% of zeolite Y seeds w.r.t. the gel were used. This mixture of seeds in gel were ball-milled in a planetary mill. Prepared with data from the work of Valtchev *et al.* (1995)[265].

Yamada *et al.* (2016) succeeded to downsize SSZ-16 (AFX) crystals, going from 2-5 μm towards <100 nm, by bead milling the original crystals and recrystallizing them with the supernatant of the first crystallization step. Using these smaller crystals, ion-exchange with Cu²⁺ is faster and more homogeneous in comparison with the original AFX crystals (no bead-milling and recrystallization step).[266] Finally, Iwasaki *et al.* (2012) successfully synthesized TS-1 and has shown that a rough estimation of the total fabrication cost was positively influenced by employing a mechanical treatment, especially if cheaper raw materials can be used. In the extreme cases, the cost (per gram of TS-1) for a conventional synthesis was calculated at $78.5, while it was only $22.4 for the cheapest mechanical treatment (allowing cheaper raw materials). Remarkably, not the planetary ball mill, but the tumbling mill, which will result in lower mechanical impact, in combination with ultrasonic irradiation to disintegrate the formed aggregates, seem to be preferred in order to reduce the estimated total TS-1 fabrication cost.[267] In general, a tumbling mill is, in comparison to a planetary ball mill, is easier to handle and consumes less energy. However, a disadvantage may be that the mechanical impact is insufficient to simplify the synthesis protocol (*e.g.* time) and/or influence final material properties (*e.g.* efficient incorporation of T-atoms).

The addition of mechanical energy can also precede a solvent-free crystallization. Here, in contrast to the above mentioned examples, mechanical energy is typically introduced in a manual way *via* grinding. The solvent-free protocol encompasses *(i)* a mixing step, *(ii)* grinding during 5 – 20 min and *(iii)* crystallization at temperature for several hours in a closed vessel. Ren *et al.* (2012) first described the synthesis of silicalite-1 (MFI) by using this dry method. By doing this, a material with more or less identical properties was obtained in comparison to the conventional way of working, but costs were said to be potentially saved by more efficient use of materials and energy, *viz.* higher solid yield, efficient use of reactor space (here: up to three times), fewer preparatory steps (*e.g.* gel formation), less (liquid) waste streams afterwards and a lower operating pressure.[268] The physical properties of the solvent-free materials are not benchmarked experimentally with those from classic hydrothermal synthesis in the work, but these values seem to be in line with literature values of the hydrothermal ones. Morris and James (2013) wrote a conceptual paper about solvent-free syntheses. Herein, the question is raised to what extent this synthesis is 100% solvent-free and how interaction takes place with the used SDAs.[269] Ren *et al.* (2012) noted that there was already some microporosity before crystallization, indicating a difference between hydrothermal and solvent-free synthesis and hinting to some mechanochemical reaction during grinding.[268] Nevertheless, more fundamental insights, such as SDA interaction or role of the headspace, into this technology are required. Moreover, a techno-economic analysis with calculation of the total cost reduction, going from a conventional towards a solvent-free synthesis, could be valuable.

At this moment, researchers have succeeded to synthesize a wide range of topologies such as MOR, BEA, FAU, TON, CHA, MFI, *etc.*, with or without the incorporation of heteroatoms using solvent-'free' approaches (at sometimes higher crystallization temperatures).[44,166,270–275] For instance, Jin *et al.* (2013) reported the successful synthesis of aluminophosphates. SAPO-34 was formed by mixing all ingredients, grinding for 10 – 20 min and finally crystallizing it in a autoclave for 8 – 24 h at 373 K. In the end, acidic and catalytic properties of the synthesized material were comparable to the conventional ones and valuable in MTO catalysis.[32,276]

Finally, the dry gel conversion (DGC) method is shortly highlighted. In fact, DGC is not a hybrid strategy since no mechanochemical steps are part of the synthesis protocol, but this way of working is somehow related to the solvent-free synthesis. Here, a hard cake or dry gel, characterized by a H_2O/Si ratio of 0.5-2 (instead of 10-500 for conventional hydrothermal synthesis), is typically obtained after drying the aged ingredient mixture.[121,277] In the end, steam-assisted crystallization (SAC) is performed in an autoclave with physical separation between the dry gel and water, so, the role of water is not to be underestimated here. Recently, Vattipalli *et al.* (2018) succeed to make *e.g.* siliceous AMH-4 (CHA) or AMH-5 (STT), using this DGC-SAC

method. Moreover, they highlighted the possibility to expand this way of working to other topologies. While conventionally F^- is sometimes needed, several siliceous zeolites can now also be synthesized in alkaline media (Figure 17).[278]

Continuous microwave experiment (CME). The CME strategy combines two physical techniques, *i.e.* the PFR-like continuous tubular set-up and microwave heating. Since both techniques mostly focus on shortening synthesis time, the major objective of a CME synthesis is also that. According to Kim *et al.* (2001), CME makes it possible to synthesize zeolites *(i)* in a short period of time, *(ii)* in a continuous way and *(iii)* without the consumption of high amounts of SDA.[279] The latter is less obvious. Given the limited literature on CME, it is necessary to further confirm this (these) advantage(s) with well-designed experiments to offer more insights. For instance, in the work of Kim *et al.* (2001), the precursor gel with seeds, was pumped continuously in the CME Teflon tube in order to synthesize ZSM-5 (MFI). By doing this, the authors succeeded to form it in just 5 minutes at 438 K obtained by microwave power up to 250 W. Moreover, zeolite Y (FAU) was said to be synthesized after 30 minutes *via* CME, operating at 423 K under microwaves, without seeds.[279] Since this group works with a continuous set-up, it is remarkable that the required synthesis time is not expressed as "residence time".
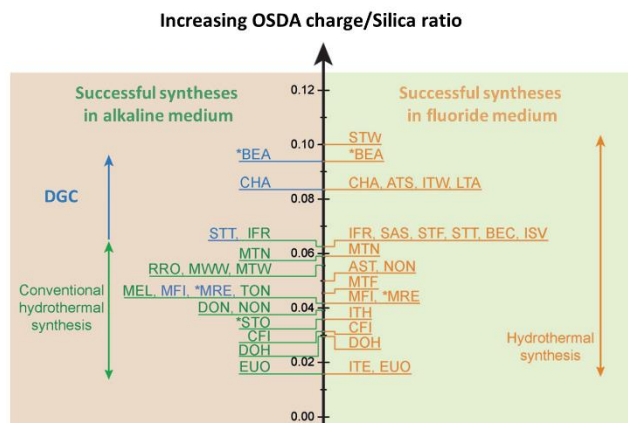

Figure 17. Dry-gel conversion overview. A summary of all siliceous zeolites, based on their OSDA charge/Si ratio. The zeolites synthesized in fluoride medium are on the right, while the zeolites synthesized in alkaline (fluoride-free) medium are shown on the left. Originally, hydrothermal synthesis in alkaline medium was only possible with an OSDA charge/Si ratio < 0.063, while ratios up to 0.1 were possible in Fluoride medium. By using the DGC method, *e.g.* AMH-4 (CHA) can now be synthesized in alkaline medium (OSDA charge/Si ratio of 0.083). Reprinted with permission from Vattipalli *et al.*[278] Copyright 2018, Wiley-VCH.

Bonaccorsi *et al.* (2008) investigated the effect of the microwave power, reactor geometry (coiled pipe *vs.* spherical vessel) and the addition of seeds in the gel on the synthesis of LTA zeolite. This zeolite was obtained after a residence time of 13 min (flow = 23 mL . min⁻¹) in a coiled pipe reactor, using 0.2 wt% seeds and operating at a microwave power

of 900 W. In comparison with conventional batch synthesis, similar size and distribution of crystals were obtained. Besides, the authors suggested that the flow rate is influencing the morphology while the reactor geometry (with its corresponding electromagnetic field distribution) the crystallization.[280] At this moment, there is insufficient data to judge the extent of potential for CME to influence final material properties, such as crystal size, porosity or Al-content and its distribution, in comparison with batch-microwave or conventional hydrothermal batch synthesis.

Microwave and ionothermal/solvothermal synthesis. Xu *et al.* (2006) pioneered this strategy noting advantages in fast crystallization rates, low synthesis pressures, and high structural selectivity over conventional heating.[281] In their work, high-purity AEL zeolites could be obtained under ambient pressure (T=150 °C) in only 1 h by the microwave-enhanced ionothermal method, while some impurities (*e.g.* CHA) were always observed in ionothermal syntheses with classic heating.[281] Likewise, a highly oriented SAPO-11 (AEL) film has been synthesized rapidly under ambient pressure and microwave heating.[282] Microwave heating could also be coupled with solvothermal syntheses. Compared to hydrothermal or solvothermal routes, a microwave-enhanced solvothermal method could realize much faster crystallization rates and more uniform crystal sizes for SAPO-16 (AST).[283] Another study showed that the morphology (*e.g.* MFI) could be tailored by using organic solvents (EG and various alcohols) with varying polarity as the microwave absorbers.[284]

POST-SYNTHETIC STRATEGIES

There are also examples of non-conventional conditions that are used after the hydrothermal step, *viz.* post-synthetic strategies, mostly to target new zeolite topologies. In what follows, topotactic transformations, assembly-disassembly-organization-reassembly and pressure-induced transformations are briefly discussed.

Topotactic transformation. Since zeolites are kinetic constructs, only metastable products that are kinetically accessible can be obtained *via* conventional hydrothermal synthesis. A sidenote should be made that 'metastability' can be quite high or for a long timeframe. The product of an OSDA-containing synthesis for instance is a hybrid organic-inorganic material with void-filling and charge-compensating stabilization. However, due to the kinetics, it is notoriously hard to predict the nature of the crystallization product (especially when there is Al[285]), making further expansion of zeolite topologies by kinetically controlled hydrothermal methods quite prone to serendipity.[286] In contrast, well defined post-synthetic methods can be more directed.[287] Topotactic transformations refer to the solid-state transformation of one (semi)crystalline zeolitic precursor into another structure by several steps of physical or chemical treatments such as dehydration, acidification and calcination.[288] The unique or non-conventional character of this method *vis-à-vis* conventional hydrothermal synthesis is that it relies on different kinetics, sometimes accessing constructs that are not found hydrothermally.

Also, it can introduce some interesting building blocks/units or enhance the pore accessibility while preserving original (parts of the) structures of the zeolite precursor, *viz.* layers, pores and cages. The main methods of topotactic transformation are condensation and delamination. Nevertheless, examples of a 3D-3D transformation, induced by a change in temperature (*e.g.* from GME to AFI[286,289]) or even by a change in pressure (see pressure-induced transformation below), are also known.

For the 2D-3D topotactic condensation, a dehydration-condensation strategy is frequently used. Silanol groups on neighboring zeolite layer surfaces will be dehydrated and condensed upon thermal treatment. The first example was the transformation of lamellar precursors into MMW zeolites, including the boron aluminosilicate MCM-22 and ERB-1, as well as the all-silica ITQ-1.[290–292] Thenceforth, a variety of zeolite topologies were prepared by virtue of this method, including CAS, SOD, FER, PCR, *etc.*[293–298] Of particular interest is the syntheses of new topologies CDO, RWR, NSI and RRO, which were never synthesized via conventional hydrothermal methods prior to their discovery.[297,299–308] More recently, a strategy of 2D-3D topotactic condensation has also been proposed, wherein the layered zeolite precursors are first expanded by additional reagents before condensation.[309,310] The interlayer-expanded zeolites, after calcination, could give access to bulky molecules and exhibit superior activity in certain catalytic processes.[310] In the meantime, the interlayer expansion also proves to be a favorable method for heteroatom incorporation, e.g. to develop new Lewis-acid catalysts.[309,311] In addition to 2D-3D condensations, the opposite operation of delamination of zeolite precursors was also realized. This methodology has been put forward mainly to tackle potential diffusional limitations in catalysis. In this field, pioneering efforts have been made by Corma and co-workers, who adopted a two-step strategy of intercalation and delamination. Among the first delaminated products was ITQ-2, from the lamellar precursor of MCM-22.[312,313] The lamellar precursor was first swollen by a quaternary alkylammonium cation and the layers were then stripped apart by sonication. Likewise, delaminated products ITQ-6 and ITQ-18 could be obtained from lamellar precursors of ferrierite (FER) and Nu-6(1) respectively.[314,315]

Since the above mentioned delamination procedures require strict conditions, Katz and co-workers introduced the usage of fluoride/chloride anions along with OSDA-like cations in order to promote exfoliation. By doing this, the delamination of the layered zeolite precursor, even in the presence of different framework heteroatoms, could be implemented under less harsh conditions, either in a near-neutral pH environment or without subsequent sonication.[316–318] As a result, the structural integrity could also be preserved in the delaminated products, including in the exfoliation of heteroatom-containing zeolites. Nevertheless, the usage of fluoride anions, although neutral, can cause additional safety concerns. Furthermore, boron atoms could be readily removed from the zeolite framework, and therefore, Katz and co-workers also developed an ele-

gant exfoliation method for the layered borosilicate precursors by a simple treatment in an $Al(NO_3)_3$ or $Zn(NO_3)_2$ solution. These delaminated materials have potential as catalyst for Friedel-Crafts acylation and, if successively functionalized with Ti, for olefin epoxidation.[319–321]

Assembly – Disassembly – Organisation – Reassembly (ADOR). It would be advantageous if one zeolite precursor could be directly transformed into new target topologies with predetermined pore architectures. In this regard, Morris, Cejka and their co-workers have put forward the concept of ADOR. The ADOR strategy starts with the assembly of parent zeolites, which are subsequently disassembled into their constituent layer precursors by removing specific structural units in them. Thereafter, the layered precursors are reorganized through the incorporation of alternative linking units or SDAs, and finally reassembled into new zeolite topologies upon calcination. Actually, the ADOR method can be treated as a specific case of the 3D-2D-3D topotactic transformation. Since the pore architecture in the target zeolites would vary with the connection of the layered precursor, and the pore sizes therein could also be flexibly adjusted, ADOR offers the opportunity to design and prepare novel zeolite topologies that can likely never be obtained using conventional hydrothermal methods.[322]

Lamellar germanosilicate zeolites are frequently employed as the disassembly precursors in the ADOR strategy because the Ge atoms prefer to occupy the double 4-membered ring (D4R) units between the 2D layers making them prone to selective hydrolysis in presence of water and acid.[323] Prior to the ADOR protocol, several trials had already been conducted to synthesize more stable or even all-silica zeolite products in this manner.[324,325] Likewise, Verheyen et al. (2012) also have a pioneering role with their inverse sigma transformation of germanosilicate UTL by germanium removal and dehydration/calcination, leading to the novel framework COK-14 (OKO), a new pure-silica large-pore structure.[324] Since the latter method above is not advantageous for porosity control, Morris, Cejka and their co-workers then reported the improved top-down method, including, besides calcination, a prior intercalation of diethoxydimethylsilane and octylamine into the delaminated UTL precursors.[298] During the final calcination single 4-membered ring units instead of the original D4R units in the parent UTL, could be formed between the layers. Compared to the 14x12 pore window in UTL, two different systems could be formed in situ, named IPC-2 (12×10 pore window) and IPC-4 (10×8 pore window) respectively. While IPC-2 also has the OKO topology, IPC-4 is a novel framework (PCR).[298,324] With ADOR, an isoreticular family of zeolites could be targeted for the first time, by delicate control over the linkage of the layered structure. The somewhat generic nature of the protocol was corroborated with other germanosilicates.[322]

Pressure-induced. Conventional syntheses are typically performed under autogenous water pressure. As mentioned at the start of 'Changing the physical environment', a recent exploration found intriguing effects of external high pressures on hydrothermal syntheses.[165] Meanwhile, some research groups have found that an already synthesized zeolite can undergo a phase-transition by increasing the pressure. Since high pressures typically cause an increase in material density and induce amorphization it was presumed that this way of working could not lead to (new) ordered materials. However, Corma and co-workers succeeded to synthesize ITQ-50 from pure silica ITQ-29 (LTA) by applying an immense pressure of $3.2 \cdot 10^4$ bar (Table 8, entry 1 and Figure 18). This new material, assigned IFY, provided a better kinetic separation between propane and propylene than ITQ-29.[326] Besides, a phase transition was also reported in case of the TON zeolite[327] and for AlPO-54 (VFI) to AlPO-8 (AET)[328] (Table 8). A pressure-induced phase transition comprises the tilting of tetrahedra and/or change(s) in the ring structure (breaking and forming T-O-T), which is illustrated in Figure 18.[326,327]

The addition of pressure can also be seen as a valuable extension of the topotactic transformation method or even a variety of ADOR. For instance, Mazur et al. (2018) described the pressure-induced ADOR transformation of the 2D precursor IPC-1P into a regular ordered 3D zeolite IPC-2 (OKO) instead of IPC-4 (PCR). While IPC-4 is obtained under atmospheric conditions and 823 K, IPC-2 is obtained under a pressure of $1 \cdot 10^4$ bar and at a temperature of 473 K. Remarkably, IPC-2 is characterized by a higher porosity in comparison to IPC-4.[329]
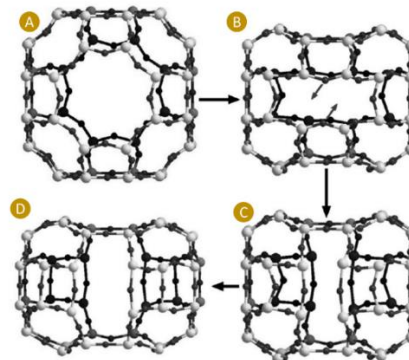

Figure 18. Suggested path from ITQ-29 to ITQ-50, corresponding with Table 8 entry 1. From (A.) to (B.): reversible deformation. From (B.) to (C.): Si-O bond breaking and formation through displacement of O atoms. From (C.) to (D.): structure relaxation. Reprinted with permission from Jordá et al.[326] Copyright 2013, Wiley-VCH.

CONCLUSIONS

Zeolite synthesis consists of a sequence of different steps involving many solid and liquid species and their complex interplays. In some respects, the formation of zeolites is still a black box, especially when Al and organics are involved. Nevertheless, if ingredients, their ratios, and the synthesis conditions (time, temperature/energy, agitation) are selected carefully, a target zeolite can be obtained with limited control over its material properties. From these DOFs in conventional syntheses, i.e. in classic batch mode

Table 8. Examples of pressure-induced phase transition.

Entry	Starting material	Transformation 1		Transformation 2	
		P (bar)	Remark	P (bar)	Remark
1 [326]	ITQ-29 (LTA)	1.2×10^4	reversible, P release = ITQ-29 (LTA) (Figure 18, A to B)	3.2×10^4	irreversible, ITQ-50 (IFY) (Figure 18, B to D)
2 [327]	TON	0.6×10^4	$Cmc2_1$ to $Pbn2_1$, pore ellipticity	$> 4.0 \times 10^4$	collapsing of the pores, amorphization
3 [328]	AlPO-54 (VFI)	$0.8 – 3 \times 10^4$	more dense state, smaller pores, AlPO-8 (AET)	$> 3.5 \times 10^4$	collapsing of the pores, amorphization

(*viz.* Figure 2), there is a lot of freedom, *i.e.* subtle parameter variations and combinations that influence the outcome. The roughly five DOFs are listed in Table 9. Deviating from conventional alterations, by making adaptations to the classic DOF (*e.g.* in terms of procedures or the use of non-classic ingredients) leads to (or is defined here as) non-conventional zeolite synthesis, with protocols targeting either the more efficient use of energy and raw materials, or control over the final material outcome in terms of properties and topology.

In academia, there are many initiatives to narrow the gap between the number of theoretically calculated frameworks and accessible (or commercially used) zeolites; or to broaden the composition of existing frameworks (*e.g.* raise Si/Al).[42,330] Presumably, there is also a gap between academia and industry in terms of what practically happens (*e.g.* batch in academia) and what is openly known. We surmise that the use of non-conventional conditions or nondisclosed tricks is probably indispensable for some commercial zeolite syntheses (*cfr.* zeolite patents).

In this review, chemical as well as physical adaptations to conventional DOFs were presented. In general, the objectives related to chemical adaptations are better defined. For instance, the purpose can be to decrease synthesis time and crystal sizes in the case of IZC or radical-assisted synthesis, while the idea behind CDM is to force OSDAs to cooperate or obtain a higher Si/Al ratio (higher stability). Another example is the goal of ionothermal syntheses to remove the competition between interactions of the framework with either the solvent or the SDA (template). In contrast, physical adaptations such as temperature, agitation, microwaves, ultrasounds and (semi-)continuous set-ups are often advantageous in terms of shortening synthesis time, saving energy or influencing crystal size. Occasionally, (small) differences due to physical adaptations are observed for material properties such as acidity, external surface and Si/Al ratio, but these effects of the non-conventional conditions are not always consistent and the underlying mechanisms are rather unclear.

The 2000s have seen innovative outcomes by adapting compositions in nonconventional ways, thus changing the chemical environment and extending the DOFs of type and ratios of ingredients (Table 9). These have proven capable of producing zeolites with different rates (activity), but also selectivity. Exemplary are the use of pre-crystallized precursors in IZC, the cooperation of two SDAs by CDM or ionic liquids a solvent and OSDA. These recently adopted techniques - although IZC has long been known - yielded novel zeolites and Al-outcomes without changing bulk overall compositions, but by altering interactions and thus kinetics (Table 9). Strikingly, only a limited amount of physical adaptations to classic DOFs (or thus external handles) have been reported to impact the selectivity. Clear phase-shifts ('selectivity' effects) are thus rare when changing the physical environment. Some illuminating examples are the use of microwaves to expand the Si/Al ratio of FAU, to tetrahedrally incorporate heteroatoms such as Ti in MEL or to steer phase selectivity between AFI and CHA. Although reactor engineering is the most common approach in organic chemistry to influence 'selectivity' when parallel and consecutive reactions are competing (Figure 11), quasi all known physical approaches for bulk zeolite synthesis focus on heat transfer and actual rate improvement ('activity'). By doing this, researchers effectively play with time and temperature/energy as DOF, thus mainly affecting activity (rates). Exemplary here are tubular liquid flow reactors, allowing synthesis in minutes, and the use of alternative heating modes such as microwaves (Table 9). Strikingly, competing and consecutive reactions are exactly what happens in zeolite synthesis.

PRACTICAL INSIGHTS

Currently, there are a lot of different tools to shorten the synthesis time of zeolites, but perhaps this parameter is not always a stumbling block on an industrial level. Other parameters and material properties seem to be more difficult to influence and are thus more interesting to work on. For instance, controlling phase selection is possible in theory if the kinetics of two competing (metastable) frameworks are changed to different degrees, but in practice, this is not straightforward. Moreover, clear demonstrations with non-classic ingredients and especially physical external handles, in order to specifically change Si/Al ratio, Al-distribution or tetrahedral heteroatom incorporation, are largely missing. Influencing the interactions between species, thus offering access to different competing kinetics, might be limited inherently by the nature of zeolite synthesis – although curious observations beg to differ (e.g. the MEL/TON phase change depending on agitation).

In order to further expand the zeolite (property) spectrum in a targeted manner, it is important to evaluate which kind of non-conventional conditions are possible in a technical way. Moreover, each researcher must consider how these conditions will be used (continuously, gradually or pulsed) and in which stage of the synthesis. The latter can be during the entire synthesis or at carefully selected stages such as aging, induction, crystallization, crystal growth or during post-treatment. For instance, the effect

of ultrasounds are often investigated during aging instead of during the hydrothermal step itself, while Figure 13 highlighted that microwaves (sometimes) need to be used at carefully selected times. In other words, an infinite number of variations are possible, and thus a well-defined experimental plan is essential in the first place. Even then, experiments will not always lead to clear insights since effects are often case- and zeolite-dependent. Secondly, in case of synthetic success, researchers must also look into how the synthesis can proceed in a cost-efficient manner with a low environmental impact. What is the total fabrication cost estimate of the conventional synthesis in comparison with the alternative one? Are the additional benefits in line with the complexity/cost of a special feature, such as additional equipment or process steps (*e.g.* an extra aerosol step to synthesize an amorphous SiAl-precursor)? Do alternative conditions lead to a simplified procedure? Consider for example the net benefit of a longer aging step at higher temperature prior to a shorter hydrothermal synthesis, or the need for several washing steps in batch after a continuous synthesis, or mechanochemical steps prior to a solvent-free approach? Can savings easily be made in terms of energy (*e.g.* ultrasounds *vs.* longer conventional heating; or post-treatments that are less energy-intensive) or raw materials (*e.g.* solvent-free, low consumption of a cheap and environmental-friendly OSDA)? Such questions are off course less urgent if new selectivities and properties are targeted, but when only rate and crystal size changes are the outcome, they are absolutely crucial and synthesis yields and mass balances should be listed to evaluate resource efficiency. Thirdly, validating the technical performance of these materials *e.g.* in catalysis, as ion exchanger or as adsorbent should be considered as much as possible. However, including catalytic reaction data cannot compensate for a lack of synthetic parametrization, adequate synthesis controls and mass balances.

Table 9. Schematic overview of non-conventional conditions adapting classic DOFs of conventional zeolite synthesis.

DOF in conventional synthesis [a]		chemical adaptations to DOF (non-conv.[b])	Physical adaptations to DOF
1	type Al	IZC	
	Si	IZC	
	H_2O	solvent-free, other solvents	steam-assisted dry gel
	OH^-, F^- $OSDA^+$	radical-assisted, CDM, ionothermal	
2	ratio of charges/ ingredients	CDM, (IZC)	
3	time	[c] radical-assisted, (solvent-free, IZC)	microwaves, ultrasounds, T profiles, PFR-type reactor
4	temperature (or energy)		
5	agitation	n.a.	type of agitation/stirrer

[a] Seeding is also a DOF. [b] Non-conv.: non-conventional chemical adaptions only, so not a new OSDA or using silica gel instead of TEOS, as that is using a classic DOF (type). [c] Not an adaptation to time or temperature/energy, but related to activity (rates): less time and/or energy required.

To make a fair evaluation of a non-conventional synthesis protocol, its material outcome, environmental impact, economics and application performance, it is essential to always compare with the - at that moment - established benchmark. Too often, a benchmark is used, with negated conditions, to which the proposed non-conventional method relates favorably. However, if one would compare to the best recipes and conditions achieved with traditional reactors (or methods), the benefit of the non-conventional one could be lost or even outweighed. Again, this is much less critical if new materials or properties are targeted (other than rate and size). In addition, it is important to only vary the non-conventional parameter during the synthesis protocol, and not also use a different Si-source or OSDA etc. Since case-dependent differences are always very real in zeolite synthesis, multi-variation experiments should be avoided in order to get a clear picture about the influence of the changed parameter or set-up. Therefore, it is important to always detail all ingredients and reactor conditions meticulously, as even reactor geometry, filling level (headspace), water content of sources, and type of stirrer can be relevant. Finally, it is important to emphasize that the conventional benchmark for comparing synthesis protocols is not necessarily the same one for comparing catalytic performance. Ideally, mature materials (optimal) from both synthesis strategies should be compared in catalysis. For one, a longer synthesis time for the conventional material could be required in order to obtain a fully crystalline sample.

OUTLOOK AND OPPORTUNITIES

A first outlook for developing non-conventional zeolite synthesis protocols - especially reactor-based ones (physical environment) - is the relative ease of transfering new methodologies or equipment to other classes of materials (zeotypes, silicas, mesoporous materials, oxides, metal-organic frameworks) in case of success.

The underlying mechanisms for some reported non-conventional synthesis effects remains clouded and could be unraveled. Do factors such as headspace, variable temperature profiles or hot spots, addition order, concentration gradients and non-uniformity alter the interactions between species and thus the crystallization processes in comparison to conventional synthesis?

Based on this review, we surmise that non-conventional protocols that directly impact the chemical environment (*e.g.* IZC) alter the interactions between species and offer new kinetics for different sub-steps in a synthesis. In such cases, one can strive for improvements in the field of selectivity instead of activity (*e.g.* new phases, a wider Si/Al ratio, controlled Al pairing[14], zoning). In contrast, most non-conventional protocols that change the physical environment seem to just tweak around the edges in terms of selectivity. Non-conventional physical approaches thus mostly impact activity, i.e. synthesis times and morphology or crystal sizes (= consequences of nucleation and growth rates). As visualized (or sorted) in Table 9, few cases of physical adaptations (external) to classic DOFs have been

reported that can impact chemical interactions among synthesis species of classic ingredients along the way, *viz.* the empty red zones Table 9. A notable example that could classify here is the steam-assisted dry gel synthesis, impacting the DOF of H_2O as ingredient in an unconventional way. Another recent example of influencing interactions of classic ingredients along the way was shown for zeolite synthesis *via* vapor-phase-transport rearrangement.[331] Further evidence that impacting the interactions between species could alter selectivity can be deduced from: *(i)* conventional syntheses where changing the ratio of species slightly has great impact, *(ii)* IZC or CDM influencing the chemical system without overall compositional changes, *(iii)* theoretically calculating concentration profiles using different reactor types (*e.g.* see Figure 11), or *(iv)* examples where the introduction of alternative energy or agitation resulted in other materials (*e.g.* see Figure 12). Therefore, straying away from the classic batch reactor to more types of reactors – *e.g.* those used in industrial and organic chemistry – could be rewarding and perhaps allow one to fill missing gaps in Table 9.

A focus could be put on reactor design (in the broadest sense) that can impact and control the critical interactions and gradients of the different species in zeolite synthesis in a direct way. Instead of only relying on starting ingredients, batching them in and letting a synthesis run its course, some 'intelligence' could and should be added along the way, as this is a kinetic game after all. That intelligence should allow additional degrees of freedom with gradual fine-control over the zeolite materials produced in terms of Al-content, Al-distribution, heteroatom integration, and zeolite type, as well as open the gates to fundamental insight into the kinetic factors that matter.

AUTHOR INFORMATION

Corresponding Author

* E-mail: michiel.dusselier@kuleuven.be (M.D.)

Author Contributions

A.D. has written all parts, with critical input by M.D., except for certain sections: J.D. has written about IZC while Q.K. has written the sections about topotactic transformation, ADOR, CDM, free-radical assisted and solvo/ionothermal syntheses, all with critical input by M.D. and A.D.

Notes

The authors declare no competing financial interests.

ACKNOWLEDGMENT

ABBREVIATIONS

DOF, degree of freedom; MTO, methanol to olefins; (O)SDA, (organic) structure directing agent; -MR, -membered ring; ADOR, assembly-disassembly-organization-reassembly; CDM, charge density mismatch; FD, framework density; TMAda(OH), N,N,N-trimethyl-1-adamantanamine (hydroxide); TEA(OH), Tetraethylammonium (hydroxide); TPA(OH), tetrapropylammonium (hydroxide); TEOS, tetraethyl orthosilicate; HMI, hexamethyleneimine; CSTR, continuous stirred tank reactor; PFR, plug flow reactor; CEC, cation exchange capacity; DGC, dry gel conversion; SAC, steam-assisted conversion. CME, continuous microwave experiment. EG, ethylene glycol. Abbreviations only used in Tables are found in the captions.

REFERENCES

(1) Cundy, C. S.; Cox, P. A. The Hydrothermal Synthesis of Zeolites: History and Development from the Earliest Days to the Present Time. *Chem. Rev.* **2003**, *103* (3), 663–701.

(2) Corma, A.; Davis, M. E. Issues in the Synthesis of Crystalline Molecular Sieves: Towards the Crystallization of Low Framework-Density Structures. *ChemPhysChem* **2004**, *5* (3), 304–313.

(3) Cundy, C. S.; Cox, P. A. The Hydrothermal Synthesis of Zeolites: Precursors, Intermediates and Reaction Mechanism. *Microporous Mesoporous Mater.* **2005**, *82* (1–2), 1–78.

(4) Cejka, J.; Corma, A.; Zones, S. *Zeolites and Catalysis*; Wiley-VCH, 2010; Vol. 1.

(5) Kirschhock, C. E. A.; Feijen, E. J. P.; Jacobs, P. A.; Martens, J. A. Hydrothermal Zeolite Synthesis. In *Handbook of Heterogeneous Catalysis*; Ertl, G., Knözinger, H., Schüth, F., Weitkamp, J., Eds.; Wiley-VCH, 2008.

(6) Lok, B. M.; Messina, C. A.; Patton, R. L.; Gajek, R. T.; Cannan, T. R.; Flanigen, E. M. Silicoaluminophosphate Molecular Sieves: Another New Class of Microporous Crystalline Inorganic Solids. *J. Am. Chem. Soc.* **1984**, *106*, 6092–6093.

(7) Burton, A. W.; Zones, S. I. Organic Molecules in Zeolite Synthesis: Their Preparation and Strcture-Directing Agents. In *Introduction to Zeolite Science and Practice*; Cejka, J., van Bekkum, H., Corma, A., Schüth, F., Eds.; Elsevier B.V., 2007.

(8) Kumar, M.; Choudhary, M. K.; Rimer, J. D. Transient Modes of Zeolite Surface Growth from 3D Gel-like Islands to 2D Single Layers. *Nat. Commun.* **2018**, *9*, 2129.

(9) Grand, J.; Awala, H.; Mintova, S. Mechanism of Zeolite Crystal Growth: New Findings and Open Questions. *CrystEngComm* **2016**, *18*, 650–664.

(10) Tsunoji, N.; Shimono, D.; Tsuchiya, K.; Sadakane, M.; Sano, T. Formation Pathway of AEI Zeolites as a Basis for a Streamlined Synthesis. *Chem. Mater.* **2019**, DOI: 10.1021/acs.chemmater.9b02227.

(11) Qin, W.; Agarwal, A.; Choudhary, M. K.; Palmer, J. C.; Rimer, J. D. Molecular Modifiers Suppress Nonclassical Pathways of Zeolite Crystallization. *Chem. Mater.* **2019**, *31* (9), 3228–3238.

(12) Choudhary, M. K.; Kumar, M.; Rimer, J. D. Regulating Nonclassical Pathways of Silicalite-1 Crystallization through Controlled Evolution of Amorphous Precursors. *Angew. Chemie* **2019**, *131* (44), 15859–15863.

(13) Zhao, Y.; Zhang, H.; Wang, P.; Xue, F.; Ye, Z.; Zhang, Y.; Tang, Y. Tailoring the Morphology of MTW Zeolite Mesocrystals: Intertwined Classical/Nonclassical Crystallization. *Chem. Mater.* **2017**, *29* (8), 3387–3396.

(14) Devos, J.; Bols, M. L.; Plessers, D.; Van Goethem, C.; Seo, J. W.; Hwang, S.-J.; Sels, B. F.; Dusselier, M. Synthesis-Structure-Activity Relations in Fe-CHA for C-H Activation: Control of Al-Distribution by Interzeolite Conversion. *Chem. Mater.* **2020**, *32* (1), 273–285.

(15) Davis, M. E. Ordered Porous Materials for Emerging Applications. *Nature* **2002**, *417* (6891), 813–821.

(16) Yang, R. T. *Gas Separation by Adsorption Processes*; Butterworht-Heinemann: London, 2013.

(17) Primo, A.; Garcia, H. Zeolites as Catalysts in Oil Refining. *Chem. Soc. Rev.* **2014**, *43* (22), 7548–7561.

(18) Dusselier, M.; Davis, M. E. Small-Pore Zeolites: Synthesis and Catalysis. *Chem. Rev.* **2018**, *118* (11), 5265–5329.

(19) Sushkevich, V. L.; Palagin, D.; Ranocchiari, M.; Van Bokhoven, J. A. Selective Anaerobic Oxidation of Methane Enables Direct Synthesis of Methanol. *Science* **2017**, *356*, 523–527.

(20) Bols, M. L.; Hallaert, S. D.; Snyder, B. E. R.; Devos, J.; Plessers, D.; Rhoda, H. M.; Dusselier, M.; Schoonheydt, R. A.; Pierloot, K.; Solomon, E. I.; et al. Spectroscopic Identification of the α-Fe/α-O Active Site in Fe-CHA Zeolite for the Low-Temperature Activation of the Methane C-H Bond. *J. Am. Chem. Soc.* **2018**, *140* (38), 12021–12032.

(21) Cheng, K.; Zhou, W.; Kang, J.; He, S.; Shi, S.; Zhang, Q.; Pan, Y.; Wen, W.; Wang, Y. Bifunctional Catalysts for One-Step Conversion of Syngas into Aromatics with Excellent Selectivity and Stability. *Chem* **2017**, *3*, 334–347.

(22) Li, G.; Jiao, F.; Miao, D.; Wang, Y.; Pan, X.; Yokoi, T.; Meng, X.; Xiao, F.; Parvulescu, A.-N.; Müller, U.; et al. Selective Conversion of Syngas to Propane over ZnCrOx-SSZ-39 OX-ZEO Catalysts. *J. Energy Chem.* **2019**, *36*, 141–147.

(23) Artz, J.; Müller, T. E.; Thenert, K.; Kleinekorte, J.; Meys, R.; Sternberg, A.; Bardow, A.; Leitner, W. Sustainable Conversion of Carbon Dioxide: An Integrated Review of Catalysis and Life Cycle Assessment. *Chem. Rev.* **2018**, *118* (2), 434–504.

(24) Dokania, A.; Ramirez, A.; Bavykina, A.; Gascon, J. Heterogeneous Catalysis for the Valorization of CO2: Role of Bifunctional Processes in the Production of Chemicals. *ACS Energy Lett.* **2019**, *4*, 167–176.

(25) Wei, J.; Ge, Q.; Yao, R.; Wen, Z.; Fang, C.; Guo, L.; Xu, H.; Sun, J. Directly Converting CO2 into a Gasoline Fuel. *Nat. Commun.* **2017**, *8*, 1–8.

(26) Gao, P.; Li, S.; Bu, X.; Dang, S.; Liu, Z.; Wang, H.; Zhong, L.; Qiu, M.; Yang, C.; Cai, J.; et al. Direct Conversion of CO2 into Liquid Fuels with High Selectivity over a Bifunctional Catalyst. *Nat. Chem.* **2017**, *9*, 1019–1024.

(27) Dusselier, M.; Van Wouwe, P.; Dewaele, A.; Jacobs, P. A.; Sels, B. F. Shape-Selective Zeolite Catalysis for Bioplastics Production. *Science* **2015**, *349*, 78–80.

(28) Ennaert, T.; Van Aelst, J.; Dijkmans, J.; De Clercq, R.; Schutyser, W.; Dusselier, M.; Verboekend, D.; Sels, B. F. Potential and Challenges of Zeolite Chemistry in the Catalytic Conversion of Biomass. *Chem. Soc. Rev.* **2016**, *45* (3), 584–611.

(29) Ferrini, P.; Dijkmans, J.; De Clercq, R.; Van de Vyver, S.; Dusselier, M.; Jacobs, P. A.; Sels, B. F. Lewis Acid Catalysis on Single Site Sn Centers Incorporated into Silica Hosts. *Coord. Chem. Rev.* **2017**, *343*, 220–255.

(30) Davis, M. E. Zeolites from a Materials Chemistry Perspective. *Chem. Mater.* **2014**, *26* (1), 239–245.

(31) Li, Y.; Li, L.; Yu, J. Applications of Zeolites in Sustainable Chemistry. *Chem* **2017**, *3* (6), 928–949.

(32) Tian, P.; Wei, Y.; Ye, M.; Liu, Z. Methanol to Olefins (MTO): From Fundamentals to Commercialization. *ACS Catal.* **2015**, *5* (3), 1922–1938.

(33) Nuttens, N.; Verboekend, D.; Deneyer, A.; Van Aelst, J.; Sels, B. F. Potential of Sustainable Hierarchical Zeolites in the Valorization of α-Pinene. *ChemSusChem* **2015**, *8* (7), 1197–1205.

(34) Sartipi, S.; Alberts, M.; Meijerink, M. J.; Keller, T. C.; Pørez-ramírez, J. Towards Liquid Fuels from Biosyngas: Effect of Zeolite Structure in Hierarchical-Zeolite-Supported Cobalt Catalysts. *ChemSusChem* **2013**, *6*, 1646–1650.

(35) Dapsens, P. Y.; Mondelli, C.; Pérez-Ramírez, J. Biobased Chemicals from Conception toward Industrial Reality: Lessons Learned and To Be Learned. *ACS Catal.* **2012**, *2*, 1487–1499.

(36) Moliner, M.; Román-leshkov, Y.; Davis, M. E. Tin-Containing Zeolites Are Highly Active Catalysts for the Isomerization of Glucose in Water. *PNAS* **2010**, *107*, 6164–6168.

(37) Jacobs, P. A.; Dusselier, M.; Sels, B. F. Will Zeolite-Based Catalysis Be as Relevant in Future Biorefineries as in Crude Oil Refineries? *Angew. Chemie - Int. Ed.* **2014**, *53*, 8621–8626.

(38) Vermeiren, W.; Gilson, J.-P. Impact of Zeolites on the Petroleum and Petrochemical Industry. *Top. Catal.* **2009**, *52*, 1131–1161.

(39) Zones, S. I. Translating New Materials Discoveries in Zeolite Research to Commercial Manufacture. *Microporous Mesoporous Mater.* **2011**, *144*, 1–8.

(40) Liu, Z.; Wakihara, T.; Oshima, K.; Nishioka, D.; Hotta, Y.; Elangovan, S. P.; Yanaba, Y.; Yoshikawa, T.; Chaikittisilp, W.; Matsuo, T.; et al. Widening Synthesis Bottlenecks: Realization of Ultrafast and Continuous-Flow Synthesis of High-Silica Zeolite SSZ-13 for NOx Removal. *Angew. Chemie - Int. Ed.* **2015**, *54* (19), 5683–5687.

(41) Ng, E.-P.; Chateigner, D.; Bein, T.; Valtchev, V.; Mintova, S. Capturing Ultrasmall EMT Zeolite from Template-Free Systems. *Science* **2012**, *335*, 70–74.

(42) Pophale, R.; Cheeseman, P. A.; Deem, M. W. A Database of New Zeolite-like Materials. *Phys. Chem. Chem. Phys.* **2011**, *13* (27), 12407.

(43) Mazur, M.; Wheatley, P. S.; Navarro, M.; Roth, W. J.; Polozij, M.; Mayoral, A.; Eliásová, P.; Nachtigall, P.; Cejka, J.; Morris, R. E. Synthesis of 'Unfeasible' Zeolites. *Nat. Chem.* **2016**, *8*, 58–62.

(44) Wu, Q.; Ma, Y.; Wang, S.; Meng, X.; Xiao, F.-S. 110th Anniversary: Sustainable Synthesis of Zeolites: From Fundamental Research to Industrial Production. *Ind. Eng. Chem. Res.* **2019**, *58*, 11653–11658.

(45) Majda, D.; Paz, F. A. A.; Friedrichs, D.; Foster, M. D.; Simperler, A.; Bell, R. G.; Klinowski, J. Hypothetical Zeolitic Frameworks: In Search of Potential Heterogeneous Catalysts. *J. Phys. Chem. C* **2008**, *112* (4), 1040–1047.

(46) Blatov, V. A.; Ilyushin, G. D.; Proserpio, D. M. The Zeolite Conundrum: Why Are There so Many Hypothetical Zeolites and so Few Observed? A Possible Answer from the Zeolite-Type Frameworks Perceived as Packings of Tiles. *Chem. Mater.* **2013**, *25* (3), 412–424.

(47) Moteki, T.; Lobo, R. F. A General Method for Aluminum Incorporation into High-Silica Zeolites Prepared in Fluoride Media. *Chem. Mater.* **2016**, *28* (2), 638–649.

(48) Knott, B. C.; Nimlos, C. T.; Robichaud, D. J.; Nimlos, M. R.; Kim, S.; Gounder, R. Consideration of the Aluminum Distribution in Zeolites in Theoretical and Experimental Catalysis Research. *ACS Catal.* **2018**, *8* (2), 770–784.

(49) Di Iorio, J. R.; Gounder, R. Controlling the Isolation and Pairing of Aluminum in Chabazite Zeolites Using Mixtures of Organic and Inorganic Structure-Directing Agents. *Chem. Mater.* **2016**, *28* (7), 2236–2247.

(50) Li, T.; Krumeich, F.; Chen, M.; Ma, Z.; van Bokhoven, J. A. Defining Aluminum-Zoning during Synthesis of ZSM-5 Zeolites. *Phys. Chem. Chem. Phys.* **2019**, DOI: 10.1039/C9CP05423E.

(51) Dědeček, J.; Sobalík, Z.; Wichterlová, B. Siting and Distribution of Framework Aluminium Atoms in Silicon-Rich Zeolites and Impact on Catalysis. *Catal. Rev. - Sci. Eng.* **2012**, *54* (2), 135–223.

(52) Javaid, R.; Urata, K.; Furukawa, S.; Komatsu, T. Factors Affecting Coke Formation on H-ZSM-5 in Naphtha Cracking. *Appl. Catal. A Gen.* **2015**, *491*, 100–105.

(53) IHS Markit. *Zeolites, Chemical Economics Handbook*; 2016.

(54) Shin, J.; Jo, D.; Hong, S. B. Rediscovery of the Importance of Inorganic Synthesis Parameters in the Search for New Zeolites. *Acc. Chem. Res.* **2019**, *52*, 1419–1427.

(55) Caro, J.; Noack, M.; Kölsch, P.; Schäfer, R. Zeolite Membranes - State of Their Development and Perspective. *Microporous Mesoporous Mater.* **2000**, *38*, 3–24.

(56) Li, Y.; Yang, W. Microwave Synthesis of Zeolite Membranes: A Review. *J. Memb. Sci.* **2008**, *316*, 3–17.

(57) Wu, Y.; Ren, X.; Lu, Y.; Wang, J. Crystallization and Morphology of Zeolite MCM-22 Influenced by Various Conditions in the Static Hydrothermal Synthesis.

Microporous Mesoporous Mater. **2008**, *112* (1–3), 138–146.

(58) Li, R.; Linares, N.; Sutjianto, J. G.; Chawla, A.; Garcia-Martinez, J.; Rimer, J. D. Ultrasmall Zeolite L Crystals Prepared from Highly Interdispersed Alkali-Silicate Precursors. *Angew. Chemie - Int. Ed.* **2018**, *57* (35), 11283–11288.

(59) Song, J.; Dai, L.; Ji, Y.; Xiao, F.-S. Organic Template Free Synthesis of Aluminosilicate Zeolite ECR-1. *Chem. Mater.* **2006**, *18* (12), 2775–2777.

(60) Itabashi, K.; Kamimura, Y.; Iyoki, K.; Shimojima, A.; Okubo, T. A Working Hypothesis for Broadening Framework Types of Zeolites in Seed-Assisted Synthesis without Organic Structure-Directing Agent. *J. Am. Chem. Soc.* **2012**, *134* (28), 11542–11549.

(61) Xie, B.; Zhang, H.; Yang, C.; Liu, S.; Ren, L.; Zhang, L.; Meng, X.; Yilmaz, B.; Müller, U.; Xiao, F.-S. Seed-Directed Synthesis of Zeolites with Enhanced Performance in the Absence of Organic Templates. *Chem. Commun.* **2011**, *47* (13), 3945–3947.

(62) Majano, G.; Delmotte, L.; Valtchev, V.; Mintova, S. Al-Rich Zeolite Beta by Seeding in the Absence of Organic Template. *Chem. Mater.* **2009**, *21* (18), 4184–4191.

(63) Kamimura, Y.; Chaikittisilp, W.; Itabashi, K.; Shimojima, A.; Okubo, T. Critical Factors in the Seed-Assisted Synthesis of Zeolite Beta and "Green Beta" from OSDA-Free Na+-Aluminosilicate Gels. *Chem. - An Asian J.* **2010**, *5* (10), 2182–2191.

(64) Majano, G.; Darwiche, A.; Mintova, S.; Valtchev, V. Seed-Induced Crystallization of Nanosized Na-ZSM-5 Crystals. *Ind. Eng. Chem. Res.* **2009**, *48* (15), 7084–7091.

(65) Yokoi, T.; Yoshioka, M.; Imai, H.; Tatsumi, T. Diversification of RTH-Type Zeolite and Its Catalytic Application. *Angew. Chemie - Int. Ed.* **2009**, *48* (52), 9884–9887.

(66) Kamimura, Y.; Itabashi, K.; Okubo, T. Seed-Assisted, OSDA-Free Synthesis of MTW-Type Zeolite and "Green MTW" from Sodium Aluminosilicate Gel Systems. *Microporous Mesoporous Mater.* **2012**, *147* (1), 149–156.

(67) Zhang, H.; Guo, Q.; Ren, L.; Yang, C.; Zhu, L.; Meng, X.; Li, C.; Xiao, F.-S. Organotemplate-Free Synthesis of High-Silica Ferrierite Zeolite Induced by CDO-Structure Zeolite Building Units. *J. Mater. Chem.* **2011**, *21* (26), 9494–9497.

(68) Zhu, J.; Liu, Z.; Endo, A.; Yanaba, Y.; Yoshikawa, T.; Wakihara, T.; Okubo, T. Ultrafast, OSDA-Free Synthesis of Mordenite Zeolite. *CrystEngComm* **2017**, *19*, 632–640.

(69) Liu, M.; Yokoi, T.; Yoshioka, M.; Imai, H.; Kondo, J. N.; Tatsumi, T. Differences in Al Distribution and Acidic Properties between RTH-Type Zeolites Synthesized with OSDAs and without OSDAs. *Phys. Chem. Chem. Phys.* **2014**, *16* (9), 4155–4164.

(70) Meng, X.; Xiao, F. Green Routes for Synthesis of Zeolites. *Chem. Rev.* **2014**, *114*, 1521–1543.

(71) Morris, R. E. Ionothermal Synthesis - Ionic Liquids as Functional Solvents in the Preparation of Crystalline Materials. *Chem. Commun.* **2009**, No. 21, 2990–2998.

(72) Morris, R. E.; Weigel, S. J. The Synthesis of Molecular Sieves from Non-Aqueous Solvents. *Chem. Soc. Rev.* **1997**, *26*, 309–317.

(73) Oliver, S.; Kuperman, A.; Ozin, G. A. A New Model for Aluminophosphate Formation : Transformation of a Linear Chain Aluminophosphate to Chain, Layer, and Framework Structures. *Angew. Chem. Int. Ed.* **1998**, *37*, 46–62.

(74) Liu, Z.; Xu, W.; Yang, G.; Xu, R. New Insights into the Crystallization Mechanism of Microporous AlPO4-21. *Microporous Mesoporous Mater.* **1998**, *22*, 33–41.

(75) Hoelderich, W.; Marosi, L.; Mross, W. D.; Schwarzmann, M. Process for the Preparation of a Crystalline Aluminosilicate (Zeolite) and Use Thereof as a Catalyst, 1982.

(76) Bibby, D. M.; Dale, M. P. Synthesis of Silica-Sodalite from Non-Aqueous Systems. *Nature* **1985**, *317*, 157–158.

(77) Kuperman, A.; Nadimi, S.; Oliver, S.; Ozin, G. A.; Garcés, J. M.; Olken, M. M. Non-Aqueous Synthesis of Giant Crystals

of Zeolites and Molecular Sieves. *Nature* **1993**, *365*, 239–242.

(78) Rakoczy, R. A.; Traa, Y.; Kortunov, P.; Vasenkov, S.; Kärger, J.; Weitkamp, J. Synthesis of Large Crystals of All-Silica Zeolite Ferrierite. *Microporous Mesoporous Mater.* **2007**, *104*, 179–184.

(79) Fechtelkord, M.; Posnatzki, B.; Buhl, J.-C. On the Synthesis of Nitrate Enclathrated Sodalite in Organic Solvents. *Zeolites* **1997**, *19*, 334–342.

(80) Yang, X.; Albrecht, D.; Caro, J. Solvothermal Synthesis of Germanosilicate-Sodalite and Silica-Sodalite: Effects of Water, Germanium and Fluoride. *Microporous Mesoporous Mater.* **2007**, *100*, 95–102.

(81) Li, R.; Xu, W.; Wang, J. Nonaqueous Synthesis: Iron Aluminosilicates with the ZSM-48 Structure. *Zeolites* **1992**, *12*, 716–719.

(82) Marthala, V. R. R.; Hunger, M.; Kettner, F.; Krautscheid, H.; Chmelik, C.; Kärger, J.; Weitkamp, J. Solvothermal Synthesis and Characterization of Large-Crystal All-Silica, Aluminum-, and Boron-Containing Ferrierite Zeolites. *Chem. Mater.* **2011**, *23*, 2521–2528.

(83) Takako, N.; Takuji, I.; Chie, A.; Yasuhisa, H.; Yoshimichi, K.; Takaaki, H. Solvothermal Synthesis of – LIT-Type Zeolite. *Cryst. Growth Des.* **2012**, *12*, 1752–1761.

(84) Huo, Q.; Xu, R.; Li, S.; Ma, Z.; Thomas, J. M.; Jones, R. H.; Chippindale, A. M. Synthesis and Characterization of a Novel Extra Large Ring of Aluminophosphate JDF-20. *J. Chem. Soc. Chem. Commun.* **1992**, 875–876.

(85) Qisheng, H.; Ruren, X. Syntheses of AlPO4-5, AlPO4-11, and AlPO 4-21 from Non-Aqueous Systems. *J. Chem. Soc. Chem. Commun.* **1990**, 783–784.

(86) Gao, Q.; Li, S.; Xu, R. Synthesis of AlPO4-17 from Non-Aqueous Systems. *J. Chem. Soc. Chem. Commun.* **1994**, 1465–1466.

(87) Sinha, A. K.; Seelan, S. Characterization of SAPO-11 and SAPO-31 Synthesized from Aqueous and Non-Aqueous Media. *Appl. Catal. A Gen.* **2004**, *270*, 245–252.

(88) Tiuliukova, I. A.; Rudina, N. A.; Lysikov, A. I.; Cherepanova, S. V.; Parkhomchuk, E. V. Screw-like Morphology of Silicoaluminophosphate-11 (SAPO-11) Crystallized in Ethanol Medium. *Mater. Lett.* **2018**, *228*, 61–64.

(89) Venkatathri, N.; Hegde, S. G.; Rajamohanan, P. R.; Sivasanker, S. Synthesis of SAPO-35 in Non-Aqueous Gels. *J. Chem. Soc. Faraday Trans.* **1997**, *93* (18), 3411–3415.

(90) Venkatathri, N. Synthesis and Characterization of High Silica Content Silicoaluminophosphate SAPO-35 from Non-Aqueous Medium. *Catal. Commun.* **2006**, *7*, 773–777.

(91) Kanno, N.; Miyake, M.; Sato, M. Syntheses of Ferrierite, ZSM-48, and ZSM-5 in Glycerol Solvent. *Zeolites* **1994**, *14*, 625–628.

(92) Wei, Y.; Tian, Z.; Gies, H.; Xu, R.; Ma, H.; Pei, R.; Zhang, W.; Xu, Y.; Wang, L.; Li, K.; et al. Ionothermal Synthesis of an Aluminophosphate Molecular Sieve with 20-Ring Pore Openings. *Angew. Chemie - Int. Ed.* **2010**, *49* (31), 5367–5370.

(93) Rogers, R. D.; Seddon, K. R. Ionic Liquids - Solvents of the Future? *Science* **2003**, *302*, 792–793.

(94) Nockemann, P.; Thijs, B.; Pittois, S.; Thoen, J.; Glorieux, C.; Van Hecke, K.; Van Meervelt, L.; Kirchner, B.; Binnemans, K. Task-Specific Ionic Liquid for Solubilizing Metal Oxides. *J. Phys. Chem. B* **2006**, *110*, 20978–20992.

(95) Reichert, W. M.; Holbrey, J. D.; Vigour, K. B.; Morgan, T. D.; Broker, G. A.; Rogers, R. D. Approaches to Crystallization from Ionic Liquids: Complex Solvents-Complex Results, or, a Strategy for Controlled Formation of New Supramolecular Architectures? *Chem. Commun.* **2006**, No. 46, 4767–4779.

(96) Cooper, E. R.; Andrews, C. D.; Wheatley, P. S.; Webb, P. B.; Wormald, P.; Morris, R. E. Ionic Liquids and Eutectic Mixtures as Solvent and Template in Synthesis of Zeolite Analogues. *Nature* **2004**, *430*, 1012–1016.

(97) Parnham, E. R.; Wheatley, P. S.; Morris, R. E. The Ionothermal Synthesis of SIZ-6 - A Layered Aluminophosphate. *Chem. Commun.* **2006**, 380–382.

(98) Wheatley, P. S.; Allan, P. K.; Teat, S. J.; Ashbrook, S. E.;

Morris, R. E. Task Specific Ionic Liquids for the Ionothermal Synthesis of Siliceous Zeolites. *Chem. Sci.* **2010**, *1*, 483–487.

(99) Parnham, E. R.; Morris, R. E. The Ionothermal Synthesis of Cobalt Aluminophosphate Zeolite Frameworks. *J. Am. Chem. Soc.* **2006**, *128*, 2204–2205.

(100) Parnham, E. R.; Morris, R. E. 1-Alkyl-3-Methyl Imidazolium Bromide Ionic Liquids in the Ionothermal Synthesis of Aluminium Phosphate Molecular Sieves. *Chem. Mater.* **2006**, *18*, 4882–4887.

(101) Ma, H.; Xu, R.; You, W.; Wen, G.; Wang, S.; Xu, Y.; Wang, B.; Wang, L.; Wei, Y.; Xu, Y.; et al. Ionothermal Synthesis of Gallophosphate Molecular Sieves in 1-Alkyl-3-Methyl Imidazolium Bromide Ionic Liquids. *Microporous Mesoporous Mater.* **2009**, *120*, 278–284.

(102) Ma, H.; Tian, Z.; Xu, R.; Wang, B.; Wei, Y.; Wang, L.; Xu, Y.; Zhang, W.; Lin, L. Effect of Water on the Ionothermal Synthesis of Molecular Sieves. *J. Am. Chem. Soc.* **2008**, *130*, 8120–8121.

(103) Wang, L.; Xu, Y.; Wei, Y.; Duan, J.; Chen, A.; Wang, B.; Ma, H.; Tian, Z.; Lin, L. Structure-Directing Role of Amines in the Ionothermal Synthesis. *J. Am. Chem. Soc.* **2006**, *128*, 7432–7433.

(104) Xing, H.; Li, J.; Yan, W.; Chen, P.; Jin, Z.; Yu, J.; Dai, S.; Xu, R. Cotemplating Ionothermal Synthesis of a New Open-Framework Aluminophosphate with Unique Al/P Ratio of 6/7. *Chem. Mater.* **2008**, *20*, 4179–4181.

(105) Xu, R.; Zhang, W.; Guan, J.; Xu, Y.; Wang, L.; Ma, H.; Tian, Z.; Han, X.; Lin, L.; Bao, X. New Insights into the Role of Amines in the Synthesis of Molecular Sieves in Ionic Liquids. *Chem. - A Eur. J.* **2009**, *15*, 5348–5354.

(106) Tuckerman, M. E.; Marx, D.; Parrinello, M. The Nature and Transport Mechanism of Hydrated Hydroxide Ions in Aqueous Solution. *Nature* **2002**, *417*, 925–929.

(107) Parnham, E. R.; Morris, R. E. Ionothermal Synthesis of Zeolites, Metal-Organic Frameworks, and Inorganic-Organic Hybrids. *Acc. Chem. Res.* **2007**, *40*, 1005–1013.

(108) Wang, Y.; Xu, Y.; Tian, Z.; Lin, L. Research Progress in Ionothermal Synthesis of Molecular Sieves. *Chinese J. Catal.* **2012**, *33*, 39–50.

(109) Li, C.; Moliner, M.; Corma, A. Building Zeolites from Precrystallized Units: Nanoscale Architecture. *Angew. Chemie - Int. Ed.* **2018**, *57*, 15330–15353.

(110) Nakazawa, N.; Ikeda, T.; Hiyoshi, N.; Yoshida, Y.; Han, Q.; Inagaki, S.; Kubota, Y. A Microporous Aluminosilicate with 12-, 12-, and 8-Ring Pores and Isolated 8-Ring Channels. *J. Am. Chem. Soc.* **2017**, *139*, 7989–7997.

(111) Martín, N.; Moliner, M.; Corma, A. High Yield Synthesis of High-Silica Chabazite by Combining the Role of Zeolite Precursors and Tetraethylammonium: SCR of NOx. *Chem. Commun.* **2015**, *51*, 9965–9968.

(112) Sano, T.; Itakura, M.; Sadakane, M. High Potential of Interzeolite Conversion Method for Zeolite Synthesis. *J. Japan Pet. Inst.* **2013**, *56* (4), 183–197.

(113) Ke, Q.; Sun, T.; Cheng, H.; Wei, X.; Guo, Y.; Zhao, S.; Zeng, S.; Wang, S. Accelerated Construction of High-Silica RHO and CHA Zeolites via Interzeolite Transformation and Their NH3–SCR Performances after Copper Exchange. *Ind. Eng. Chem. Res.* **2018**, *57*, 16763–16771.

(114) Goel, S.; Zones, S. I.; Iglesia, E. Synthesis of Zeolites via Interzeolite Transformations without Organic Structure-Directing Agents. *Chem. Mater.* **2015**, *27*, 2056–2066.

(115) Martín, N.; Boruntea, C. R.; Moliner, M.; Corma, A. Efficient Synthesis of the Cu-SSZ-39 Catalyst for DeNOx Applications. *Chem. Commun.* **2015**, *51*, 11030–11033.

(116) Maruo, T.; Yamanaka, N.; Tsunoj, N.; Sadakane, M.; Sano, T. Facile Synthesis of AEI Zeolites by Hydrothermal Conversion of FAU Zeolites in the Presence of Tetraethylphosphonium Cations. *Chem. Lett.* **2014**, *43*, 302–304.

(117) Sonoda, T.; Maruo, T.; Yamasaki, Y.; Tsunoji, N.; Takamitsu, Y.; Sadakane, M.; Sano, T. Synthesis of High-Silica AEI Zeolites with Enhanced Thermal Stability by Hydrothermal Conversion of FAU Zeolites, and Their Activity in the Selective Catalytic Reduction of NOx with NH3. *J. Mater. Chem. A* **2015**, *3*, 857–865.

(118) Xu, H.; Wu, Q.; Chu, Y.; Jiang, J.; Zhang, L.; Pan, S.; Zhang, C.; Zhu, L.; Deng, F.; Meng, X.; et al. Efficient Synthesis of Aluminosilicate RTH Zeolite with Good Catalytic Performances in NH3-SCR and MTO Reactions. *J. Mater. Chem. A* **2018**, *6*, 8705–8711.

(119) Schmidt, J. E.; Deimund, M. A.; Xie, D.; Davis, M. E. Synthesis of RTH-Type Zeolites Using a Diverse Library of Imidazolium Cations. *Chem. Mater.* **2015**, *27*, 3756–3762.

(120) Boruntea, C. R.; Lundegaard, L. F.; Corma, A.; Vennestrøm, P. N. R. Crystallization of AEI and AFX Zeolites through Zeolite-to-Zeolite Transformations. *Microporous Mesoporous Mater.* **2019**, *278*, 105–114.

(121) Nakazawa, N.; Inagaki, S.; Kubota, Y. Direct Hydrothermal Synthesis of High-Silica SSZ-39 Zeolite with Small Particle Size. *Chem. Lett.* **2016**, *45*, 919–921.

(122) Nakazawa, N.; Inagaki, S.; Kubota, Y. Novel Technique to Synthesize AFX-Type Zeolite Using a Bulky and Rigid Diquaternary Ammonium Cation. *Adv. Porous Mater.* **2016**, *4*, 219–229.

(123) Ji, Y.; Deimund, M. A.; Bhawe, Y.; Davis, M. E. Organic-Free Synthesis of CHA-Type Zeolite Catalysts for the Methanol-to-Olefins Reaction. *ACS Catal.* **2015**, *5*, 4456–4465.

(124) Itakura, M.; Goto, I.; Takahashi, A.; Fujitani, T.; Ide, Y.; Sadakane, M.; Sano, T. Synthesis of High-Silica CHA Type Zeolite by Interzeolite Conversion of FAU Type Zeolite in the Presence of Seed Crystals. *Microporous Mesoporous Mater.* **2011**, *144*, 91–96.

(125) Zones, S. I. Conversion of Faujasites to High-Silica Chabazite SSZ-13 in the Presence of N,N,N-Trimethyl-l -Adamantammonium Iodide. *J. Chem. Soc. Faraday Trans.* **1991**, *87* (22), 3709–3716.

(126) Itakura, M.; Inoue, T.; Takahashi, A.; Fujitani, T.; Oumi, Y.; Sano, T. Synthesis of High-Silica CHA Zeolite from FAU Zeolite in the Presence of Benzyltrimethylammonium Hydroxide. *Chem. Lett.* **2008**, *37* (9), 908–909.

(127) Xiong, X.; Yuan, D.; Wu, Q.; Chen, F.; Meng, X.; Lv, R.; Dai, D.; Maurer, S.; McGuire, R.; Feyen, M.; et al. Efficient and Rapid Transformation of High Silica CHA Zeolite from FAU Zeolite in the Absence of Water. *J. Mater. Chem. A* **2017**, *5*, 9076–9080.

(128) Jon, H.; Ikawa, N.; Oumi, Y.; Sano, T. An Insight into the Process Involved in Hydrothermal Conversion of FAU to *BEA Zeolite. *Chem. Mater.* **2008**, *20*, 4135–4141.

(129) Honda, K.; Yashiki, A.; Itakura, M.; Ide, Y.; Sadakane, M.; Sano, T. Influence of Seeding on FAU –*BEA Interzeolite Conversions. *Microporous Mesoporous Mater.* **2011**, *142*, 161–167.

(130) Piccione, P. M.; Laberty, C.; Yang, S.; Camblor, M. A.; Navrotsky, A.; Davis, M. E. Thermochemistry of Pure-Silica Zeolites. *J. Phys. Chem. B* **2000**, *104*, 10001–10011.

(131) Anthony, J. L.; Davis, M. E. Assembly of Zeolites and Crystalline Molecular Sieves. In *Self-Organized Nanoscale Materials*; Adachi, M., Lockwood, D. J., Eds.; Springer New York,: New York, NY, 2006; pp 159–185.

(132) Van Tendeloo, L.; Gobechiya, E.; Breynaert, E.; Martens, J. A.; Kirschhock, C. E. A. Alkaline Cations Directing the Transformation of FAU Zeolites into Five Different Framework Types. *Chem. Commun.* **2013**, *49*, 11737–11739.

(133) Xu, H.; Zhang, J.; Wu, Q.; Chen, W.; Lei, C.; Zhu, Q.; Han, S.; Fei, J.; Zheng, A.; Zhu, L.; et al. Direct Synthesis of Aluminosilicate SSZ-39 Zeolite Using Colloidal Silica as a Starting Source. *ACS Appl. Mater. Interfaces* **2019**, *11*, 23112–23117.

(134) Khan, N. A.; Yoo, D. K.; Bhadra, B. N.; Jun, J. W.; Kim, T.-W.; Kim, C.-U.; Jhung, S. H. Preparation of SSZ-13 Zeolites from Beta Zeolite and Their Application in the Conversion of Ethylene to Propylene. *Chem. Eng. J.* **2019**, *377*, 119546.

(135) Tang, L.; Haw, K.-G.; Zhang, Y.; Fang, Q.; Qiu, S.; Valtchev,

V. Fast and Efficient Synthesis of SSZ-13 by Interzeolite Conversion of Zeolite Beta and Zeolite L. *Microporous Mesoporous Mater.* **2019**, *280*, 306–314.

(136) Xu, H.; Chen, W.; Wu, Q.; Lei, C.; Zhang, J.; Han, S.; Zhang, L.; Zhu, Q.; Meng, X.; Dai, D.; et al. Transformation Synthesis of Aluminosilicate SSZ-39 Zeolite from ZSM-5 and Beta Zeolite. *J. Mater. Chem. A* **2019**, *7*, 4420–4425.

(137) Cizmek, A.; Subotic, B.; Aiello, R.; Crea, F.; Nastro, A.; Tuoto, C. Dissolution of High-Silica Zeolites in Alkaline Solutions I. Dissolution of Silicalite-1 and ZSM-5 with Different Aluminum Content. *Microporous Mater.* **1995**, 159–168.

(138) Goto, I.; Itakura, M.; Shibata, S.; Honda, K.; Ide, Y.; Sadakane, M.; Sano, T. Transformation of LEV-Type Zeolite into Less Dense CHA-Type Zeolite. *Microporous Mesoporous Mater.* **2012**, *158*, 117–122.

(139) Honda, K.; Itakura, M.; Matsuura, Y.; Onda, A.; Ide, Y.; Sadakane, M.; Sano, T. Role of Structural Similarity Between Starting Zeolite and Product Zeolite in the Interzeolite Conversion Process. *J. Nanosci. Nanotechnol.* **2013**, *13*, 3020–3026.

(140) Joichi, Y.; Shimono, D.; Tsunoji, N.; Takamitsu, Y.; Sadakane, M.; Sano, T. Stepwise Gel Preparation for High-Quality CHA Zeolite Synthesis: A Common Tool for Synthesis Diversification. *Cryst. Growth Des.* **2018**, *18* (9), 5652–5662.

(141) Qin, W.; Jain, R.; Robles Hernández, F. C.; Rimer, J. D. Organic-Free Interzeolite Transformation in the Absence of Common Building Units. *Chem. - A Eur. J.* **2019**, *25* (23), 5893–5898.

(142) Barrer, R. M.; Denny, P. J. Hydrothermal Chemistry of the Silicates. Part IX. Nitrogeneous Aluminosilicates. *J. Chem. Soc.* **1961**, 971–982.

(143) Lobo, R. F.; Zones, S. I.; Davis, M. E. Structure-Direction in Zeolite Synthesis. *J. Incl. Phenom. Mol. Recognit. Chem.* **1995**, *21*, 47–78.

(144) Blackwell, C. S.; Broach, R. W.; Gatter, M. G.; Holmgren, J. S.; Jan, D.-Y.; Lewis, G. J.; Mezza, B. J.; Mezza, T. M.; Miller, M. A.; Moscoso, J. G.; et al. Open-Framework Materials Synthesized in the TMA+/TEA+ Mixed-Template System: The New Low Si/Al Ratio Zeolites UZM-4 and UZM-5. *Angew. Chemie Int. Ed.* **2003**, *42*, 1737–1740.

(145) Miller, M. A.; Moscoso, J. G.; Koster, S. C.; Gatter, M. G.; Lewis, G. J. Synthesis and Characterization of the 12-Ring Zeolites UZM-4 (BPH) and UZM-22 (MEI) via the Charge Density Mismatch Approach in the Choline-Li2O-SrO-Al2O3-SiO2 System. In *Studies in Surface Science and Catalysis*; Elsevier B.V., 2007; Vol. 170, pp 347–354.

(146) Park, M. B.; Jo, D.; Jeon, H. C.; Nicholas, C. P.; Lewis, G. J.; Hong, S. B. Zeolite Synthesis from a Charge Density Perspective: The Charge Density Mismatch Synthesis of UZM-5 and UZM-9. *Chem. Mater.* **2014**, *26*, 6684–6694.

(147) Broach, R. W.; Boldingh, E. P.; Jan, D.-Y.; Lewis, G. J.; Moscoso, J. G.; Bricker, J. C. Tailoring Zeolite Morphology by Charge Density Mismatch for Aromatics Processing. *J. Catal.* **2013**, *308*, 142–153.

(148) Kim, S. H.; Park, M. B.; Min, H.; Hong, S. B. Zeolite Synthesis in the Tetraethylammonium – Tetramethylammonium Mixed-Organic Additive System. *Microporous Mesoporous Mater.* **2009**, *123*, 160–168.

(149) Lee, J. H.; Park, M. B.; Lee, J. K.; Min, H.; Song, M. K.; Hong, S. B. Synthesis and Characterization of ERI-Type UZM-12 Zeolites and Their Methanol-to-Olefin Performance. *J. Am. Chem. Soc.* **2010**, *132*, 12971–12982.

(150) Park, M. B.; Cho, S. J.; Hong, S. B. Synthesis of Aluminosilicate and Gallosilicate Zeolites via a Charge Density Mismatch Approach and Their Characterization. *J. Am. Chem. Soc.* **2011**, *133*, 1917–1934.

(151) Park, M. B.; Ahn, H. A.; Nicholas, C. P.; Lewis, G. J.; Hong, S. B. Charge Density Mismatch Synthesis of Zeolite Beta in the Presence of Tetraethylammonium, Tetramethylammonium, and Sodium Ions: Influence of Tetraethylammonium Decomposition. *Microporous Mesoporous Mater.* **2017**, *240*,

159–168.

(152) Guo, Y.; Sun, T.; Liu, X.; Ke, Q.; Wei, X.; Gu, Y.; Wang, S. Cost-Effective Synthesis of CHA Zeolites with Controllable Morphology and Size. *Chem. Eng. J.* **2019**, *358*, 331–339.

(153) Lewis, G. J.; Miller, M. A.; Moscoso, J. G.; Wilson, B. A.; Knight, L. M.; Wilson, S. T. Experimental Charge Density Matching Approach to Zeolite Synthesis. *Stud. Surf. Sci. Catal.* **2004**, *154*, 364–372.

(154) Moteki, T.; Okubo, T. From Charge Density Mismatch to a Simplified, More Efficient Seed-Assisted Synthesis of UZM-4. *Chem. Mater.* **2013**, *25* (13), 2603–2609.

(155) Feng, G.; Cheng, P.; Yan, W.; Boronat, M.; Li, X.; Su, J.; Wang, J.; Li, Y.; Corma, A.; Xu, R.; et al. Accelerated Crystallization of Zeolites via Hydroxyl Free Radicals. *Science* **2016**, *351* (6278), 1188–1192.

(156) Cheng, P.; Feng, G.; Sun, C.; Xu, W.; Su, J.-H.; Yan, W.; Yu, J. An Efficient Synthetic Route to Accelerate the Zeolite Synthesis via Radicals. *Inorg. Chem. Front.* **2018**, *5* (9), 2106–2110.

(157) Miyazawa, K.; Inagaki, S. Control of the Microporosity within the Pore Walls of Ordered Mesoporous Silica SBA-15. *Chem. Commun.* **2000**, 2121–2122.

(158) Feng, G.; Wang, J.; Boronat, M.; Li, Y.; Su, J.; Huang, J.; Ma, Y.; Yu, J. Radical-Facilitated Green Synthesis of Highly Ordered Mesoporous Silica Materials. *J. Am. Chem. Soc.* **2018**, *140*, 4770–4773.

(159) Cheng, P.; Song, M.; Zhang, H.; Xuan, Y.; Wu, C. Accelerated Synthesis of Zeolites via Radicalized Seeds. *J. Mater. Sci.* **2019**, *54* (6), 4573–4578.

(160) Watanabe, T.; Isobe, T.; Senna, M. Mechanisms of Incipient Chemical Reaction between Ca(OH)2 and SiO2 under Moderate Mechanical Stressing II: Examination of a Radical Mechanism by an EPR Study. *J. Solid State Chem.* **1996**, *122*, 291–296.

(161) Watanabe, T.; Hasegawa, S.; Wakiyama, N.; Usui, F.; Kusai, A.; Isobe, T.; Senna, M. Solid State Radical Recombination and Charge Transfer across the Boundary between Indomethacin and Silica under Mechanical Stress. *J. Solid State Chem.* **2002**, *164*, 27–33.

(162) Inaki, Y.; Yoshida, H.; Yoshida, T.; Hattori, T. Active Sites on Mesoporous and Amorphous Silica Materials and Their Photocatalytic Activity: An Investigation by FTIR, ESR, VUV-UV and Photoluminescence Spectroscopies. *J. Phys. Chem. B* **2002**, *106*, 9098–9106.

(163) Zeleňák, V.; Zeleňáková, A.; Kováč, J. Insight into Surface Heterogenity of SBA-15 Silica: Oxygen Related Defects and Magnetic Properties. *Colloids Surfaces A Physicochem. Eng. Asp.* **2010**, *357*, 97–104.

(164) Shi, D.; Xu, L.; Chen, P.; Ma, T.; Lin, C.; Wang, X.; Xu, D.; Sun, J. Hydroxyl Free Radical Route to the Stable Siliceous Ti-UTL with Extra-Large Pores for Oxidative Desulfurization. *Chem. Commun.* **2019**, *55*, 1390–1393.

(165) Tan, C.; Liu, Z.; Yonezawa, Y.; Sukenaga, S.; Ando, M.; Shibata, H.; Sasaki, Y.; Okubo, T.; Wakihara, T. Unique Crystallization Behavior in Zeolite Synthesis under External High Pressures. *Chem. Commun.* **2020**, *56*, 2811–2814.

(166) Bian, C.; Zhang, C.; Pan, S.; Chen, F.; Zhang, W.; Meng, X.; Maurer, S.; Dai, D.; Parvulescu, A. N.; Müller, U.; et al. Generalized High-Temperature Synthesis of Zeolite Catalysts with Unpredictably High Space-Time Yields (STYs). *J. Mater. Chem. A* **2017**, *5*, 2613–2618.

(167) Li, Q.; Creaser, D.; Sterte, J. The Nucleation Period for TPA-Silicalite-1 Crystallization Determined by a Two-Stage Varying-Temperature Synthesis. *Microporous Mesoporous Mater.* **1999**, *31*, 141–150.

(168) Sun, H.; Wang, J.; Hu, J.; Zhou, J. Rapid Synthesis of Small Crystal FeZSM-5 by a Two-Stage Varying-Temperature Technique. *Catal. Letters* **2000**, *69*, 245–250.

(169) Sang, S.; Liu, Z.; Tian, P.; Liu, Z.; Qu, L.; Zhang, Y. Synthesis of Small Crystals Zeolite NaY. *Mater. Lett.* **2006**, *60*, 1131–1133.

(170) Li, Q.; Creaser, D.; Sterte, J. An Investigation of the

Nucleation/Crystallization Kinetics of Nanosized Colloidal Faujasite Zeolites. *Chem. Mater.* **2002**, *14* (3), 1319–1324.

(171) Hui, K. S.; Chao, C. Y. H. Effects of Step-Change of Synthesis Temperature on Synthesis of Zeolite 4A from Coal Fly Ash. *Microporous Mesoporous Mater.* **2006**, *88*, 145–151.

(172) Yin, X.; Chu, N.; Lu, X.; Li, Z.; Guo, H. Cost-Effective Two-Stage Varying-Temperature Rapid Crystallization of Zeolite T and SAPO-34. *J. Cryst. Growth* **2016**, *441*, 1–11.

(173) Cheng, Y.; Lu, M.; Li, J.; Su, X.; Pan, S.; Jiao, C.; Feng, M. Synthesis of MCM-22 Zeolite Using Rice Husk as a Silica Source under Varying-Temperature Conditions. *J. Colloid Interface Sci.* **2012**, *369* (1), 388–394.

(174) Güray, I.; Warzywoda, J.; Baç, N.; Sacco Jr., A. Synthesis of Zeolite MCM-22 under Rotating and Static Conditions. *Microporous Mesoporous Mater.* **1999**, *31*, 241–251.

(175) Deneyer, A.; Ennaert, T.; Cavents, G.; Dijkmans, J.; Vanneste, J.; Courtin, C. M.; Dusselier, M.; Sels, B. F. Compositional and Structural Feedstock Requirements of a Liquid Phase Cellulose-to-Naphtha Process in a Carbon- and Hydrogen-Neutral Biorefinery Context. *Green Chem.* **2016**, *18* (20), 5594–5606.

(176) Wang, P.; Yang, D.; Hu, J.; Xu, J.; Lu, G. Synthesis of SAPO-34 with Small and Tunable Crystallite Size by Two-Step Hydrothermal Crystallization and Its Catalytic Performance for MTO Reaction. *Catal. Today* **2013**, *212*, 62.e1-62.e8.

(177) Guo, Z.; Miao, P.; Zhu, W.; Guo, L.; Li, F.; Xue, Y.; Yin, Q.; Yuan, R.; Xu, L. Synthesis of SAPO-34 Molecular Sieves via Novel Intermittent Hydrothermal Treatment and Its Effect on the Crystallization and Product Properties. *Catalysts* **2017**, *7*.

(178) Luo, M.; Wang, D.; Fu, Y.; Mao, G.; Wang, B. Three-Stage Crystallization : An Effective Way to Reduce the Crystal Size and Improve the Catalytic Performance of SAPO-34 for MTO. *Eur. J. Inorg. Chem.* **2018**, 3491–3495.

(179) Bakhtiar, S. ul H.; Ali, S.; Wang, X.; Yuan, F.; Li, Z.; Zhu, Y. Synthesis of Sub-Micrometric SAPO-34 by Morpholine Assisted Two-Step Hydrothermal Route and Its Excellent Catalytic MTO Performance. *Dalt. Trans.* **2019**, *48*, 2606–2616.

(180) Deimund, M. A.; Harrison, L.; Lunn, J. D.; Liu, Y.; Malek, A.; Shayib, R.; Davis, M. E. Effect of Heteroatom Concentration in SSZ-13 on the Methanol-to-Olefins Reaction. *ACS Catal.* **2016**, *6*, 542–550.

(181) Martín, N.; Li, Z.; Martínez-Triguero, J.; Yu, J.; Moliner, M.; Corma, A. Nanocrystalline SSZ-39 Zeolite as an Efficient Catalyst for the Methanol-to-Olefin (MTO) Process. *Chem. Commun.* **2016**, *52*, 6072–6075.

(182) Gharibeh, M.; Tompsett, G.; Lu, F.; Auerbach, S. M.; Yngvesson, K. S.; Conner, W. C. Temperature Distributions within Zeolite Precursor Solutions in the Presence of Microwaves. *J. Phys. Chem. B* **2009**, *113*, 12506–12520.

(183) Liu, Z.; Wakihara, T.; Nishioka, D.; Oshima, K.; Takewaki, T.; Okubo, T. One-Minute Synthesis of Crystalline Microporous Aluminophosphate (AlPO4 -5) by Combining Fast Heating with a Seed-Assisted Method. *Chem. Commun.* **2014**, *50*, 2526–2528.

(184) Xu, X. T.; Zhai, J. P.; Li, I. L.; Tang, J. N.; Ruan, S. C. Synthesis of Large Single Crystals of SAPO-47 in the Presence of Diethylamine Using Two-Step Temperature Process. *Microporous Mesoporous Mater.* **2012**, *148*, 122–130.

(185) Nag, A.; Baksi, A.; Ghosh, J.; Kumar, V.; Bag, S.; Mondal, B.; Ahuja, T.; Pradeep, T. Tribochemical Degradation of Polytetrafluoroethylene in Water and Generation of Nanoplastics. *ACS Sustain. Chem. Eng.* **2019**, *7* (21), 17554–17558.

(186) Pentsak, E. O.; Eremin, D. B.; Gordeev, E. G.; Ananikov, V. P. Phantom Reactivity in Organic and Catalytic Reactions as a Consequence of Microscale Destruction and Contamination-Trapping Effects of Magnetic Stir Bars. *ACS Catal.* **2019**, *9*, 3070–3081.

(187) Chen, C.-T.; Iyoki, K.; Yamada, H.; Sukenaga, S.; Ando, M.;

(188) Shibata, H.; Ohara, K.; Wakihara, T.; Okubo, T. Zeolite Crystallization Triggered by Intermediate Stirring. *J. Phys. Chem. C* **2019**, *123*, 20304–20313.

(188) Di Renzo, F. Zeolites as Tailor-Made Catalysts : Control of the Crystal Size. *Catal. Today* **1998**, *41*, 37–40.

(189) Ding, L.; Zheng, Y.; Zhang, Z.; Ring, Z.; Chen, J. Effect of Agitation on the Synthesis of Zeolite Beta and Its Synthesis Mechanism in Absence of Alkali Cations. *Microporous Mesoporous Mater.* **2006**, *94*, 1–8.

(190) Bohström, Z.; Arstad, B.; Petter, K. Preparation of High Silica Chabazite with Controllable Particle Size. *Microporous Mesoporous Mater.* **2014**, *195*, 294–302.

(191) Zhan, B.; White, M. A.; Lumsden, M.; Mueller-neuhaus, J.; Robertson, K. N.; Cameron, T. S.; Gharghouri, M. Control of Particle Size and Surface Properties of Crystals of NaX Zeolite. *Chem. Mater.* **2002**, No. 14, 3636–3642.

(192) Mainganye, D.; Ojumu, T. V.; Petrik, L. Synthesis of Zeolites Na-P1 from South African Coal Fly Ash: Effect of Impeller Design and Agitation. *Materials (Basel).* **2013**, *6*, 2074–2089.

(193) Derewinski, M.; Machowska, M. Effect of Stirring on the Selective Synthesis of MEL or TON Zeolites in the Presence of 1,8-Diaminooctane. *Stud. Surf. Sci. Catal.* **2004**, *154*, 349–354.

(194) Bedard, R. L. Synthesis of Zeolites and Manufacture of Zeolitic Catalysts and Adsorbents. In *Zeolites in Industrial Separation and Catalysis*; Kulprathipanja, S., Ed.; Wiley, 2010; pp 61–83.

(195) Rollmann, L. D.; Valyocsik, E. W. Continuous-Stream Method of Preparing Crystalline Zeolites (EP0021675B1), 1980.

(196) Bretaudeau, D.; Delprato, F.; Malassis, M. Process for Preparing Crystallized 4A Zeolite (EP0485262B1), 1996.

(197) Frilette, V. J.; Kerr, G. T. Process for Making Crystalline Zeolites (US3071434), 1963.

(198) Hirsh, W. Production of Crystalline Zeolites (US3425800), 1969.

(199) Deabriges, J. Industrial Process for Continuous Production of Zeolite A (US4314979), 1982.

(200) Bretaudeau, D.; Delprato, F.; Malassis, M. Preparation of Crystalline 4A Zeolites (US5474753), 1995.

(201) Tannous, M. K.; Marchioretto, S.; Monson, L. E. Process for Synthesizing and Controlling the Particle Size and Particle Size Distribution of a Molecular Sieve (US6656447B1), 2003.

(202) Roland, E. Industrial Production of Zeolites. In *Zeolites as Catalysts, Sorbents and Detergent Builders*; Karge, H. G., Weitkamp, J., Eds.; Elsevier Science Publishers B.V., 1989.

(203) Liu, Z.; Wakihara, T.; Nomura, N.; Matsuo, T.; Anand, C.; Elangovan, S. P.; Yanaba, Y.; Yoshikawa, T.; Okubo, T. Ultrafast and Continuous Flow Synthesis of Silicoaluminophosphates. *Chem. Mater.* **2016**, *28*, 4840–4847.

(204) Liu, Z.; Okabe, K.; Anand, C.; Yonezawa, Y.; Zhu, J.; Yamada, H.; Endo, A.; Yanaba, Y.; Yoshikawa, T.; Ohara, K.; et al. Continuous Flow Synthesis of ZSM-5 Zeolite on the Order of Seconds. *PNAS* **2016**, *113* (50), 14267–14271.

(205) Liu, Z.; Zhu, J.; Wakihara, T.; Okubo, T. Ultrafast Synthesis of Zeolites: Breakthrough, Progress and Perspective. *Inorg. Chem. Front.* **2019**, *6*, 14–31.

(206) Peng, C.; Liu, Z.; Okubo, T.; Wakihara, T. Fast Synthesis of SSZ-24 : A Pure Silica Zeolite with AFI Framework. *Chem. Lett.* **2018**, *47* (5), 654–656.

(207) Zhu, J.; Liu, Z.; Sukenaga, S.; Ando, M.; Shibata, H.; Okubo, T.; Wakihara, T. Ultrafast Synthesis of * BEA Zeolite without the Aid of Aging Pretreatment. *Microporous Mesoporous Mater.* **2018**, *268*, 1–8.

(208) Zhu, J.; Liu, Z.; Iyoki, K.; Anand, C.; Yoshida, K.; Sasaki, Y.; Sukenaga, S.; Ando, M.; Shibata, H.; Okubo, T.; et al. Ultrafast Synthesis of High-Silica Erionite Zeolites with Improved Hydrothermal Stability. *Chem. Commun.* **2017**, *53*, 6796–6799.

(209) Liu, Z.; Wakihara, T.; Anand, C.; Keoh, S. H.; Nishioka, D.;

Hotta, Y.; Matsuo, T.; Takewaki, T.; Okubo, T. Ultrafast Synthesis of Silicalite-1 Using a Tubular Reactor with a Feature of Rapid Heating. *Microporous Mesoporous Mater.* **2016**, *223*, 140–144.

(210) Vandermeersch, T.; Van Assche, T. R. C.; Denayer, J. F. M.; De Malsche, W. A Continuous Flow Reactor Setup as a Tool for Rapid Synthesis of Micron Sized NaA Zeolite. *Microporous Mesoporous Mater.* **2016**, *226*, 133–139.

(211) Ju, J.; Zeng, C.; Zhang, L.; Xu, N. Continuous Synthesis of Zeolite NaA in a Microchannel Reactor. *Chem. Eng. J.* **2006**, *116*, 115–121.

(212) Tassopoulos, M.; Thompson, R. . Comparative Study of Zeolite A Synthesis in Batch and Semibatch Reactors. In *7th Int. Conf. Zeolites*; 1986; pp 153–160.

(213) Tassopoulos, M.; Thompson, R. W. Transformation Behaviour of Zeolite A to Hydroxysodalite in Batch and Semi-Batch Crystallizers. *Zeolites* **1987**, *7* (3), 243–248.

(214) Cundy, C. S.; Henty, M. S.; Plaisted, R. Zeolite Synthesis Using a Semicontinuous Reactor, Part 1 : Controlled Nucleation and Growth of ZSM-5 Crystals Having Well-Defined Morphologies. *Zeolites* **1995**, *15*, 353–372.

(215) Cundy, C. S.; Hentyt, M. S.; Plaisted, R. J. Zeolite Synthesis Using a Semicontinuous Reactor, Part 2 : Synthesis at High Nucleation Rates. *Zeolites* **1995**, *14*, 400–407.

(216) Metcalfe, I. S. *Chemical Reaction Engineering: A First Course*; Oxford University Press: Oxford, 1997.

(217) Chu, P.; Dwyer, F. G.; Vartuli, J. C. Crystallization Method Employing Microwave Radiation, 1988.

(218) Tompsett, G. A.; Conner, C.; Yngvesson, K. S. Microwave Synthesis of Nanoporous Materials. *ChemPhysChem* **2006**, *7*, 296–319.

(219) Arafat, A.; Jansen, J. C.; Ebaid, A. R.; van Bekkum, H. Microwave Preparation of Zeolite Y and ZSM-5. *Zeolites* **1993**, *13*, 162–165.

(220) Cundy, C. S.; Plaisted, R. J.; Zhao, J. P. Remarkable Synergy between Microwave Heating and the Addition of Seed Crystals in Zeolite Synthesis — a Suggestion Verified. *Chem. Commun.* **1998**, 1465–1466.

(221) Katsuki, H.; Furuta, S.; Komarneni, S. Microwave Versus Conventional-Hydrothermal Synthesis of NaY Zeolite. *J. Porous Mater.* **2001**, *8*, 5–12.

(222) Serrano, D. P.; Uguina, M. A.; Sanz, R.; Castillo, E.; Rodríquez, A.; Sánchez, P. Synthesis and Crystallization Mechanism of Zeolite TS-2 by Microwave and Conventional Heating. *Microporous Mesoporous Mater.* **2004**, *69*, 197–208.

(223) Jhung, S. H.; Chang, J.-S.; Hwang, J. S.; Park, S.-E. Selective Formation of SAPO-5 and SAPO-34 Molecular Sieves with Microwave Irradiation and Hydrothermal Heating. *Microporous Mesoporous Mater.* **2003**, *64*, 33–39.

(224) Slangen, P. M.; Jansen, J. C.; Van Bekkum, H. The Effect of Ageing on the Microwave Synthesis of Zeolite NaA. *Microporous Mater.* **1997**, *9*, 259–265.

(225) Chandrasekhar, S.; Pramada, P. N. Microwave Assisted Synthesis of Zeolite A from Metakaolin. *Microporous Mesoporous Mater.* **2008**, *108*, 152–161.

(226) Bonaccorsi, L.; Proverbio, E. Microwave Assisted Crystallization of Zeolite A from Dense Gels. *J. Cryst. Growth* **2003**, *247*, 555–562.

(227) Bukhari, S. S.; Behin, J.; Kazemian, H.; Rohani, S. Conversion of Coal Fly Ash to Zeolite Utilizing Microwave and Ultrasound Energies : A Review. *Fuel* **2015**, *140*, 250–266.

(228) Querol, X.; Alastuey, A.; López-Soler, A.; Plana, F.; Andrés, J. M.; Juan, R.; Ferrer, P.; Ruiz, C. R. A Fast Method for Recycling Fly Ash : Microwave-Assisted Zeolite Synthesis. *Environ. Sci. Technol.* **1997**, *31* (9), 2527–2533.

(229) Anuwattana, R.; Balkus Jr., K. J.; Asavapisit, S.; Khummongkol, P. Conventional and Microwave Hydrothermal Synthesis of Zeolite ZSM-5 from the Cupola Slag. *Microporous Mesoporous Mater.* **2008**, *111*, 260–266.

(230) Inada, M.; Tsujimoto, H.; Eguchi, Y.; Enomoto, N.; Hojo, J. Microwave-Assisted Zeolite Synthesis from Coal Fly Ash in

Hydrothermal Process. *Fuel* **2005**, *84*, 1482–1486.

(231) Conner, W. C.; Tompsett, G.; Lee, K.; Yngvesson, K. S. Microwave Synthesis of Zeolites: 1. Reactor Engineering. *J. Phys. Chem. B* **2004**, *108* (37), 13913–13920.

(232) Panzarella, B.; Tompsett, G. A.; Yngvesson, K. S.; Conner, W. C. Microwave Synthesis of Zeolites. 2. Effect of Vessel Size, Precursor Volume, and Irradiation Method. *J. Phys. Chem. B* **2007**, *111*, 12657–12667.

(233) Gharibeh, M.; Tompsett, G. A.; Yngvesson, K. S.; Conner, W. C. Microwave Synthesis of Zeolites: Effect of Power Delivery. *J. Phys. Chem. B* **2009**, *113*, 8930–8940.

(234) Askari, S.; Alipour, S. M.; Halladj, R.; Farahani, M. H. D. A. Effects of Ultrasound on the Synthesis of Zeolites : A Review. *J. Porous Mater.* **2013**, *20*, 285–302.

(235) Suslick, K. S. Sonochemistry. *Science* **1990**, *247*, 1439–1445.

(236) Mu, Y.; Zhang, Y.; Fan, J.; Guo, C. Effect of Ultrasound Pretreatment on the Hydrothermal Synthesis of SSZ-13 Zeolite. *Ultrason. Sonochem.* **2017**, *38*, 430–436.

(237) Behin, J.; Kazemian, H.; Rohani, S. Sonochemical Synthesis of Zeolite NaP from Clinoptilolite. *Ultrason. Sonochem.* **2016**, *28*, 400–408.

(238) Andaç, Ö.; Tatlier, M.; Sirkecioğlu, A.; Ece, I.; Erdem-Şenatalar, A. Effects of Ultrasound on Zeolite A Synthesis. *Microporous Mesoporous Mater.* **2005**, *79*, 225–233.

(239) Kim, D. S.; Chang, J.; Hwang, J.; Park, S.; Kim, J. M. Synthesis of Zeolite Beta in Fluoride Media under Microwave Irradiation. *Microporous Mesoporous Mater.* **2004**, *68*, 77–82.

(240) Youssef, H.; Ibrahim, D.; Komarneni, S. Microwave-Assisted versus Conventional Synthesis of Zeolite A from Metakaolinite. *Microporous Mesoporous Mater.* **2008**, *115*, 527–534.

(241) Romero, M. D.; Gómez, J. M.; Overjero, G.; Rodríguez, A. Synthesis of LSX Zeolite by Microwave Heating. *Mater. Res. Bull.* **2004**, *39*, 389–400.

(242) Wu, Y.; Ren, X.; Wang, J. Effect of Microwave-Assisted Aging on the Static Hydrothermal Synthesis of Zeolite MCM-22. *Microporous Mesoporous Mater.* **2008**, *116*, 386–393.

(243) Wang, B.; Wu, J.; Yuan, Z.; Li, N.; Xiang, S. Synthesis of MCM-22 Zeolite by an Ultrasonic-Assisted Aging Procedure. *Ultrason. Sonochem.* **2008**, *15*, 334–338.

(244) Han, J.; Ha, Y.; Guo, M.; Zhao, P.; Liu, Q.; Liu, C.; Song, C.; Ji, N.; Lu, X.; Ma, D.; et al. Synthesis of Zeolite SSZ-13 from Coal Gangue via Ultrasonic Pretreatment Combined with Hydrothermal Growth Method. *Ultrason. - Sonochemistry* **2019**, *59*, 104703.

(245) Charghand, M.; Haghighi, M.; Saedy, S.; Aghamohammadi, S. Efficient Hydrothermal Synthesis of Nanostructured SAPO-34 Using Ultrasound Energy: Physicochemical Characterization and Catalytic Performance toward Methanol Conversion to Light Olefins. *Adv. Powder Technol.* **2014**, *25*, 1728–1736.

(246) Ahmadova, R.; Ibragimov, H.; Kondratenko, E.; Rodemerc, U. Synthesis of SAPO-34 Catalysts via Sonochemically Prepared Method and Its Catalytic Performance in Methanol Conversion to Light Olefins. *Appl. Petrochemical Res.* **2018**, *8*, 13–20.

(247) Ng, E.-P.; Awala, H.; Ghoy, J.-P.; Vicente, A.; Ling, T. C.; Ng, Y. H.; Mintova, S.; Adam, F. Effects of Ultrasonic Irradiation on Crystallization and Structural Properties of EMT-Type Zeolite Nanocrystals. *Mater. Chem. Phys.* **2015**, *159*, 38–45.

(248) Jusoh, N.; Yeong, Y. F.; Mohamad, M.; Lau, K. K.; Shariff, A. M. Rapid-Synthesis of Zeolite T via Sonochemical-Assisted Hydrothermal Growth Method. *Ultrason. Sonochem.* **2017**, *34*, 273–280.

(249) Mendoza, H. R.; Jordens, J.; Pereira, M. V. L.; Lutz, C.; Van Gerven, T. Effects of Ultrasonic Irradiation on Crystallization Kinetics, Morphological and Structural Properties of Zeolite FAU. *Ultrason. Sonochem.* **2020**, *64*, 105010.

(250) Subotic, B.; Smit, I.; Madzija, O.; Sekovanic, L. Kinetic Study of the Transformation of Zeolite A into Zeolite P. *Zeolites*

1982, 2, 135–142.

(251) Azizi, S. N.; Tilami, S. E. Recrystallization of Zeolite Y to Analcime and Zeolite P with d -Methionine as Structure-Directing Agent (SDA). *Zeitschrift für Anorg. und algemeine Chemie* 2009, 635, 2660–2664.

(252) Hoffmann, J.; Nüchter, M.; Ondruschka, B.; Wasserscheid, P. Ionic Liquids and Their Heating Behaviour during Microwave Irradiation - A State of the Art Report and Challenge to Assessment. *Green Chem.* 2003, 5, 296–299.

(253) Leadbeater, N. E.; Torenius, H. M. A Study of the Ionic Liquid Mediated Microwave Heating of Organic Solvents. *J. Org. Chem.* 2002, 67, 3145–3148.

(254) Debecker, D. P.; Le Bras, S.; Boissière, C.; Chaumonnot, A.; Sanchez, C. Aerosol Processing: A Wind of Innovation in the Field of Advanced Heterogeneous Catalysts. *Chem. Soc. Rev.* 2018, 47, 4112–4155.

(255) Guo, Z.; Xiong, G.; Liu, L.; Yin, J.; Zhao, R.; Yu, S. Facile and Green Aerosol-Assisted Synthesis of Zeolites. *RSC Adv.* 2015, 5, 71433–71436.

(256) Xiong, G.; Feng, M.; Liu, J.; Meng, Q.; Liu, L.; Guo, H. The Synthesis of Hierarchical High-Silica Beta Zeolites in NaF Media. *RSC Adv.* 2019, 9, 3653–3660.

(257) Xiong, G.; Yin, J.; Liu, J.; Liu, X.; Guo, Z.; Liu, L. Aerosol-Assisted Synthesis of Nano-Sized ZSM-5 Aggregates. *RSC Adv.* 2016, 6, 101365–101371.

(258) Xiong, G.; Liu, X.; Zhao, R.; Liu, J.; Yin, J.; Meng, Q.; Guo, Z.; Liu, L. Synthesis and Crystallization Mechanism of Nano-Sized Zeolite Beta Aggregates via Aerosol-Assisted Method. *Microporous Mesoporous Mater.* 2017, 249, 97–104.

(259) Meng, Q.; Liu, J.; Xiong, G.; Liu, X.; Liu, L.; Guo, H. Aerosol-Seed-Assisted Hydrothermal Synthesis of Sn-Beta Zeolite and Its Catalytic Performance in Baeyer–Villiger Oxidation. *Microporous Mesoporous Mater.* 2018, 266, 242–251.

(260) Guo, Z.; Xiong, G.; Liu, L.; Song, W.; Jia, Q. Crystallization Mechanism and Catalytic Performance of TS-1 Synthesized by an Aerosol-Assisted Method. *CrystEngComm* 2017, 19, 2695–2701.

(261) Pega, S.; Boissière, C.; Grosso, D.; Azaïs, T.; Chaumonnot, A.; Sanchez, C. Direct Aerosol Synthesis of Large-Pore Amorphous Mesostructured Aluminosilicates with Superior Acid-Catalytic Properties. *Angew. Chemie - Int. Ed.* 2009, 48, 2784–2787.

(262) Fiorilli, S.; Cauda, V.; Pontiroli, L.; Vitale-Brovarone, C.; Onida, B. Aerosol-Assisted Synthesis of Mesoporous Aluminosilicate Microspheres: The Effect of the Aluminum Precursor. *New J. Chem.* 2016, 40, 4420–4427.

(263) Smeets, V.; Boissière, C.; Sanchez, C.; Gaigneaux, E. M.; Peeters, E.; Sels, B. F.; Dusselier, M.; Debecker, D. P. Aerosol Route to TiO2 -SiO2 Catalysts with Tailored Pore Architecture and High Epoxidation Activity. *Chem. Mater.* 2019, 31 (5), 1610–1619.

(264) Majano, G.; Borchardt, L.; Mitchell, S.; Valtchev, V.; Pérez-ramírez, J. Rediscovering Zeolite Mechanochemistry – A Pathway beyond Current Synthesis and Modification Boundaries. *Microporous Mesoporous Mater.* 2014, 194, 106–114.

(265) Valtchev, V.; Mintova, S.; Dimov, V.; Toneva, A.; Radev, D. Tribochemical Activation of Seeds for Rapid Crystallization of Zeolite Y. *Zeolites* 1995, 15, 193–197.

(266) Yamada, H.; Iida, T.; Liu, Z.; Naraki, Y.; Ohara, K.; Kohara, S.; Okubo, T.; Wakihara, T. Downsizing AFX Zeolite Crystals to Nanoscale by a Postmilling Recrystallization Method. *Cryst. Growth Des.* 2016, 16, 3389–3394.

(267) Iwasaki, T.; Isaka, M.; Nakamura, H.; Yasuda, M.; Watano, S. Synthesis of Titanosilicate TS-1 Crystals via Mechanochemical Route Using Low Cost Materials. *Microporous Mesoporous Mater.* 2012, 150, 1–6.

(268) Ren, L.; Wu, Q.; Yang, C.; Zhu, L.; Li, C.; Zhang, P.; Zhang, H.; Meng, X.; Xiao, F. Solvent-Free Synthesis of Zeolites from Solid Raw Materials. *J. Am. Chem. Soc.* 2012, 134, 15173–15176.

(269) Morris, R. E.; James, S. L. Solventless Synthesis of Zeolites.

(270) Wu, Q.; Wang, X.; Qi, G.; Guo, Q.; Pan, S.; Meng, X.; Xu, J.; Deng, F.; Fan, F.; Feng, Z.; et al. Sustainable Synthesis of Zeolites without Addition of Both Organotemplates and Solvents. *J. Am. Chem. Soc.* 2014, 136, 4019–4025.

(271) Wang, X.; Wu, Q.; Chen, C.; Pan, S.; Zhang, W.; Meng, X.; Maurer, S.; Feyen, M.; Müller, U.; Xiao, F. Atom-Economical Synthesis of a High Silica CHA Zeolite Using a Solvent-Free Route. *Chem. Commun.* 2015, 51, 16920–16923.

(272) Wu, Q.; Liu, X.; Zhu, L.; Ding, L.; Gao, P.; Wang, X.; Pan, S.; Bian, C.; Meng, X.; Xu, J.; et al. Solvent-Free Synthesis of Zeolites from Anhydrous Starting Raw Solids. *J. Am. Chem. Soc.* 2015, 137, 1052–1055.

(273) Zhu, L.; Zhang, J.; Wang, L.; Wu, Q.; Bian, C.; Pan, S.; Meng, X.; Xiao, F.-S. Solvent-Free Synthesis of Titanosilicate Zeolites. *Journals Mater. Chem. A* 2015, 3, 14093–14095.

(274) Xiao, Y.; Sheng, N.; Chu, Y.; Wang, Y.; Wu, Q.; Liu, X.; Deng, F.; Meng, X.; Feng, Z. Mechanism on Solvent-Free Crystallization of NaA Zeolite. *Microporous Mesoporous Mater.* 2017, 237, 201–209.

(275) Wu, Q.; Meng, X.; Gao, X.; Xiao, F.-S. Solvent-Free Synthesis of Zeolites: Mechanism and Utility. *Acc. Chem. Res.* 2018, 51, 1396–1403.

(276) Jin, Y.; Sun, Q.; Qi, G.; Yang, C.; Xu, J.; Chen, F.; Meng, X.; Deng, F.; Xiao, F.-S. Solvent-Free Synthesis of Silicoaluminophosphate Zeolites. *Angew. Chemie - Int. Ed.* 2013, 52, 9172–9175.

(277) Nakai, M.; Miyake, K.; Inoue, R.; Ono, K.; Al Jabri, H.; Hirota, Y.; Uchida, Y.; Miyamoto, M.; Nishiyama, N. Synthesis of High Silica *BEA Type Ferrisilicate (Fe-Beta) by Dry Gel Conversion Method Using Dealuminated Zeolites and Its Catalytic Performance on Acetone to Olefins (ATO) Reaction. *Microporous Mesoporous Mater.* 2019, 273, 189–195.

(278) Vattipalli, V.; Paracha, A. M.; Hu, W.; Chen, H.; Fan, W. Broadening the Scope for Fluoride-Free Synthesis of Siliceous Zeolites. *Angew. Chemie - Int. Ed.* 2018, 57 (14), 3607–3611.

(279) Kim, D. S.; Kim, J. M.; Chang, J.-S.; Park, S.-E. Rapid and Mass Production of Porous Materials Using a Continuous Microwave Equipment. *Stud. Surf. Sci. Catal.* 2001, 135, 333–340.

(280) Bonaccorsi, L.; Proverbio, E. Influence of Process Parameters in Microwave Continuous Synthesis of Zeolite LTA. *Microporous Mesoporous Mater.* 2008, 112, 481–493.

(281) Xu, Y.-P.; Tian, Z.-J.; Wang, S.-J.; Hu, Y.; Wang, L.; Wang, B. C.; Ma, Y.-C.; Hou, L.; Yu, J.-Y.; Lin, L.-W. Microwave-Enhanced Ionothermal Synthesis of Aluminophosphate Molecular Sieves. *Angew. Chemie - Int. Ed.* 2006, 45, 3965–3970.

(282) Cai, R.; Sun, M.; Chen, Z.; Munoz, R.; O'Neill, C.; Beving, D. E.; Yan, Y. Ionothermal Synthesis of Oriented Zeolite AEL Films and Their Application as Corrosion-Resistant Coatings. *Angew. Chemie - Int. Ed.* 2008, 47, 525–528.

(283) Suresh, S.; Reddy, I. A. K.; Venkatathri, N. Synthesis of SAPO-16 Molecular Sieve in Non-Aqueous Medium by Microwave Method Using Hexamethyleneimine as a Template. *Microporous Mesoporous Mater.* 2018, 263, 275–281.

(284) Chen, X.; Yan, W.; Shen, W.; Yu, J.; Cao, X.; Xu, R. Morphology Control of Self-Stacked Silicalite-1 Crystals Using Microwave-Assisted Solvothermal Synthesis. *Microporous Mesoporous Mater.* 2007, 104, 296–304.

(285) Boruntea, C.; Sastre, G.; Lundegaard, L. F.; Corma, A.; Vennestrøm, P. N. R. Synthesis of High-Silica ERI Driven by Computational Screening of Hypothetical Zeolites. *Chem. Mater.* 2019, 31 (22), 9268–9276.

(286) Dusselier, M.; Kang, J. H.; Xie, D.; Davis, M. E. CIT-9 : A Fault-Free Gmelinite Zeolite. *Angew. Chemie - Int. Ed.* 2017, 56, 13475–13478.

(287) Schwalbe-Koda, D.; Jensen, Z.; Olivetti, E.; Gómez-

Bombarelli, R. Graph Similarity Drives Zeolite Diffusionless Transformations and Intergrowth. *Nat. Mater.* **2019**, *18*, 1177–1181.

(288) Li, J.; Corma, A.; Yu, J. Synthesis of New Zeolite Structures. *Chem. Soc. Rev.* **2015**, *44* (20), 7112–7127.

(289) Alberti, A.; Parodi, I.; Cruciani, G.; Dalconi, M. C.; Martuccci, A. Dehydration and Rehydration Processes in Gmelinite: An in Situ X-Ray Single-Crystal Study. *Am. Mineral.* **2010**, *95*, 1773–1782.

(290) Leonowicz, M. E.; Lawton, J. A.; Lawton, S. L.; Rubin, M. K. MCM-22: A Molecular Sieve with Two Independent Multidimensional Channel Systems. *Science* **1994**, *264*, 1910–1913.

(291) Millini, R.; Perego, G.; Parker, W. O.; Bellussi, G.; Carluccio, L. Layered Structure of ERB-1 Microporous Borosilicate Precursor and Its Intercalation Properties towards Polar Molecules. *Microporous Mater.* **1995**, *4* (2–3), 221–230.

(292) Camblor, M. A.; Corma, A.; Díaz-Cabañas, M. J.; Baerlocher, C. Synthesis and Structural Characterization of MWW Type Zeolite ITQ-1, the Pure Silica Analog of MCM-22 and SSZ-25. *J. Phys. Chem. B* **1998**, *102* (1), 44–51.

(293) Marler, B.; Camblor, M. A.; Gies, H. The Disordered Structure of Silica Zeolite EU-20b, Obtained by Topotactic Condensation of the Piperazinium Containing Layer Silicate EU-19. *Microporous Mesoporous Mater.* **2006**, *90*, 87–101.

(294) Moteki, T.; Chaikittisilp, W.; Shimojima, A.; Okubo, T. Silica Sodalite without Occluded Organic Matters by Topotactic Conversion of Lamellar Precursor. *J. Am. Chem. Soc.* **2008**, *130*, 15780–15781.

(295) Ikeda, T.; Kayamori, S.; Mizukami, F. Synthesis and Crystal Structure of Layered Silicate PLS-3 and PLS-4 as a Topotactic Zeolite Precursor. *J. Mater. Chem.* **2009**, *19*, 5518–5525.

(296) Moteki, T.; Chaikittisilp, W.; Sakamoto, Y.; Shimojima, A.; Okubo, T. Role of Acidic Pretreatment of Layered Silicate RUB-15 in Its Topotactic Conversion into Pure Silica Sodalite. *Chem. Mater.* **2011**, *23*, 3564–3570.

(297) Zhao, Z.; Zhang, W.; Ren, P.; Han, X.; Müller, U.; Yilmaz, B.; Feyen, M.; Gies, H.; Xiao, F.-S.; De Vos, D.; et al. Insights into the Topotactic Conversion Process from Layered Silicate RUB-36 to FER-Type Zeolite by Layer Reassembly. *Chem. Mater.* **2013**, *25*, 840–847.

(298) Roth, W. J.; Nachtigall, P.; Morris, R. E.; Wheatley, P. S.; Seymour, V. R.; Ashbrook, S. E.; Chlubná, P.; Grajciar, L.; Polozij, M.; Zukal, A.; et al. A Family of Zeolites with Controlled Pore Size Prepared Using a Top-down Method. *Nat. Chem.* **2013**, *5*, 628–633.

(299) Ikeda, T.; Akiyama, Y.; Oumi, Y.; Kawai, A.; Mizukami, F. The Topotactic Conversion of a Novel Layered Silicate into a New Framework Zeolite. *Angew. Chemie - Int. Ed.* **2004**, *43*, 4892–4896.

(300) Wang, Y. X.; Gies, H.; Marler, B.; Müller, U. Synthesis and Crystal Structure of Zeolite RUB-41 Obtained as Calcination Product of a Layered Precursor: A Systematic Approach to a New Synthesis Route. *Chem. Mater.* **2005**, *17* (12), 43–49.

(301) Knight, L. M.; Miller, M. A.; Koster, S. C.; Gatter, M. G.; Benin, A. I.; Willis, R. R.; Lewis, G. J.; Broach, R. W. UZM-13, UZM-17, UZM-19 and UZM-25: Synthesis and Structure of New Layered Precursors and a Zeolite Discovered via Combinatorial Chemistry Techniques. *Stud. Surf. Sci. Catal.* **2007**, *170*, 338–346.

(302) Martínez-franco, R.; Paris, C.; Martínez-triguero, J.; Moliner, M.; Corma, A. Direct Synthesis of the Aluminosilicate Form of the Small Pore CDO Zeolite with Novel OSDAs and the Expanded Polymorphs. *Microporous Mesoporous Mater.* **2017**, *246*, 147–157.

(303) Dorset, D. L.; Kennedy, G. J. Crystal Structure of MCM-65: An Alternative Linkage of Ferrierite Layers. *J. Phys. Chem. B* **2010**, *108* (39), 15216–15222.

(304) Marler, B.; Ströter, N.; Gies, H. The Structure of the New Pure Silica Zeolite RUB-24, Si32O64, Obtained by Topotactic Condensation of the Intercalated Layer Silicate RUB-18.

(305) Oumi, Y.; Takeoka, T.; Ikeda, T.; Yokoyama, T.; Sano, T. Convenient Conversion of Crystalline Layered Silicate Octosilicate into RWR-Type Zeolite by Acetic Acid Intercalation. *New J. Chem.* **2007**, *31* (4), 593–597.

(306) Ikeda, T.; Oumi, Y.; Takeoka, T.; Yokoyama, T.; Sano, T.; Hanaoka, T. Preparation and Crystal Structure of RUB-18 Modified for Synthesis of Zeolite RWR by Topotactic Conversion. *Microporous Mesoporous Mater.* **2008**, *110*, 488–500.

(307) Asakura, Y.; Osada, S.; Hosaka, N.; Terasawa, T.; Kuroda, K. Optimal Topotactic Conversion of Layered Octosilicate to RWR-Type Zeolite by Separating the Formation Stages of Interlayer Condensation and Elimination of Organic Guest Molecules. *Dalt. Trans.* **2014**, *43*, 10392–10395.

(308) Zanardi, S.; Alberti, A.; Cruciani, G.; Corma, A.; Fornés, V.; Brunelli, M. Crystal Structure Determination of Zeolite Nu-6(2) and Its Layered Precursor Nu-6(1). *Angew. Chemie Int. Ed.* **2004**, *116*, 5041–5045.

(309) De Baerdemaeker, T.; Gies, H.; Yilmaz, B.; Müller, U.; Feyen, M.; Xiao, F.; Zhang, W.; Yokoi, T.; Bao, X.; De Vos, D. E. A New Class of Solid Lewis Acid Catalysts Based on Interlayer Expansion of Layered Silicates of the RUB-36 Type with Heteroatoms. *J. Mater. Chem. A* **2014**, *2*, 9709–9717.

(310) Wu, P.; Ruan, J.; Wang, L.; Wu, L.; Wang, Y.; Liu, Y.; Fan, W.; He, M.; Terasaki, O.; Tatsumi, T. Methodology for Synthesizing Crystalline Metallosilicates with Expanded Pore Windows Through Molecular Alkoxysilylation of Zeolitic Lamellar Precursors. *J. Am. Chem. Soc.* **2008**, *130*, 8178–8187.

(311) Schmidt, J. E.; Xie, D.; Davis, M. E. High-Silica, Healandite-Type Zeolites Prepared by Direct Synthesis and Topotactic Condensation. *J. Mater. Chem. A* **2015**, *3*, 12890–12897.

(312) Corma, A.; Fornes, V.; Bergher, S. B.; Maesen, T. L. M.; Buglass, J. G. Delaminated Zeolite Precursors as Selective Acidic Catalysts. *Nature* **1998**, *396*, 353–356.

(313) Corma, A.; Fornés, V.; Guil, J. M.; Pergher, S.; Maesen, T. L. M.; Buglass, J. G. Preparation, Characterisation and Catalytic Activity of ITQ-2, a Delaminated Zeolite. *Microporous Mesoporous Mater.* **2000**, *38*, 301–309.

(314) Corma, A.; Fornés, V.; Díaz, U. ITQ-18 a New Delaminated Stable Zeolite. *Chem. Commun.* **2001**, *6*, 2642–2643.

(315) Corma, A.; Diaz, U.; Domine, M. E.; Fornés, V. AlITQ-6 and TiITQ-6: Synthesis, Characterization, and Catalytic Activity. *Angew. Chemie Int. Ed.* **2000**, *39*, 1499–1501.

(316) Ogino, I.; Nigra, M. M.; Hwang, S.; Ha, J.; Rea, T.; Zones, S. I.; Katz, A. Delamination of Layered Zeolite Precursors under Mild Conditions: Synthesis of UCB-1 via Fluoride/Chloride Anion-Promoted Exfoliation. *J. Am. Chem. Soc.* **2011**, *133*, 3288–3291.

(317) Eilertsen, E. A.; Ogino, I.; Hwang, S.; Rea, T.; Yeh, S.; Zones, S. I.; Katz, A. Nonaqueous Fluoride/Chloride Anion-Promoted Delamination of Layered Zeolite Precursors: Synthesis and Characterization of UCB-2. *Chem. Mater.* **2011**, *23*, 5404–5408.

(318) Ogino, I.; Eilertsen, E. A.; Hwang, S.; Rea, T.; Xie, D.; Ouyang, X.; Zones, S. I.; Katz, A. Heteroatom-Tolerant Delamination of Layered Zeolite Precursor Materials. *Chem. Mater.* **2013**, *25*, 1502–1509.

(319) Okrut, A.; Aigner, M.; Schöttle, C.; Grosso-giordano, N. A.; Hwang, S.; Ouyang, X.; Zones, S.; Katz, A. SSZ-70 Borosilicate Delamination without Sonication: Effect of Framework Topology on Olefin Epoxidation Catalysis. *Dalt. Trans.* **2018**, *47*, 15082–15090.

(320) Ouyang, X.; Hwang, S.; Runnebaum, R. C.; Xie, D.; Wanglee, Y.; Rea, T.; Zones, S. I.; Katz, A. Single-Step Delamination of a MWW Borosilicate Layered Zeolite Precursor under Mild Conditions without Surfactant and Sonication. *J. Am. Chem. Soc.* **2014**, *136*, 1449–1461.

(321) Ouyang, X.; Wanglee, Y.-J.; Hwang, S.-J.; Xie, D.; Rea, T.; Zones, S. I.; Katz, A. Novel Surfactant-Free Route to

Delaminated All-Silica and Titanosilicate Zeolites Derived from a Layered Borosilicate MWW Precursor. *Dalt. Trans.* **2014**, *43*, 10417–10429.

(322) Eliasova, P.; Opanasenko, M.; Wheatley, P. S.; Shamzhy, M.; Mazur, M.; Nachtigall, P.; Roth, W. J.; Morris, R. E.; Cejka, J. The ADOR Mechanism for the Synthesis of New Zeolites. *Chem. Soc. Rev.* **2015**, *44*, 7177–7206.

(323) Henkelis, S. E.; Mazur, M.; Rice, C. M.; Bignami, G. P. M.; Wheatley, P. S.; Ashbrook, S. E.; Čejka, J.; Morris, R. E. A Procedure for Identifying Possible Products in the Assembly–Disassembly–Organization–Reassembly (ADOR) Synthesis of Zeolites. *Nat. Protoc.* **2019**, *14*, 781–794.

(324) Verheyen, E.; Joos, L.; Van Havenbergh, K.; Breynaert, E.; Kasian, N.; Gobechiya, E.; Houthoofd, K.; Martineau, C.; Hinterstein, M.; Taulelle, F.; et al. Design of Zeolite by Inverse Sigma Transformation. *Nat. Mater.* **2012**, *11*, 1059–1064.

(325) Roth, W. J.; Shvets, O. V; Shamzhy, M.; Chlubná, P.; Kubu, M.; Nachtigall, P.; Cejka, J. Postsynthesis Transformation of Three-Dimensional Framework into a Lamellar Zeolite with Modifiable Architecture. *J. Am. Chem. Soc.* **2011**, *133*, 6130–6133.

(326) Jordá, J. L.; Rey, F.; Sastre, G.; Valencia, S.; Palomino, M.; Corma, A.; Segura, A.; Errandonea, D.; Lacomba, R.; Manjón, F. J.; et al. Synthesis of a Novel Zeolite through a Pressure-Induced Reconstructive Phase Transition Process. *Angew. Chemie - Int. Ed.* **2013**, *52*, 10458–10462.

(327) Thibaud, J.; Rouquette, J.; Hermet, P.; Dziubek, K.; Gorelli, F. A.; Santoro, M.; Garbarino, G.; Alabarse, F. G.; Cambon, O.; Di Renzo, F.; et al. High-Pressure Phase Transition, Pore Collapse, and Amorphization in the Siliceous 1D Zeolite, TON. *J. Phys. Chem. C* **2017**, *121*, 4283–4292.

(328) Alabarse, F. G.; Brubach, J.; Roy, P.; Haidoux, A.; Levelut, C.; Bantignies, J.; Cambon, O.; Haines, J. $AlPO_4$-54 – $AlPO_4$-8 Structural Phase Transition and Amorphization under High Pressure. *J. Phys. Chem. C* **2015**, *119*, 7771–7779.

(329) Mazur, M.; Arévalo-López, A. M.; Wheatley, P. S.; Bignami, G. P. M.; Ashbrook, S. E.; Morales-Garcia, Á.; Nachtigall, P.; Attfield, J. P.; Cejka, J.; Morris, R. E. Pressure-Induced Chemistry for the 2D to 3D Transformation of Zeolites. *J. Mater. Chem. A* **2018**, *6*, 5255–5259.

(330) Moliner, M.; Román-Leshkov, Y.; Corma, A. Machine Learning Applied to Zeolite Synthesis: The Missing Link for Realizing High-Throughput Discovery. *Acc. Chem. Res.* **2019**, *52* (10), 2971–2980.

(331) Kasneryk, V.; Shamzhy, M.; Zhou, J.; Yue, Q.; Mazur, M.; Mayoral, A.; Luo, Z.; Morris, R. E.; Cejka, J.; Opanasenko, M. Vapour-Phase-Transport Rearrangement Technique for the Synthesis of New Zeolites. *Nat. Commun.* **2019**, *10* (1), 5129.

This review highlights and critically discusses non-conventional zeolite synthesis conditions – leading to new or adaptations of classic degrees of freedom (DOF) during synthesis – that are used to render syntheses more efficient or improve the resulting material's properties.